NASA CR-134774

HIGH POWER FERRITE MICROWAVE SWITCH

by

Irwin Bardash and Nicholas K. Roschak

SEDCO SYSTEMS INC.
Farmingdale, New York

Prepared for:

NATIONAL AERONAUTICS AND SPACE ADMINISTRATION
NASA Lewis Research Center
Contract NAS3-16752

NASA CR-134774

HIGH POWER FERRITE MICROWAVE SWITCH

by

Irwin Bardash and Nicholas K. Roschak

Sedco Systems Inc.
Farmingdale, New York

Prepared for:

National Aeronautics and Space Administration
NASA Lewis Research Center
Contract NAS3-16752

TABLE OF CONTENTS

LIST OF ILLUSTRATIONS

LIST OF ILLUSTRATIONS - Continued

LIST OF ILLUSTRATIONS - Continued

I INTRODUCTION

This report describes the work conducted under Contract No. NAS3-16752 conducted for NASA-Lewis Research Center. The program involved the development of a High Power Ferrite Microwave Switch and associated electronic driver circuits for operation in a spaceborne high power microwave transmitter in geostationary orbit.

Figure 1 is a photograph of the final switch configuration. Three such units were built and tested in a space environment to demonstrate conformance to the required performance characteristics. Each unit consisted of an input magic-tee hybrid, two non-reciprocal latching ferrite phase shifters, an output short-slot 3 db quadrature coupler, a dual driver electronic circuit, and input logic interface circuitry. The basic mode of operation of the High Power Ferrite Microwave Switch is identical to that of a four-port, differential phase shift, switchable circulator. By appropriately designing the phase shifters and electronic driver circuits to operate in the flux-transfer magnetization mode, power and temperature insensitive operation was achieved. A list of the realized characteristics of the developed units is as follows:

Frequency.....	12 GHz $\pm$ .25 GHz
Insertion Loss.....	0.3 db Maximum
VSWR.....	1.25 Maximum

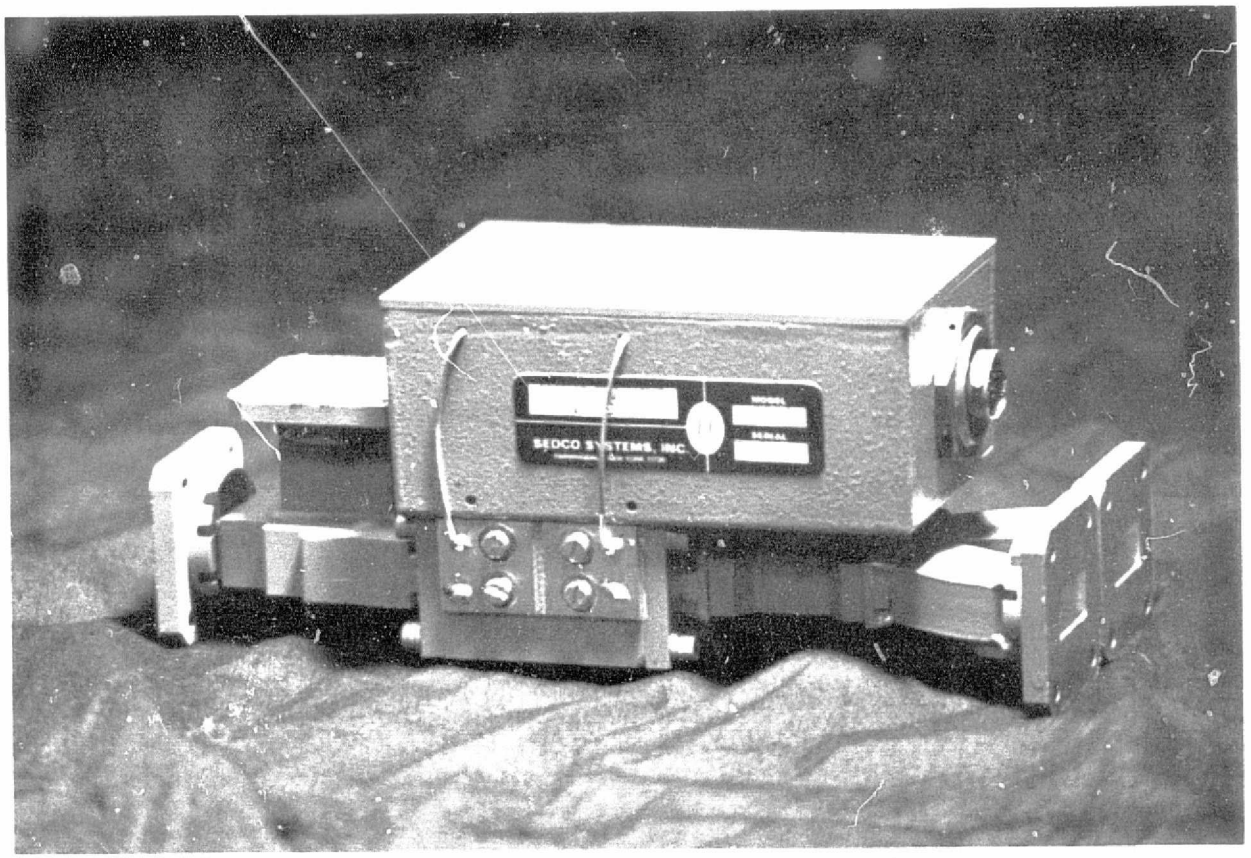

Figure 1 - Photograph of High Power Ferrite Microwave Switch

Isolation.....30 db Minimum

Power Handling..... 750 Watts C.W. Minimum

Switching Speed..... 1.0 usec. Maximum

Environment.....Vacuum (10^{-6} torr)

Weight..... 22 Ounces

Overall Outside Dimensions

Length.....Less than 7"

Height.....Less than 3"

Width.....Less than 3"

The High Power Ferrite Microwave Switch was designed to function in a missile launch environment as well as a space environment. This was achieved by eliminating any material prone to outgassing and using mechanical and electrical designs which can operate over highly severe shock, vibration, and temperature conditions.

Considerable effort was involved in realizing the final results and many problems had to be overcome in order to achieve the above listed performance. Major problems were encountered relative to high power operation in a vacuum environment and it was concluded that any material, whatsoever, which may produce outgassing or contain air pockets was unacceptable for space application. The following report will describe in detail the fundamental theory of operation of the High Power Ferrite Microwave Switch, initial design and test data results, redesign efforts, as well as all final test data.

II THEORY OF OPERATION

A. Switchable Four-Port Differential Phase Shift Circulators

The core of the High Power Ferrite Microwave Switch is a four-port differential phase shift circulator. A block diagram of this device is shown in Figure 2. Also shown in the block diagram are the required driver circuits and inputs from the logic interface circuitry. Reference planes are drawn for purposes of discussion and will be used to illustrate the relative phases of the propagating waves internal to the device.

The r.f. input terminal is the sum port of the magic tee hybrid. When the device is used as a switch, the difference port should be terminated with a matched load, as illustrated. If an r.f. voltage of unity amplitude is applied to the input port, in-phase voltage levels of 0.707 volts will be present in the upper and lower arms of the device at Reference Plane A. For Switch State 1, Phase Shifter 1 is set to 90°, while Phase Shifter 2 is set to 0°. Hence at Reference Plane B the voltage level in the upper arm will be $0.707 \angle 90°$ and in the lower arm the voltage will be $0.707 \angle 0°$. If we first consider the splitting of the voltage from the upper arm at the 3 db short-slot quadrature coupler, the voltage levels at Output 1 and Output 2 associated with the upper arm of the device will be $0.500 \angle 90°$ and $0.500 \angle 180°$ respectively. The voltage levels at Output 1 and 2 associated with the wave in the lower portion of the device will be $.500 \angle 90°$ and $.500 \angle 0°$ respectively. Hence at Output 1 there will occur

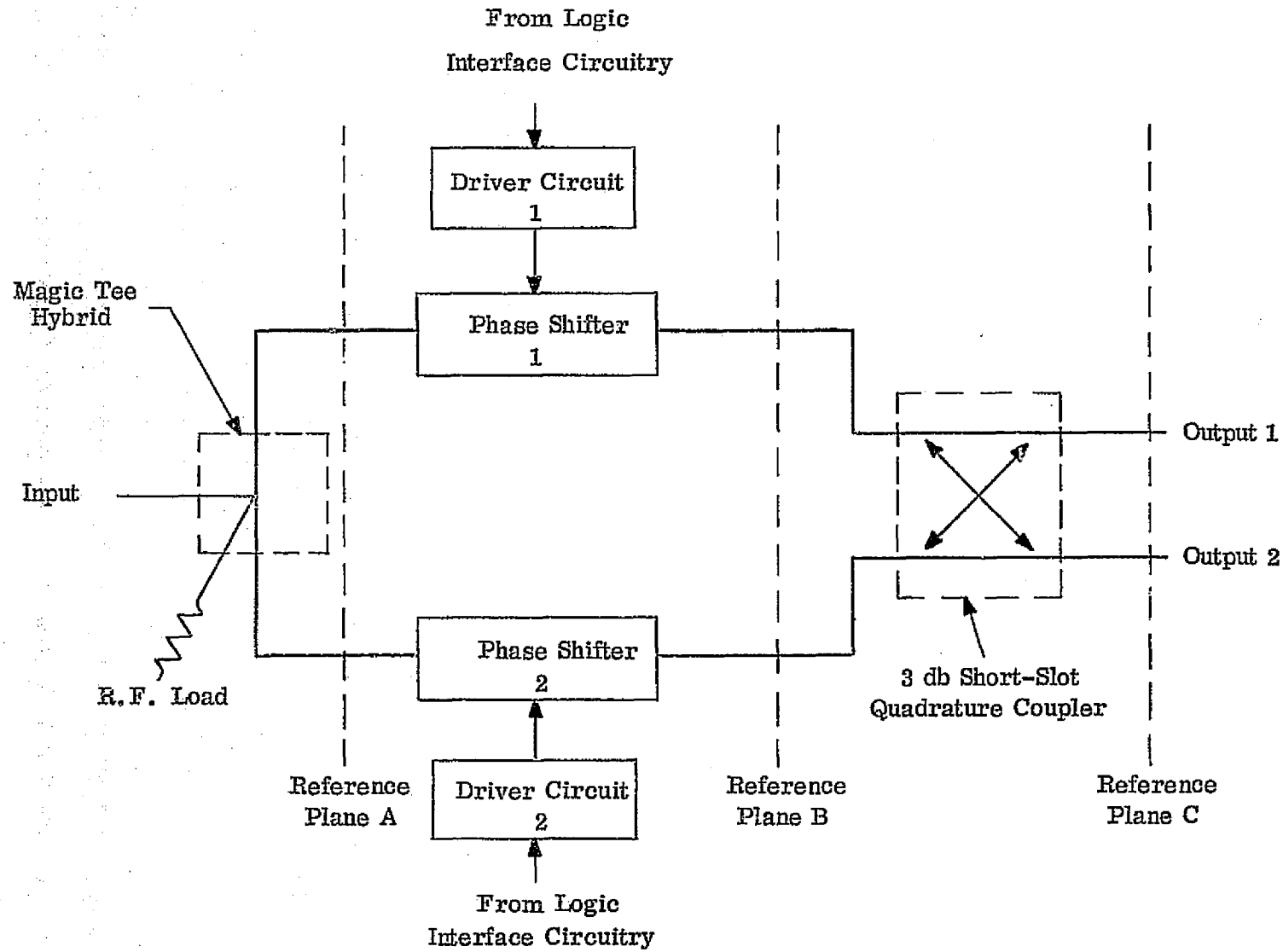

Figure 2 - BLOCK DIAGRAM OF HIGH POWER FERRITE MICROWAVE SWITCH

the summation of 0.500 $\angle 90°$ and 0.500 $\angle 90°$ or a total of 1.00 $\angle 90°$ volts. At Output 2 there will occur a sum of 0.500 $\angle 180°$ and 0.500 $\angle 0°$ which results in a null. It is seen from this simple vectoral consideration that all the output power will appear at Output 1 while zero power appears at Output 2. By setting Phase Shifter 1 to 0° and Phase Shifter 2 to 90°, it can be shown using the same simple vector considerations that all of the r.f. power will appear at Output 2 while a null will exist at Output 1. A summary of the voltage phase relations for the two output conditions at the three reference planes is listed in Table 1. As an aside, should it be desirable to feed r.f. input to the difference port of the magic tee hybrid, while terminating the sum port, Output 1 and Output 2 would be interchanged for the phase relations listed.

It is appropriate at this time to discuss some of the physical limitations and effects of errors on theoretical switch performance. In the previous discussion it was assumed that no errors or losses existed in the various sections of the switch. In reality, however, r.f. losses do occur as well as errors in phase settings within the two phase shifters. In addition, amplitude and phase imbalance may be introduced due to the limitations of the magic tee hybrid as well as the 3 db short-slot quadrature coupler.

It can be shown that, within the existing state-of-the-art, the magic tee and quadrature coupler hybrids introduce a minimum of losses and

CASE 1 - POWER OUT AT OUTPUT 1

	R. F. Voltage at Plane A	R. F. Voltage at Plane B	R. F. Voltage at Plane C
Upper Arm of Switch	$0.707 \angle 0°$	$0.707 \angle 90°$	$0.50 \angle 90° + 0.50 \angle 90° = 1.0 \angle 90°$
Lower Arm of Switch	$0.707 \angle 0°$	$0.707 \angle 0°$	$0.50 \angle 180° + 0.50 \angle 0° = 0$

CASE 2 - POWER OUT AT OUTPUT 2

	R. F. Voltage at Plane A	R. F. Voltage at Plane B	R. F. Voltage at Plane C
Upper Arm of Switch	$0.707 \angle 0°$	$0.707 \angle 0°$	$0.50 \angle 0° + 0.50 \angle 180° = 0$
Lower Arm of Switch	$0.707 \angle 0°$	$0.707 \angle 90°$	$0.50 \angle 90° + 0.50 \angle 90° = 1.0 \angle 90°$

TABLE 1 - LIST OF R. F. VOLTAGES INDICATING PHASE RELATIONS FOR TWO OUTPUT CONDITIONS OF HIGH POWER FERRITE MICROWAVE SWITCH

phase imbalance over the frequency range of the High Power Ferrite Microwave Switches. The primary cause of errors is traceable to the two phase shifter sections. It can further be stated that if the two phase shifters are fabricated properly, so as to produce minimum insertion loss, negligible amplitude imbalance will occur. Hence, the major cause of performance degradation is introduced by phase errors within the phase shifter devices themselves. Non-reciprocal latching ferrite phase shifters were used in the High Power Ferrite Microwave Switches. These devices will be described in a later section. The effects of phase errors, however, will be discussed here.

Figure 3 is a curve illustrating insertion loss or isolation as a function of relative phase between the two phase shifters ($\phi_2 - \phi_1$) for a four-port differential phase shift circulator. As can be seen, perfect theoretical operation occurs when the relative phase is either -90° or +90°. For the -90° condition energy is directed from the Input to Output 2 while the power level at Output 1 is nulled. For the +90° condition all the input power would appear at Output 1 while a null would exist at Output 2. If a phase error of 20° existed for either output condition, an isolation of approximately 15 db would be realized and an insertion loss to the coupled output port of approximately 0.13 db would occur. If the phase error is reduced to $\pm 10°$ the isolation would increase to better than 21 db and the insertion loss would be below 0.1 db. It is apparent from the curve that the insertion loss to the coupled output port is relatively insensitive to phase errors while the

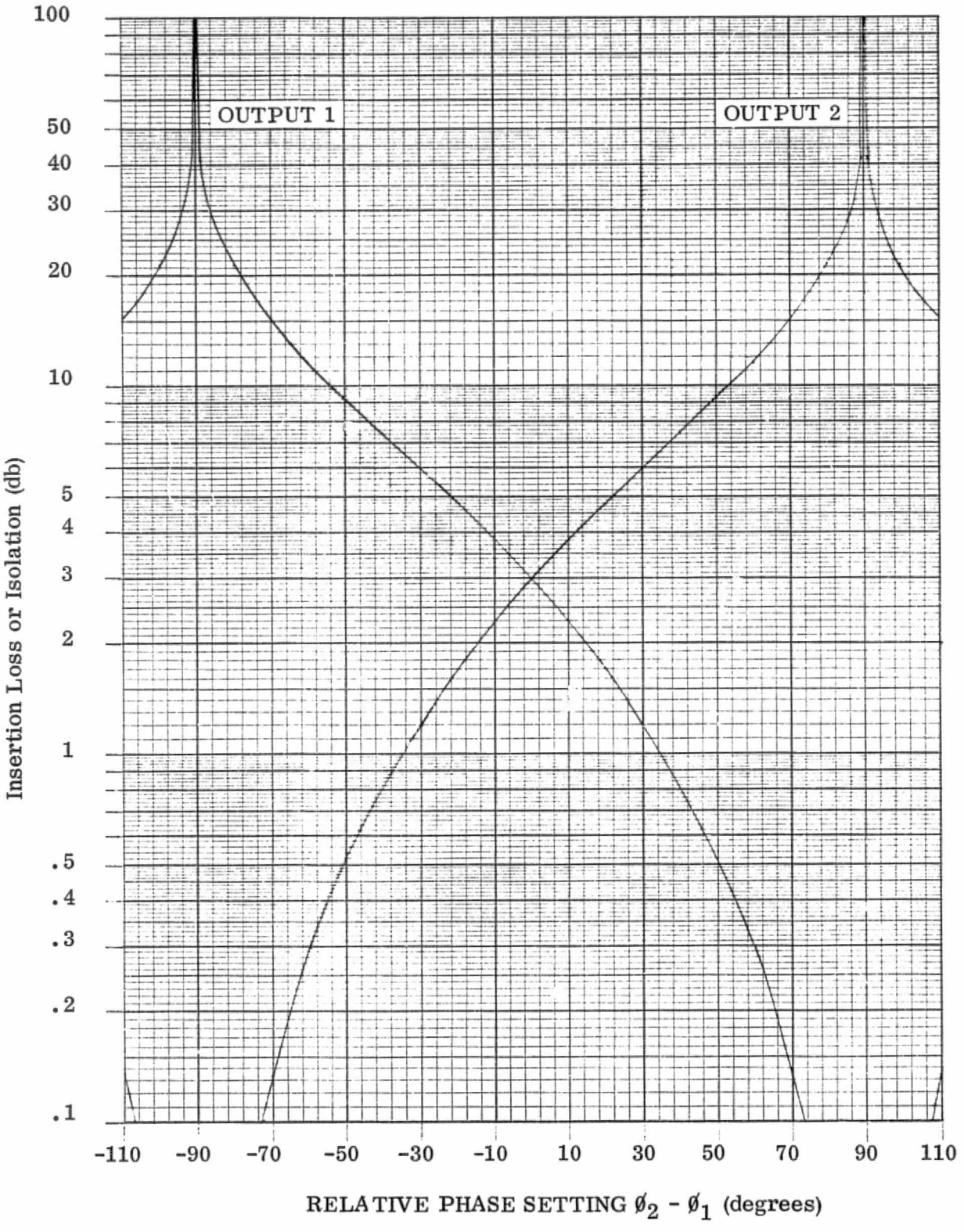

Figure 3 - Insertion Loss or Isolation vs Relative Phase Setting

isolation to the uncoupled port is effected rapidly. The specified isolation requirement for the High Power Ferrite Microwave Switch was 25 db minimum with 30 db as an objective. The isolation objective of 30 db was achieved. Referring back to Figure 3, this implies that a relative phase error of less than 4° was achieved across the entire operating frequency range as well as over the required temperature and power ranges. The observed insertion loss of 0.3 db was due to dissipative losses in the phase shifter sections and hybrids and was unrelated to phase errors, since a 4° phase imbalance would produce an immeasureable level of insertion loss. The curves shown in Figure 3 may be used to predict anticipated isolation levels as a function of phase errors for any type of four-port differential phase shift circulator whether it be latching or non-latching. The characteristics of the phase shifters and driver circuits used in the developed High Power Ferrite Microwave Switch will be discussed in the next sections and it will become evident how the achieved results were realized.

B. Non-Reciprocal Latching Ferrite Phase Shifter

The theory of operation of the non-reciprocal latching ferrite phase shifter is virtually the same as the twin slab, oppositely magnetized ferrite phase shifter. The latter device was described by Lax, Button, and Roth of the MIT Lincoln Laboratory in the early 1950s but due to its poor switching properties, as well as its cumbersome physical size, it was never utilized in any system which required practical variable phase shifter devices.

Figure 4 is a cross-sectional view of this device. As indicated in the sketch, d.c. magnetic bias is applied to the ferrite slab with two electromagnet devices located outside of the waveguide transmission line. Current in the electromagnets is applied to produce opposite diredtions of magnetization in the ferrite slabs. In the latching device internal magnetic bias is achieved by utilizing the hysteresis properties of the microwave ferrite material. By providing a closed magnetic path in the top and bottom of the twin slabs, internal bias fields as high as the remanent magnetization of the microwave ferrite may be realized. This will be discussed in more detail further in the text.

Differential phase shift is produced in the twin slab, oppositely magnetized ferrite phase shifter by the non-reciprocal interaction between the r.f. propagating wave and the oppositely biased ferrite slabs. The fundamental mode (TE_{10}) of an unloaded waveguide has two planes of circularly polarized magnetic field lines located approximately one quarter of the waveguide width away from each of the waveguide sidewalls. Two such planes also exist in the twin slab device but are drawn into the ferrite regions due to the dielectric properties of both the loading strip and the ferrite itself. The senses of circular polarization of the planes are opposite, that is, one is clockwise while the other is counterclockwise. Since the two ferrite slabs, as shown in Figure 4 are biased in opposite directions, they will interact with the two opposite senses of circularly polarized H fields

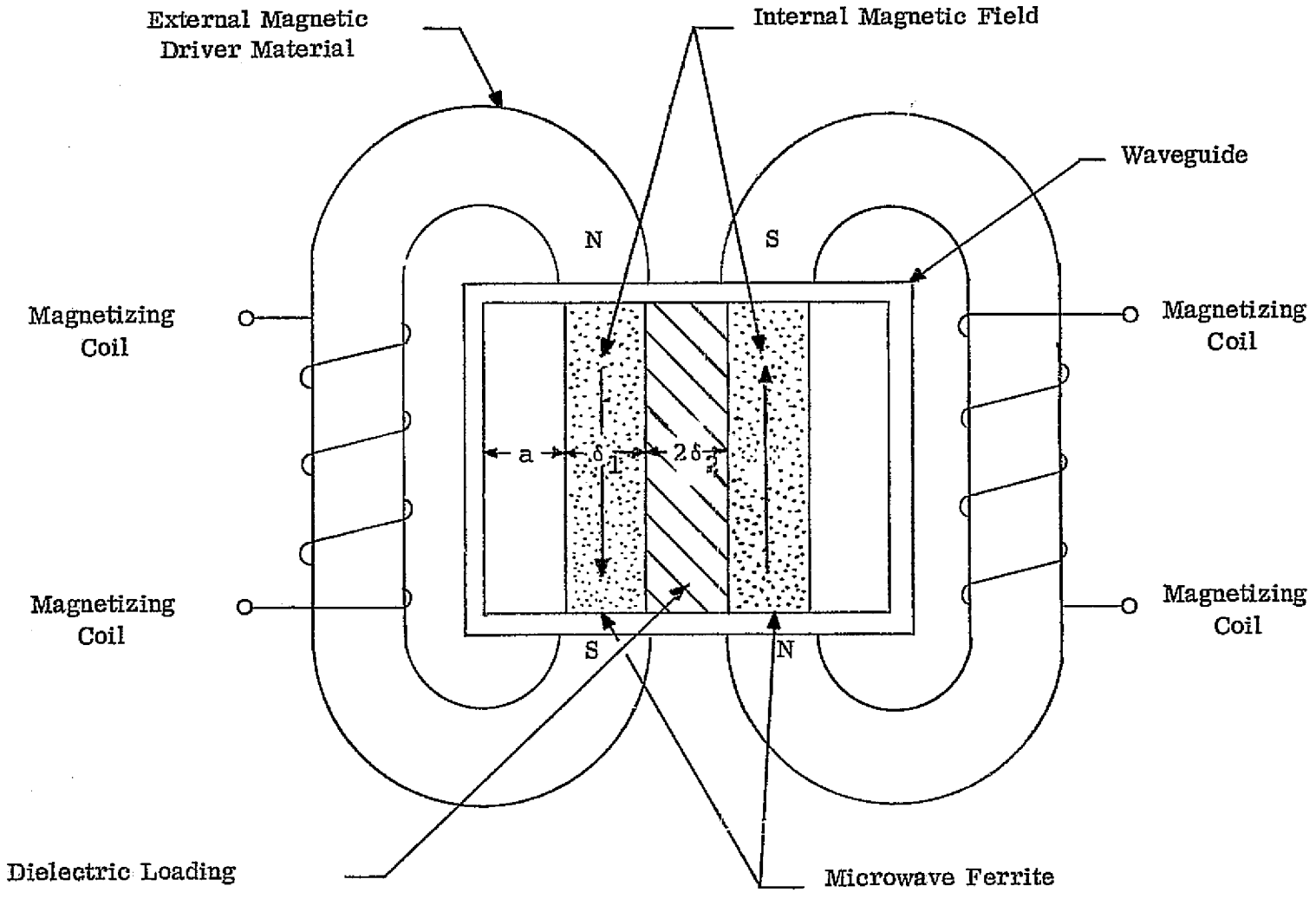

Figure 4 - Nonreciprocal, Oppositely Magnetized, Twin-Slab Ferrite Phase Shifter

equally for propagation in one direction. This interaction will be of a certain magnitude. For propagation in the opposite direction this interaction will be of a different magnitude. The difference in the two magnitudes of interaction is the useable differential phase shift of the twin slab ferrite phase shifter.

Figure 5 is a sketch of the non-reciprocal latching ferrite phase shifter. Note that a closed magnetic circuit is obtained by using return magnetic paths at the top and bottom of the ferrite slabs and that the entire magnetic circuit is composed of the microwave ferrite material itself. Also note that the entire magnetic circuit is located within the waveguide transmission line. The internal d. c. fields in the ferrite toroid are produced by the remanent magnetization of the microwave ferrite material.

Figure 6 is a typical B-H loop of a ferrite material. For current pulses applied to the magnetizing wire in one direction, the internal fields may be considered to be $+B_r$ (B_r is the symbol for remanent magnetization). Application of a current pulse in the opposite direction will result in shifting of the direction of the internal fields to $-B_r$. Differential phase shift is the difference in the insertion phases associated with the $+B_r$ and $-B_r$ magnetic states. It should be pointed out that the ferrite material for this type of operation is always magnetized to either $+B_r$ or $-B_r$, which are the two extremes of the B-H loop. Such operation has certain disadvantages in that these flux states are, in general, temperature sensitive. In addition

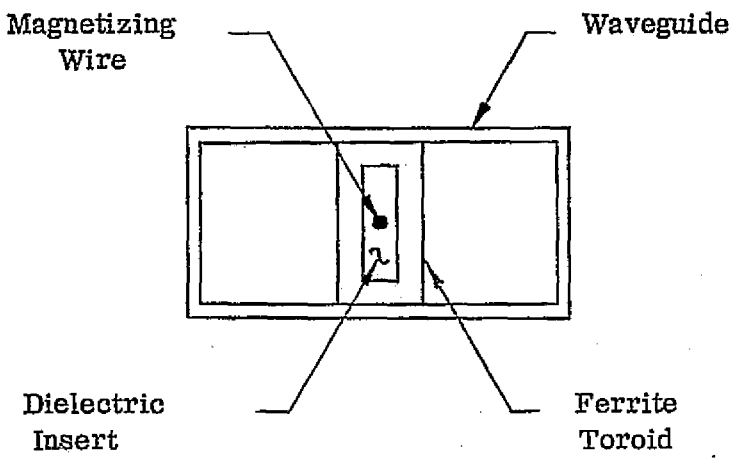

Figure 5 - Cross-Section of Nonreciprocal Latching Ferrite Phase Shifter

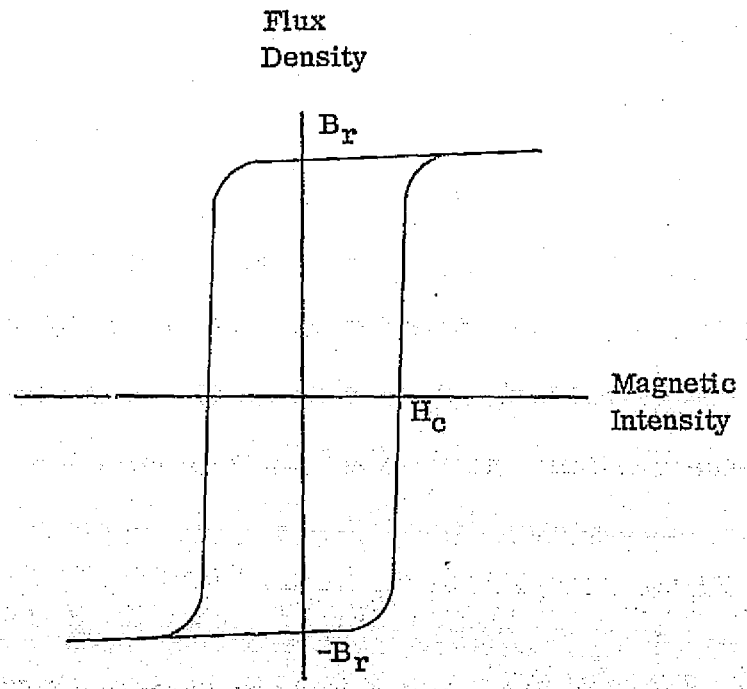

Figure 6 - B-H Loop for a Typical Ferrite Material

variations in magnetic parameters of the ferrite material from piece to piece, or batch to batch, will cause variations in differential phase shift.

A practical device is realized by adjusting the length of the ferrite toroid to yield a required differential phase shift when magnetized between the two remanent states. For use in the High Power Ferrite Microwave Switch this would involve adjusting the toroid length to yield a differential phase shift of 90° when pulsed between $-B_r$ and $+B_r$. However, due to the shortcomings listed above, phase shifter sections which produced more than 90° of differential phase shift were used. These devices were pulsed using the flux-transfer magnetization technique which overcomes these shortcomings. This technique will be described in a later section.

In general, the solution of boundary value problems in devices containing ferrite materials are very difficult to achieve. Fortunately, propagation characteristics of the twin slab oppositely magnetized ferrite phase shifter can be theoretically formulated. Since the latching configuration closely resembles the former device, very good theoretical data can be obtained to predict performance of the latching ferrite phase shifter as a function of material characteristics, material dimensions, waveguide dimensions, etc. This is accomplished in the following fashion. The ferrite tensor permeability is incorporated into Maxwell's equations for the two ferrite slabs. A set of four equations may then be derived, one for each of the four interfaces in the cross-section of the device. These interfaces are

the sidewall of the waveguide, the air to ferrite interface, the ferrite to dielectric interface, and a plane in the center of the dielectric which is equivalent to a mirror image of the second half of the device. The resultant equation that is obtained by solving these four equations is given in Equation 1.

The physical dimensions of the ferrite, dielectric and unloaded sections of the device (as shown in Figure 4) are indicated by the quantities δ_1, δ_2, and a, respectively.

$$\tan (k_a a) = \frac{k_a \left[\frac{k_e}{\rho^2} - j\frac{\beta}{\rho\theta} \cot (k_e\delta_2) \quad \frac{k_m}{\rho}\cot (k_m\delta_1) \cot(k_e\delta_2) \right]}{\left(\frac{\beta^2}{\theta^2} - k_m^2\right) \cot (k_e\delta_2) - \frac{k_m k_e}{\rho}\cot (k_m\delta_1) + j\frac{\beta k_e}{\rho\theta}} \quad (1)$$

The quantities k_a, k_m, and k_e are the transverse wave numbers in the air, ferrite, and dielectric sections of the device. The quanties θ and ρ are functions of the ferrite tensor susceptibility which, in turn, are functions of frequency, internal bias fields, and ferrite magnetic properties. This equation is a transcendental equation where the parameter of interest is β, the propagation constant defining the phase shift through the device. There is one β associated with propagation in one direction, and a second β for propagation in the opposite direction. The difference in these β's is the previously mentioned differential phase shift of the device. By varying the differential parameters in the equation such as dimensions, magnetic

properties, dielectric properties, etc., a host of design curves may be realized. Optimum devices may then be designed with practical considerations of size, and available materials parameters incorporated. This technique was used during the early stages of the program for determining an optimum configuration for the 90° non-reciprocal latching ferrite phase shifter.

Figure 7 is a plot of differential phase shift vs. ferrite slab width for a fixed dielectric width where two different dielectric constant materials were used between the ferrite slabs (ε_r = 12.0 and 1.0). Note that as ferrite slab dimensions are increased there is initially a rapid rise in differential phase shift. As slab width is increased further, a point is reached where very little additional increase in differential phase shift is realized and in fact a reduction in differential phase shift can be observed for further increase in ferrite slab width. Also observe from Figure 7 that the dielectric constant of the loading material has a marked effect on overall differential phase shift and that loading with high dielectric constant materials is desirable. Better than 100% phase shift improvement is achieved when loading the toroid with dielectric material whose dielectric constant is the same as the ferrite (ε_r = 12), in comparison to loading with air (ε_r = 1.0).

Figure 8 more clearly illustrates the dependence of differential phase shift on dielectric loading. This curve is a plot of differential phase shift

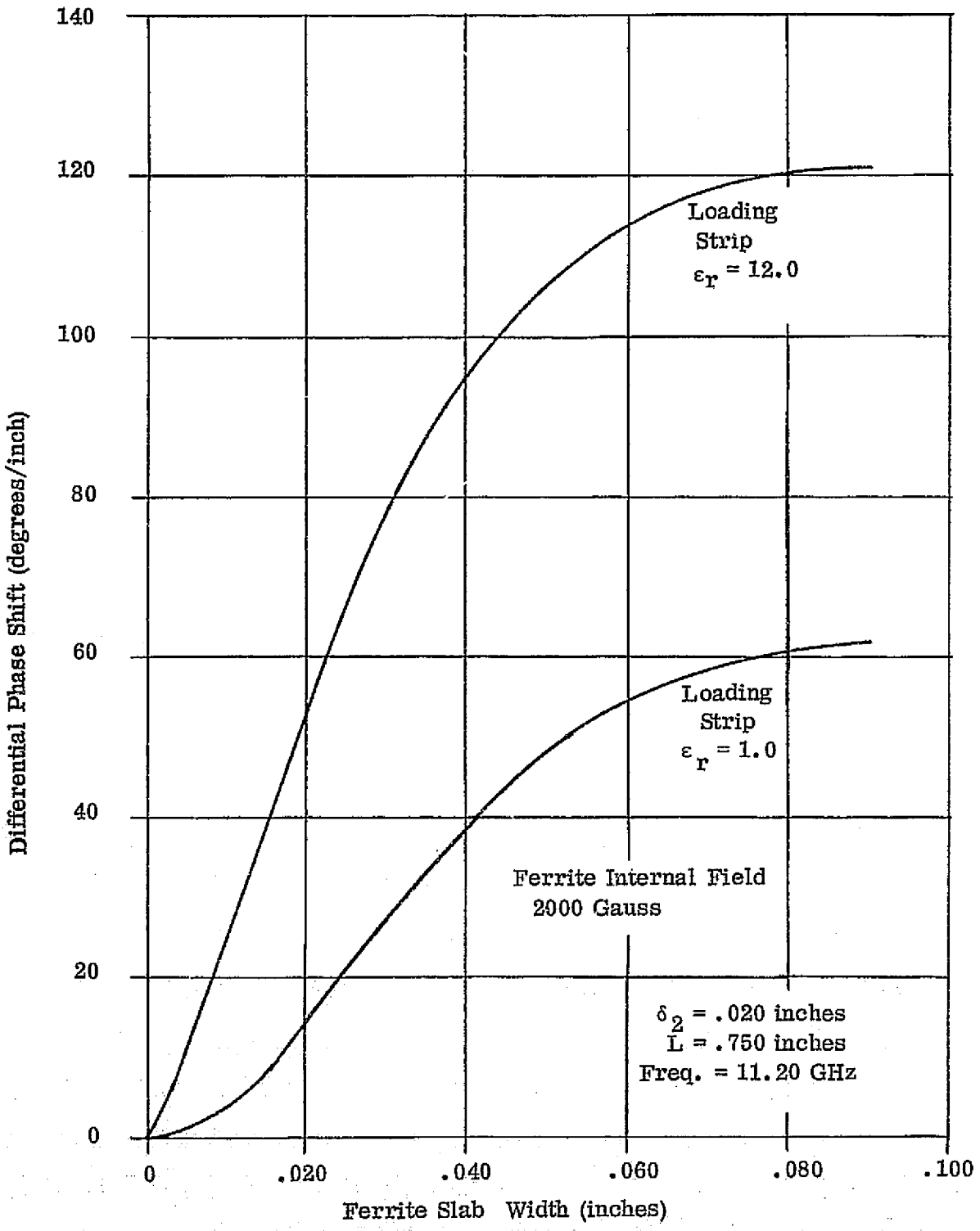

Figure 7 - Differential Phase Shift vs Ferrite Slab Width

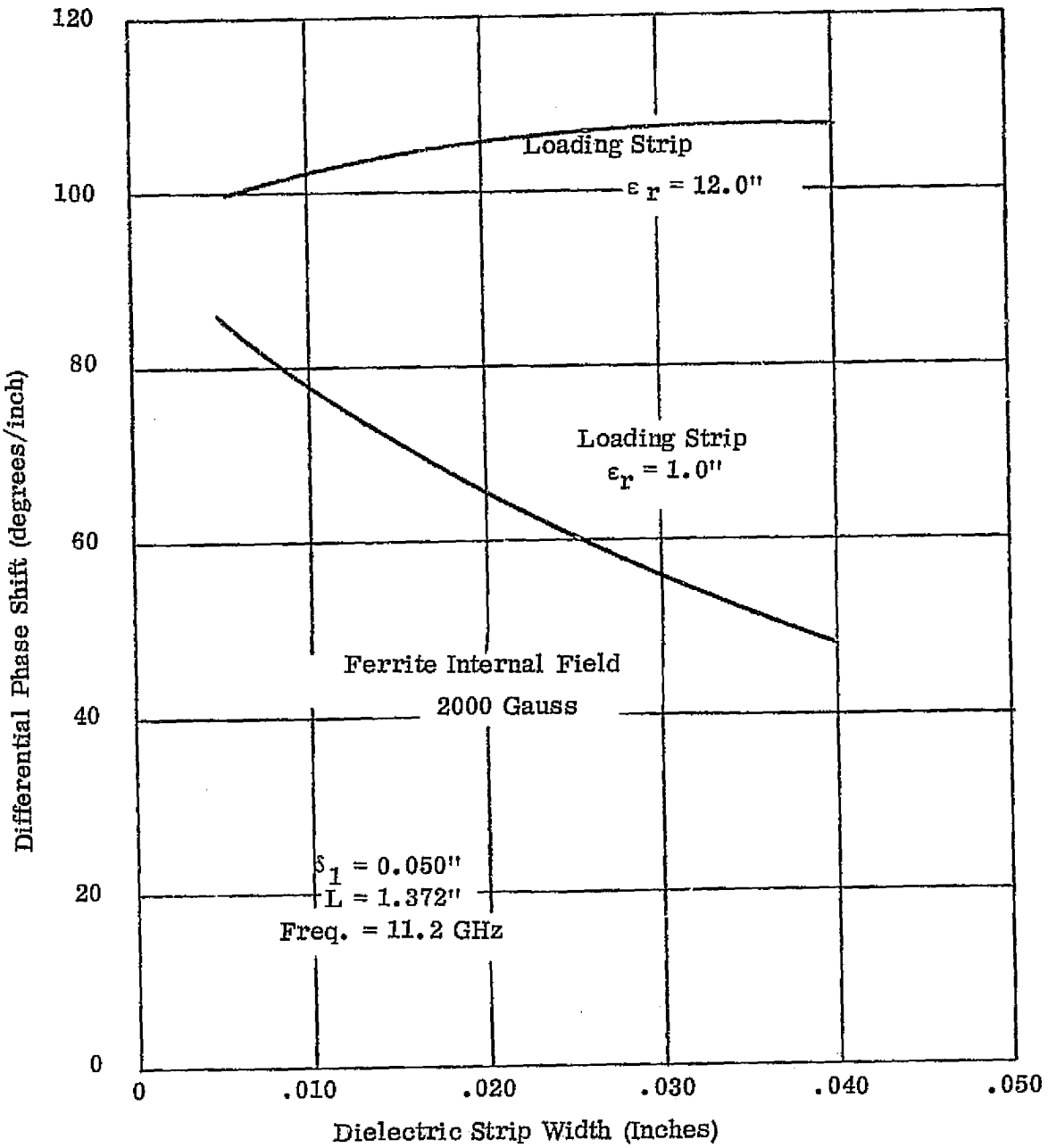

Figure 8 - Differential Phase Shift vs Dielectric Strip Width

as a function of dielectric strip width. Here it is seen that for a dielectric material whose dielectric constant is unity (air), differential phase shift starts at some initial value and falls off rapidly with increased ferrite slab spacing. For higher dielectric constant materials differential phase shift is seen to be relatively independent of slab width. Hence an optimum design may be realized if the space between the two ferrite slabs is loaded with dielectric material. Such design procedures have been used and excellent correlation between theory and experiment has been achieved. Slight modifications must be made to consider the decrease in measured data brought about by the ferrite return magnetic paths required for achieving latching action. In general, however, correlation within 10% of predicted performance can be obtained. Figures 7 and 8 were presented to indicate that design data for optimum latching devices can be computed and that this data may be used to achieve optimum designs.

C. FLUX-TRANSFER DRIVER

As mentioned earlier, operation in the digital latching ferrite configuration has several definite disadvantages. The principal disadvantage is that this method of magnetization is temperature sensitive. The flux-transfer magnetization technique overcomes this disadvantage and has several other major advantages. These include insertion phase compensation, excellent repeatability, while maintaing all the advantages of the standard latching technique.

The basis for realization of the flux-transfer technique is the linear variation of differential phase shift as a function of internal flux density within the ferrite toroid. By pulsing a well controlled flux change in the toroid, a proportional change in differential phase shift may be obtained. Since the ferrite toroid is a closed magnetic circuit, and has hysteresis properties, the amount of switch flux will be maintained or latched in the ferrite itself, even though the material is not in a totally saturated state.

The flux-transfer concept may be predicted from Faraday's law of induction, $E = \frac{d\phi}{dt}$; where E = induced voltage, ϕ = magnetic flux, and t = time. Simple manipulation of this equation yields

$$d\phi = E\,dt$$

$$\int_{\phi^1}^{\phi^2} d\phi = E \int_{t_1}^{t_2} dt \qquad (E \neq f(t))$$

$$\Delta\phi = E\ \Delta t$$

Upon integrating as done above, it can be seen that differential flux change is the integral of induced voltage over a given period of time. If this voltage is a controlled pulse where the pulse magnitude is constant, the induced flux changes are the voltage-pulse width products. Hence, by applying well controlled voltage pulse to the single magnetizing wire of a latching ferrite phase shifter, well controlled flux changes may be obtained.

When using this magnetization mode it is very important that the driver circuits appear as true voltage sources with very low internal impedances. This is important since IR voltage drops within the circuits themselves would produce errors in the above theoretical assumptions as well as the realized induced flux changes. Fortunately, high current transistor circuits when operated in the saturated mode appear as very low impedance voltage sources and are ideally suited for flux-transfer circuit applications.

Figure 9 illustrates the flux-transfer technique in terms of the B-H loop characteristics of the ferrite toroid. In effect, the latching ferrite phase shifter may be considered to be an analog latching device with the capability of producing any phase between the two phase limits that have been designed into the device. For the High Power Ferrite Microwave Switch the phase limit must be greater than 90°.

The main advantage of the flux-transfer magnetization technique is its intrinsic temperature compensation. The magnetic properties of all ferrite and garnet materials are temperature sensitive to one degree or another. Even when using the most temperature sensitive ferrite the flux-transfer technique adjusts automatically for parametric temperature variations. This enables the use of certain magnesium-manganese ferrite materials, as opposed to more expensive garnet materials, even though the former exhibit poorer temperature characteristics. The advantages of

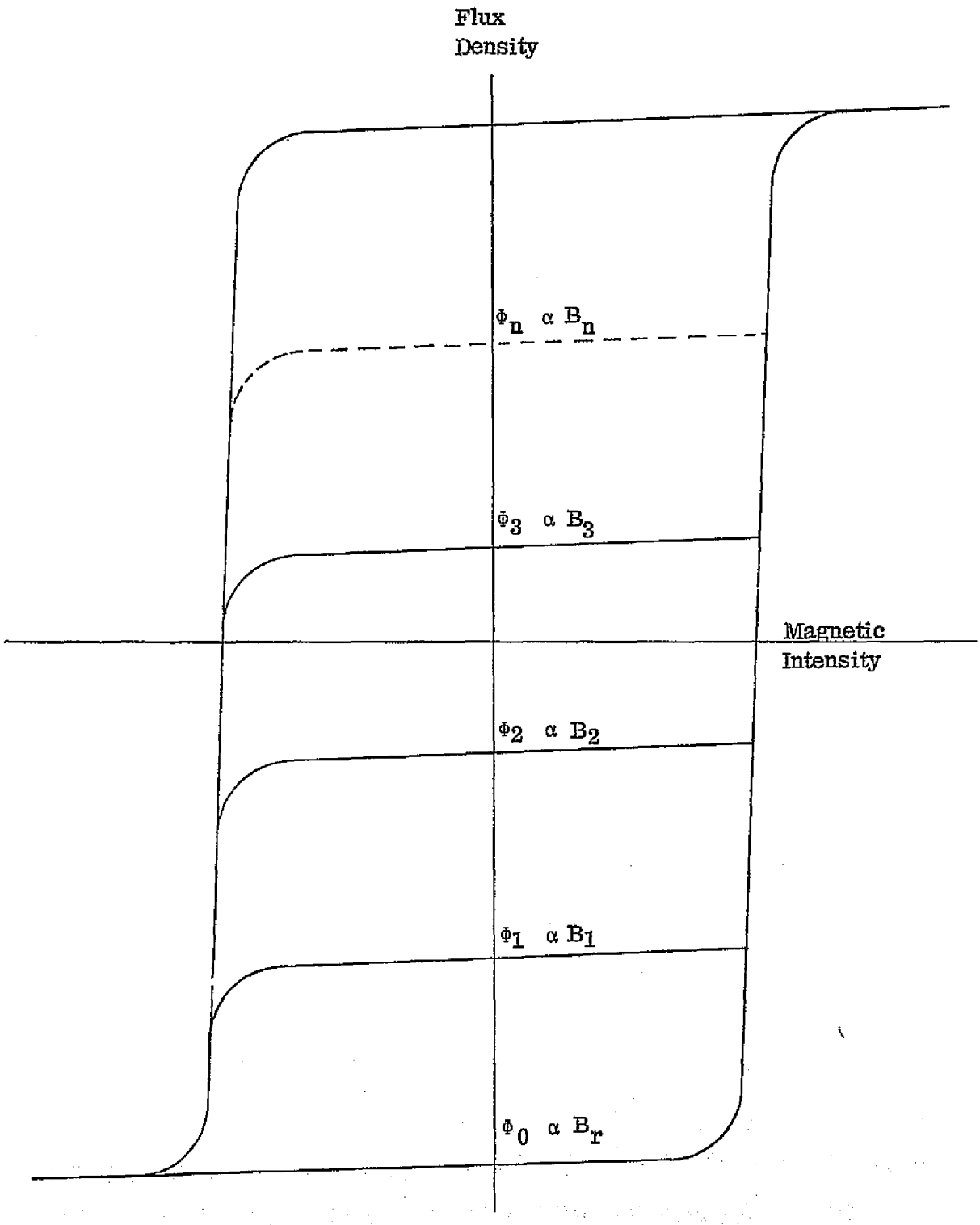

R. F. Phase Shift is Proportional to Internal Flux Density

Figure 9 - B-H Loop Indicating Flux-Transfer Concept

using these ferrites are not only based on cost, but on their superior square loop and magneto-striction properties. The intrinsic temperature compensation is the result of the linear relationship between differential phase shift and internal flux density. Even though the two extreme remanent magnetizations of the ferrite are temperature sensitive, changes in internal magnetization are independent of temperature provided these changes are limited to values less than the difference between the two extremes. In other words, if a device is constructed which will always yield at least 90 degrees of differential phase shift over the entire required temperature range, temperature compensation will be automatically realized. Hence, the length of this device is adjusted such that even at the most extreme temperatures, 90 degrees of differential phase shift is available. This implies that at room temperatures, the device may be capable of more than 90 degrees, but at no temperature will it yield less than this number. Measurements have been made which indicate that less than $\pm$ 5 degrees of differential phase shift variation can be achieved over temperature ranges from -55 to +90°C.

A second advantage of the flux-transfer magnetization technique is that variations in magnetic and dielectric properties of the materials used may be compensated by appropriate "zero phase" adjustments. This means that even though large insertion phase errors may exist between two units, "zero phase" adjustments may be made within the driver circuit of each

unit. These adjustments can be applied at the input of the driver circuit during initial test evaluations. Once these "zero adjustments" are made both phase shifter units are set to yield equal "zero phase" insertion phases. This compensation technique is a big advantage over standard latching devices since material variations may be compensated without any dimensional adjustments.

III INITIAL DESIGN DATA AND TEST RESULTS

A. Latching Ferrite Phase Shifter

Design of the latching ferrite phase shifter involved the use of the theoretical curves discussed earlier in this report. These curves were used to define the electrical magnetic and dimensional parameters of the 90° phase shifter section. In addition, major consideration was given to define a cross-sectional configuration that would inhibit the propagation of higher order modes. The orthogonal modes that propagate in inhomogeneously loaded waveguide are called Longitudinal Section Magnetic and Electric modes (abbreviated LSM_{mn} and LSE_{mn}). The LSM modes contain no magnetic r.f. fields perpendicular to the air-dielectric interface while the LSE modes contain no electric r.f. fields perpendicular to the air-dielectric interface. The dominant mode that propagates in non-reciprocal latching ferrite phase shifters is the LSE_{10} mode. This mode is similar to the TE_{10} mode for propagation in unloaded rectangular waveguide except that the E fields are highly concentrated in the ferrite/dielectric loaded portion of the device. It can be shown that no practical ferrite phase shifter may be constructed which does not allow at least one higher order mode to propagate, namely the LSE_{11} mode. This mode may be prevented from propagating by maintaining good symmetry within the device. By specifying tight mechanical tolerances of the ferrite toroid, dielectric insert, and magnetizing wire, the required symmetry can indeed be achieved. The next order mode that can propagate in these devices is the LSM_{11} mode. This mode is characterized by a horizontal E field and can only propagate in the vicinity of the ferrite

portion of the device. If energy does couple to this mode, it tends to resonate at that frequency where the length of the ferrite toroid is an integral number of half wavelengths. Such resonance produces sharp loss spikes which can get as high as 3 to 4 db. The existence of such spikes in the High Power Switch would cause considerable heating as well as loss of RF power. It was therefore necessary to design the ferrite cross-section of the switch so that the LSM_{11} mode may not propagate.

The propagation characteristics of the LSM_{11} mode were formulated using Hertz potential notation and deriving the wave equation for ferrite/dielectrically loaded waveguides. A transcendental equation was generated which contained the transverse wave number associated with the LSM_{11} mode. This wave number was calculated using a number of arithmetical and graphical techniques. The wave number was then used to calculate the cutoff frequency of the LSM_{11} mode. The first consideration for the phase shifter cross-section consisted of a 0.375" x 0.390" metal waveguide containing a 0.120" x 0.375" ferrite toroid centrally located within the metal waveguide. Upon calculating the transverse wave number and corresponding cutoff frequency for this configuration, it was found that the LSM_{11} mode could propagate in the band of interest (the cutoff frequency was calculated as 11.5 GHz which is below the operating frequency of the switch). It was then necessary to evaluate other cross-sections. After four more such analyses, a suitable configuration was defined which has the cutoff frequency of 12.4 GHz. Hence, the LSM_{11} mode could not propagate in the device with this final cross-section. This cross-section

is 0.375" x 0.390" waveguide with a ferrite toroid whose width and height are 0.100" x 0.375". Based on this series of calculations, ferrite toroids were order with the previously mentioned outer dimensions and an internal slot dimension of 0.030" x 0.305". Ceramic inserts made up of Trans-Tech material D-13 were also ordered to fit into the slots in each ferrite toroid. The ferrite material that was ordered was Trans-Tech TT1-105 which is a magnesium manganese ferrite that has exceptionally good square loop characteristics for latching devices.

A thermal analysis was conducted to determine the exact temperature rises that might be anticipated in the ferrite section of the device. This analysis started with the generalized partial differential equation governing heat flow in solids and was then converted to be compatible with the waveguide-ferrite cross-sectional configuration. Steady state heat conditions were assumed and the first calculation was based on heat transfer to the top and bottom walls of the waveguide only. The thermal characteristics of the TT1-105 ferrite and the dimensions mentioned in the previous paragraph were used. This initial analysis indicated that a maximum temperature of 85.6°C above the boundary temperature of the waveguide might be generated assuming a power flow of 1,000 watts through the ferrite with an accompanying 0.15 db of attenuation. This maximum temperature rise would occur halfway up the ferrite (at 0.187" from the top or bottom wall).

It was therefore concluded that beryllia heat sinks located on the sides of the ferrite toroids would be required to remove heat to the sidewalls of the device. A two-dimensional thermal analysis was conducted to determining the maximum temperature that might result in the ferrite portion of the switch under full power operation.

The two-dimensional model that was used is shown in Figure 10.

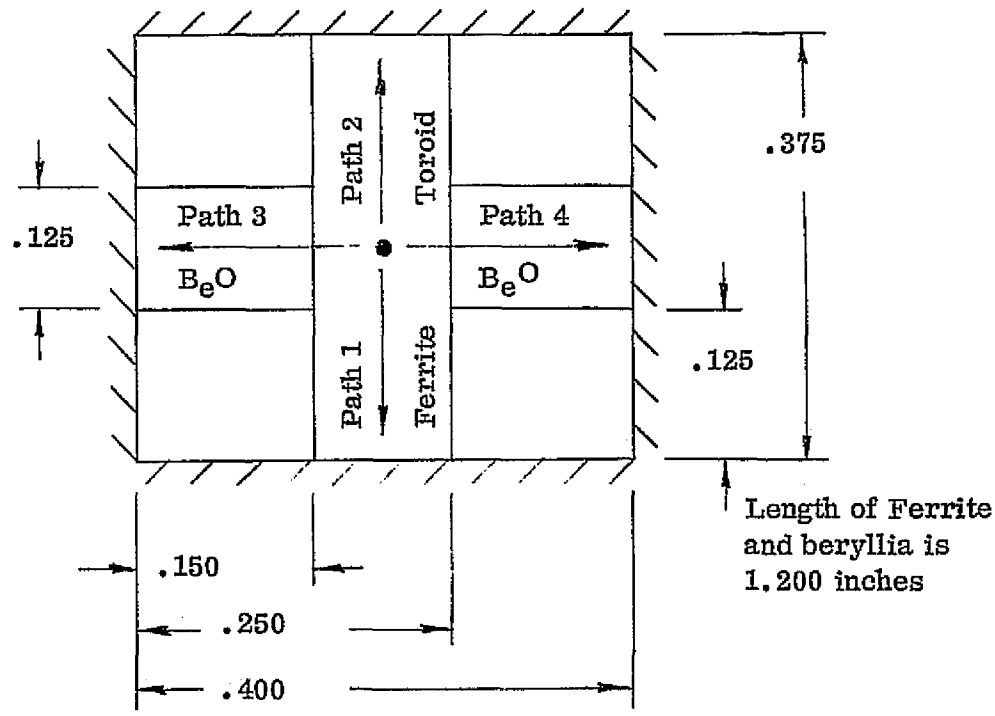

Figure 10 - Phase Shifter Cross-Section Used for Thermal Analysis

The fourpaths of heat flow from the ferrite to the top walls and sidewalls of the phase shifter consist of flow through the ferrite (paths 1 and 2), and flow through the beryllia heat sinks (paths 3 and 4). Beryllia is a low loss,

dielectric material ideally suited for heat conduction in microwave devices. This is due to the fact that it has a reasonably low dielectric constant as well as a high thermal conductivity. Its thermal conductivity exceeds that of brass.

It was assumed that 35 watts of power would be dissipated in a ferrite section of the switch and that this power is generated along a line source centrally located within the ferrite. This is a "worst case" type of assumption and in actuality heat is generated almost uniformly throughout the entire cross-section of the ferrite toroid. It was also assumed that the heat was generated uniformly along this line source throughout the entire length of the ferrite toroid.

The thermal resistance or impedance in a thermal conductor may be given by the following equation:

$$R_T = \frac{\rho L}{A}$$

where R_t is the thermal drop across a length of conduction in °C/Q

ρ = the thermal impedance factor for a given material in °C/W/in^2/in

L = the length of the thermal path

A = the cross-sectional area of the thermal path.

Note that this formula is very similar to that used for calculating electrical resistance in a bulk conductor material. The parallel path impedances for the four paths leading from the center of the toroid to the sidewalls of the

phase shifter may be calculated using the above formula and are as follows:

$$R_{T1} = R_{T2} = 6.0° \text{ per watt}$$

$$R_{T3} = R_{T4} = 1.433° \text{ per watt}$$

Since these thermal paths are all in parallel, the equivalent thermal resistance for the configuration shown in the figure may be calculated using the following formula:

$$\frac{1}{R_{(total)}} = \frac{1}{R_{T1}} + \frac{1}{R_{T2}} + \frac{1}{R_{T3}} + \frac{1}{R_{T4}}$$

Hence $R_{(total)} = 0.578°$ per watt.

The total thermal rise from the sidewalls and/or the top walls of the phase shifter to the center of the ferrite should be 20.23°C. This is considerably less than the 85°C discussed earlier and indicates that relatively straightforward cooling techniques can be used to remove the heat that will be dissipated in the ferrite portions of the device. It is interesting to note the affect of removing thermal paths T1 and T2 from the calculations. Even if this is done, R_T is only 0.716° per watt which would yield a maximum thermal rise of only 26.5°C. This indicates the effectiveness of the beryllia cooling technique for removing heat from the ferrite sections of the device. When high power measurements were made it was found that a maximum thermal rise of approximately 25°C occurred on the ferrite at rated power. This agrees quite well with the calculations made above.

Measurements were made to determine the differential phase shift produced by a 1.5" ferrite toroid with cross-sectional dimensions as follows: 0.100" wide and 0.375" high (which is the full height of WR 75 waveguide) with slot dimensions of 0.030" wide by 0.305" high. The slot was loaded with a ceramic insert of relative dielectric constant 13. This is the configuration discussed earlier and is optimized for suppression of most higher order modes while providing efficient differential phase shift per unit length. Measurements made on a section of this phase shifter configuration indicated that 165° of total differential phase shift was available from the 1.5" long section. A total of 90° of differential phase shift is required for switch operation. The device was not shortened proportionately because the flux transfer magnetization technique, which was used to drive the switch, requires more than 90° of maximum phase shift. A room temperature phase shift of 138° was used which resulted in a section 1.25" long. This guaranteed proper performance at the extreme high temperature operating point of +85°C.

Matching sections were designed to achieve low VSWR operation into and out of the phase shifter sections. Initial transformers were designed using rexolite which has a relative dielectric constant of 2.54. For this material the width of the matching transformer was approximately 0.162" wide, which is practical from a mechanical standpoint. Upon reviewing the characteristics of rexolite however, it was found that this material

ages with time and also is vulnerable to deterioration from radiation. It was therefore concluded that rexolite would not be used in the High Power Microwave Ferrite Switch. The first alternative was to use a ceramic. Upon reviewing the characteristics of available ceramics for microwave applications a material with a dielectric constant of 6.3 could have been used. However, at the frequency of operation of the High Power Switch the width of a transformer using this material would be approximately 0.02" wide which would make the transformer fragile and susceptible to breaking in a severe vibration environment. Further research indicated that fused silica was suitable for a space environment and since it has a relatively low dielectric constant, (3.8), it would yield a configuration wide enough to provide good mechanical integrity. The width that was finally used was approximately 0.070" wide.

Detailed measurements on the ferrite phase shifter sections of the High Power Microwave Switch were initially conducted at low power. These measurements were made with the beryllia heat sinks required to provide a thermal path from the ferrite toroid to the waveguide sidewalls. The following data was measured: VSWR vs. frequency, insertion loss vs. frequency, differential phase shift vs. frequency, and differential phase shift vs. temperature.

Figure 11 is a plot of the VSWR vs. frequency of the phase shifter. Note that throughout the band from 11.7 to 12.3 GHz the VSWR maximum is

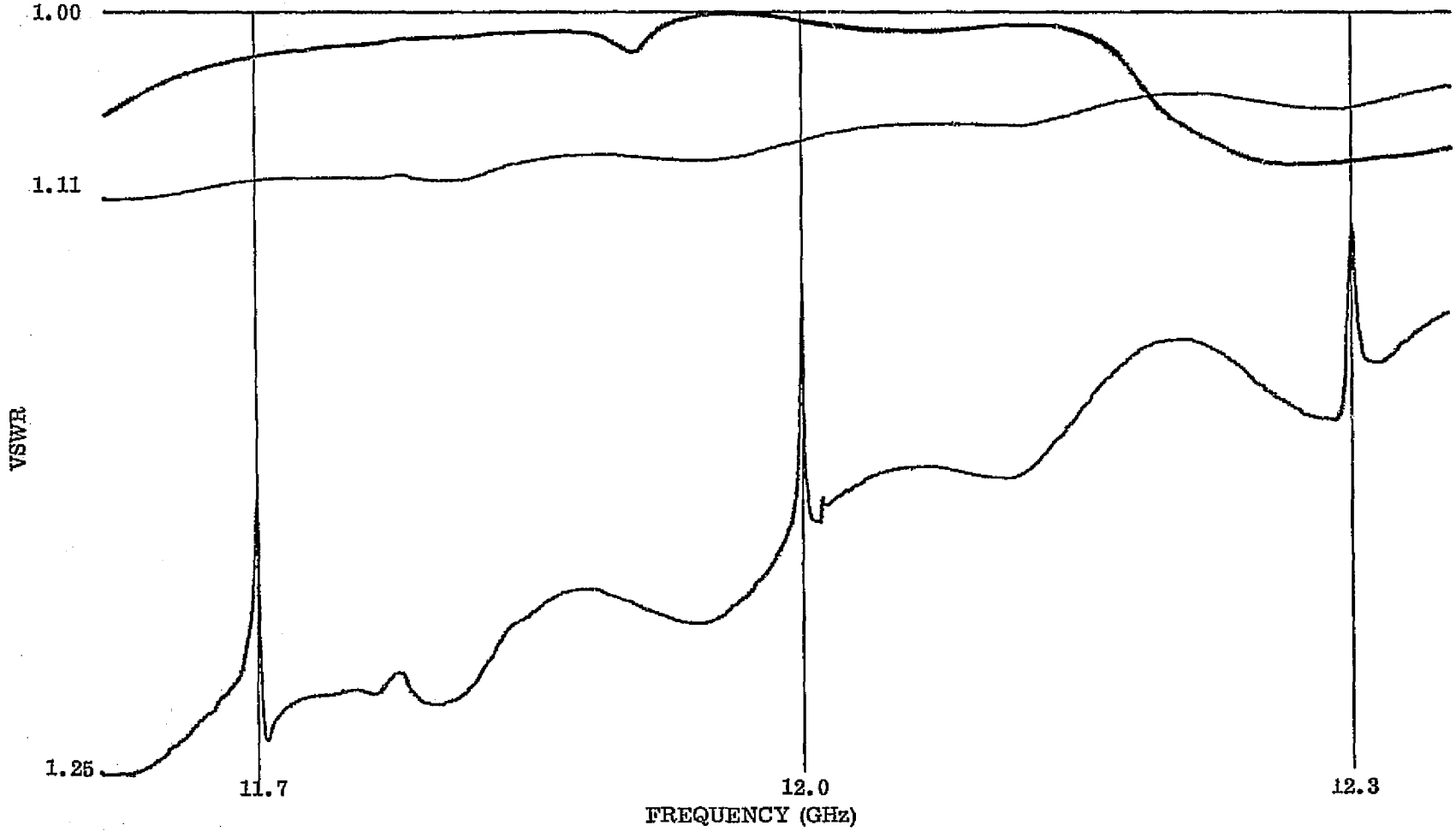

FIGURE 11 - VSWR VS FREQUENCY OF FERRITE PHASE SHIFTER
FOR HIGH POWER MICROWAVE SWITCH

approximately 1.15:1 and in the vicinity of the center frequency of the switch (11.75 GHz) it is vertually a perfect match. These measurements were made on a completed phase shifter and indicate the total mismatch associated with both the input and output interfaces of the phase shifter. This data illustrates that the phase shifters will contribute almost no reflection when used in the high power switch. It was expected that the total VSWR produced by the high power switch would be easily kept under 1.15:1.

Figure 12 is a plot of insertion loss vs. frequency for the phase shifter and it indicates that over the entire band the insertion loss falls between 0.2 and 0.25 db. Some of the ripples on the data, particularly close to 12.3 GHz, were caused by the coupling of energy to some high order modes which may propagate. However, in the final device, when the unit was assembled with all magnetizing wires pulled tight and all covers clamped tight, no such coupling occurred. The two curves indicated in the figure are for the 0° and maximum phase states and represent the losses that were expected to occur when the phase shifters were incorporated in the high power switch. It was expected that the maximum insertion loss for an entire switch would be 0.3 db since the input and output couplers, in general, have less than 0.05 db of loss. This was indeed realized.

Figure 13 is a curve of maximum differential phase shift vs. frequency from 11.7 to 12.3 GHz. Note that the phase variation is $\pm$ 1° over the full band. The driver circuits that were used in the final switch set the

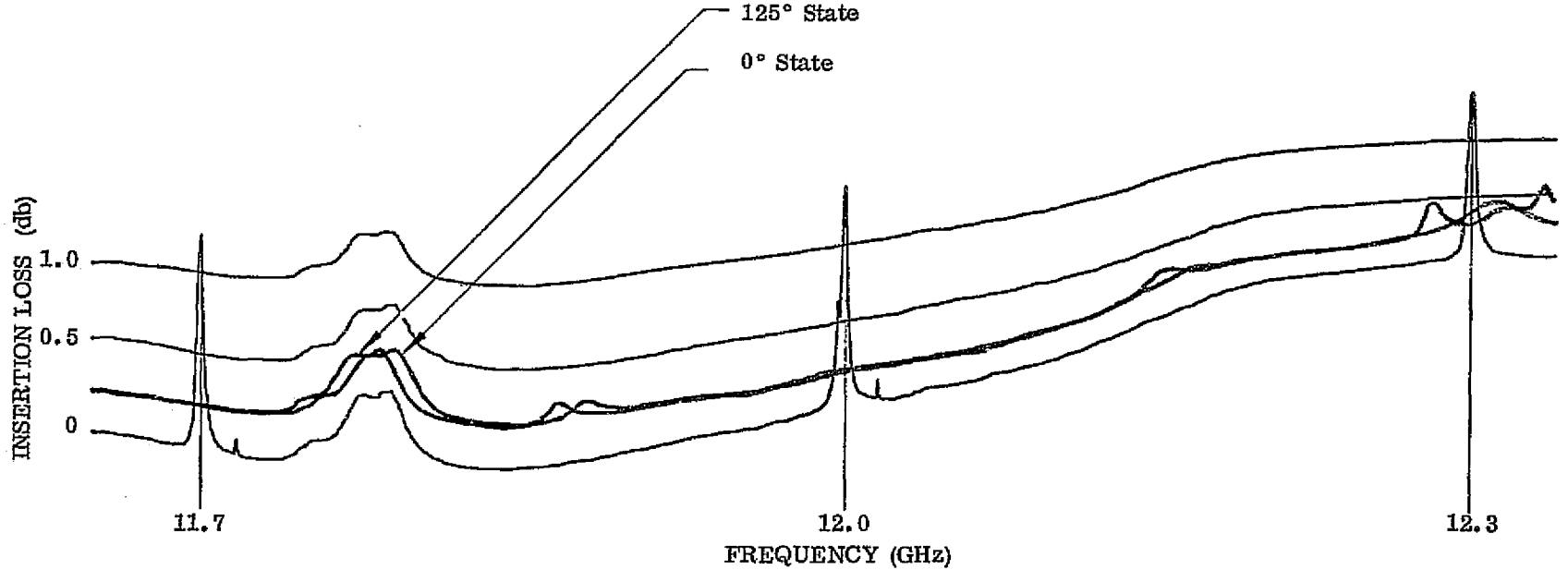

FIGURE 12 - INSERTION LOSS VS. FREQUENCY OF FERRITE PHASE SHIFTER FOR HIGH POWER MICROWAVE SWITCH

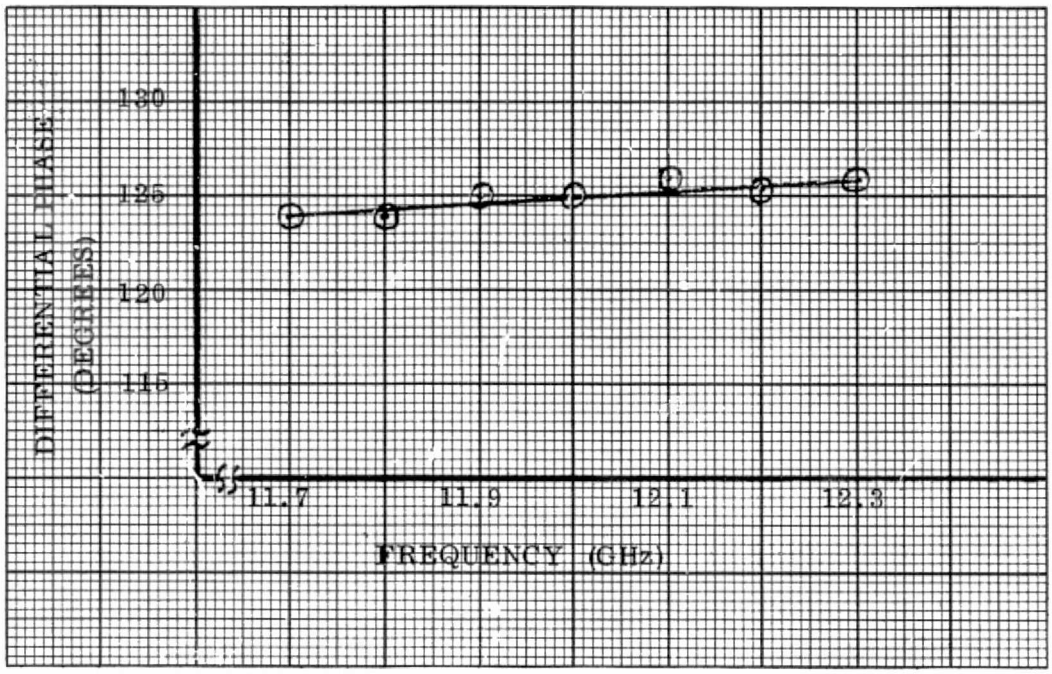

Figure 13 - Maximum Differential Phase Shift vs. Frequency of High Power Switch Phasor

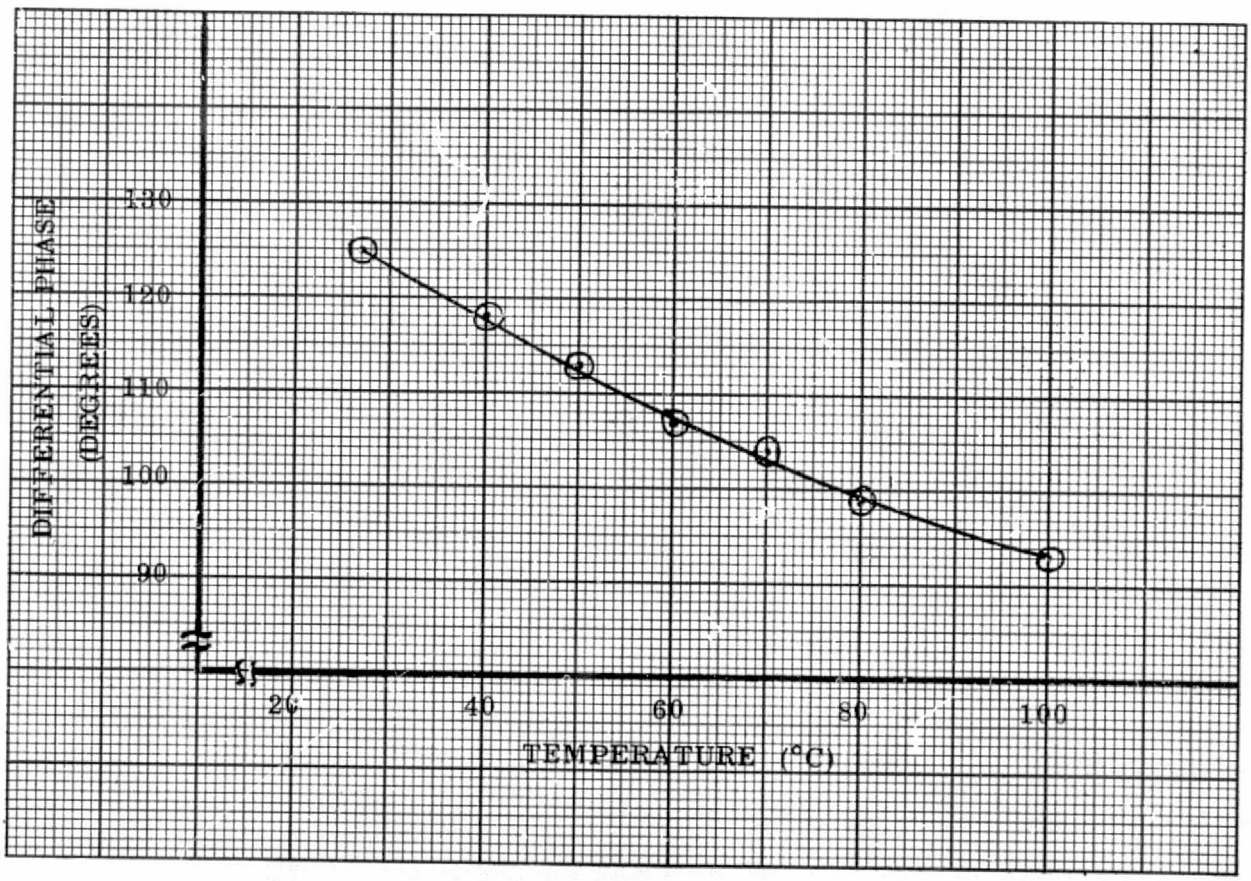

Figure 14 - Maximum Differential Phase Shift vs. Temperature of High Power Switch Phasor

differential phase shift to 90° rather than a full, saturated, 125°. The frequency dependence of the phase when set to 90° was even less than the maximum indicated in the curve. This meant that less than $\pm$ 1° of phase error occurred over the frequency range which, in turn, implies that better than 30 db of isolation should be achieved and, in fact, 40 db of isolation is feasible. Final measurements on the High Power Microwave Ferrite Switch verified that better than 30 db of isolation was achieved across the entire band.

Figure 14 is a curve of maximum differential phase shift vs. temperature from room temperature up to 100°C. Note that the maximum differential phase shift goes from 125° at room temperature to a low of 93° at 100°C. This means that at least 90° of phase is available to perform the switching function in the high power switch. Since the cold plate that the switch is mounted on will be maintained at a maximum temperature of 50°C, it was felt that no problems as far as temperature is concerned would be experienced. The anticipated temperature rise in the ferrite when operated at full power was approximately 25° so that the maximum temperature anywhere in the device was expected to be about 75°C.

B. Electronic Driver Circuit Design

Each High Power Microwave Ferrite Switch requires an Electronic Driver Circuit to program the two ferrite phase shifters for achieving required switch operation. As discussed earlier, the flux-transfer magnetization technique was used. The driver and logic circuitry that was designed and built satisfied all specification requirements. Switching speed and switching rate performance exceeded the requirement by more than an order of magnitude.

Figure 15 is a block diagram of the complete logic and dual driver circuitry built for each switch. The two input blocks consists of a Position Memory Flip-Flop, and an Update Generator. The input position command data is applied to the Position Memory Flip-Flop while the update rate and activate inputs are applied to the Update Generator. The outputs of both of these circuits are applied, in parallel, to an Enable Steering Circuit and a Leading Edge Differentiator. The output of the Leading Edge Differentiator, in turn, is applied to a Timing Generator which generates a reset pulse and a set trigger pulse. The reset pulse and set trigger pulse with the enable lines from the Enable Steering Circuit is fed into a set of AND gates which properly program the two high current driver stages for achieving the desired switch position.

A typical sequence for achieving a given switch position is as follows: Application of a 5-volt level signal to the Position 1 input of the Position Memory Flip-Flop results in the generation of a 5-volt level to the

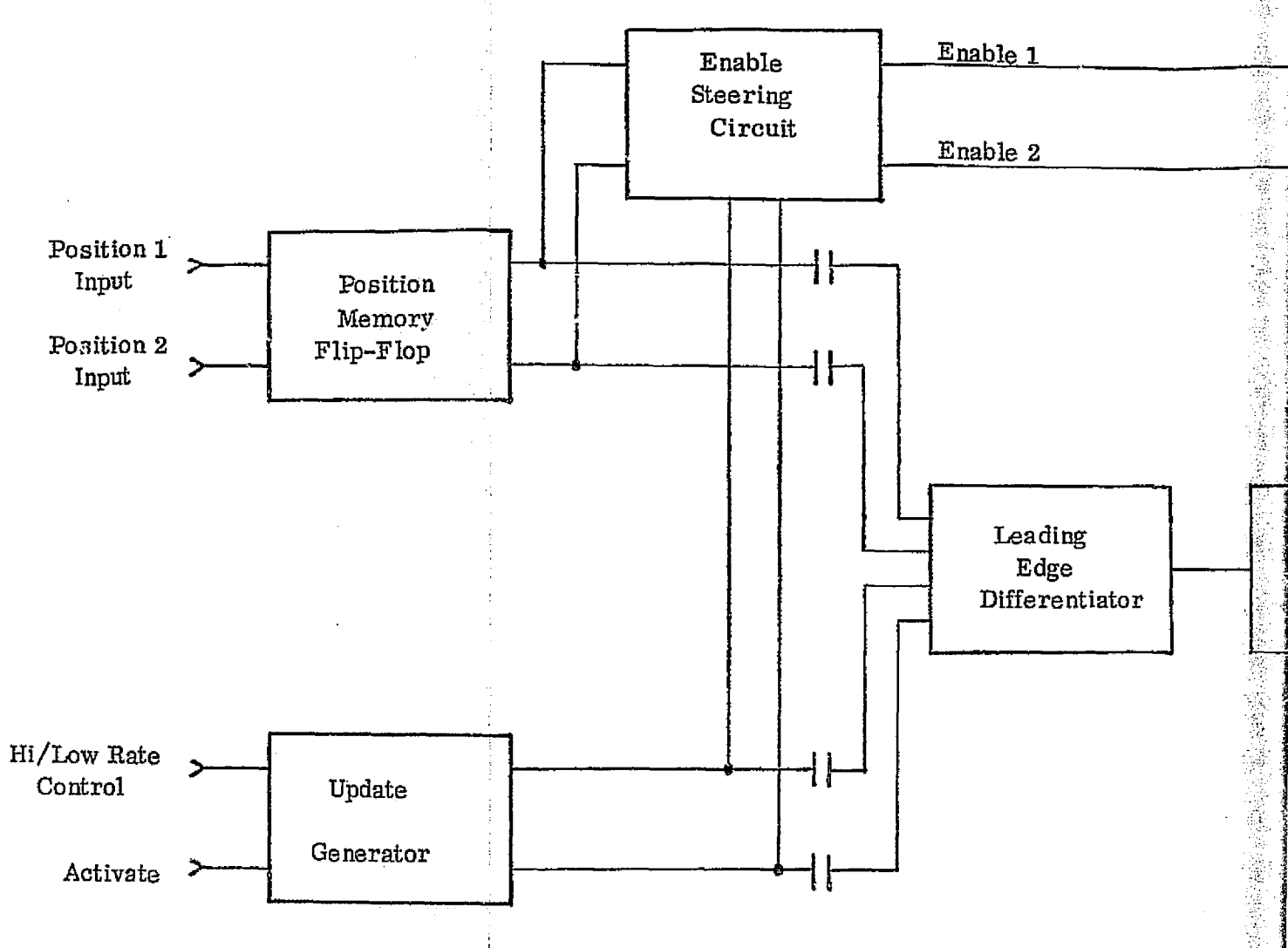

Figure 15 - BLOCK DIAGRAM OF ELECTRONIC DRIVE

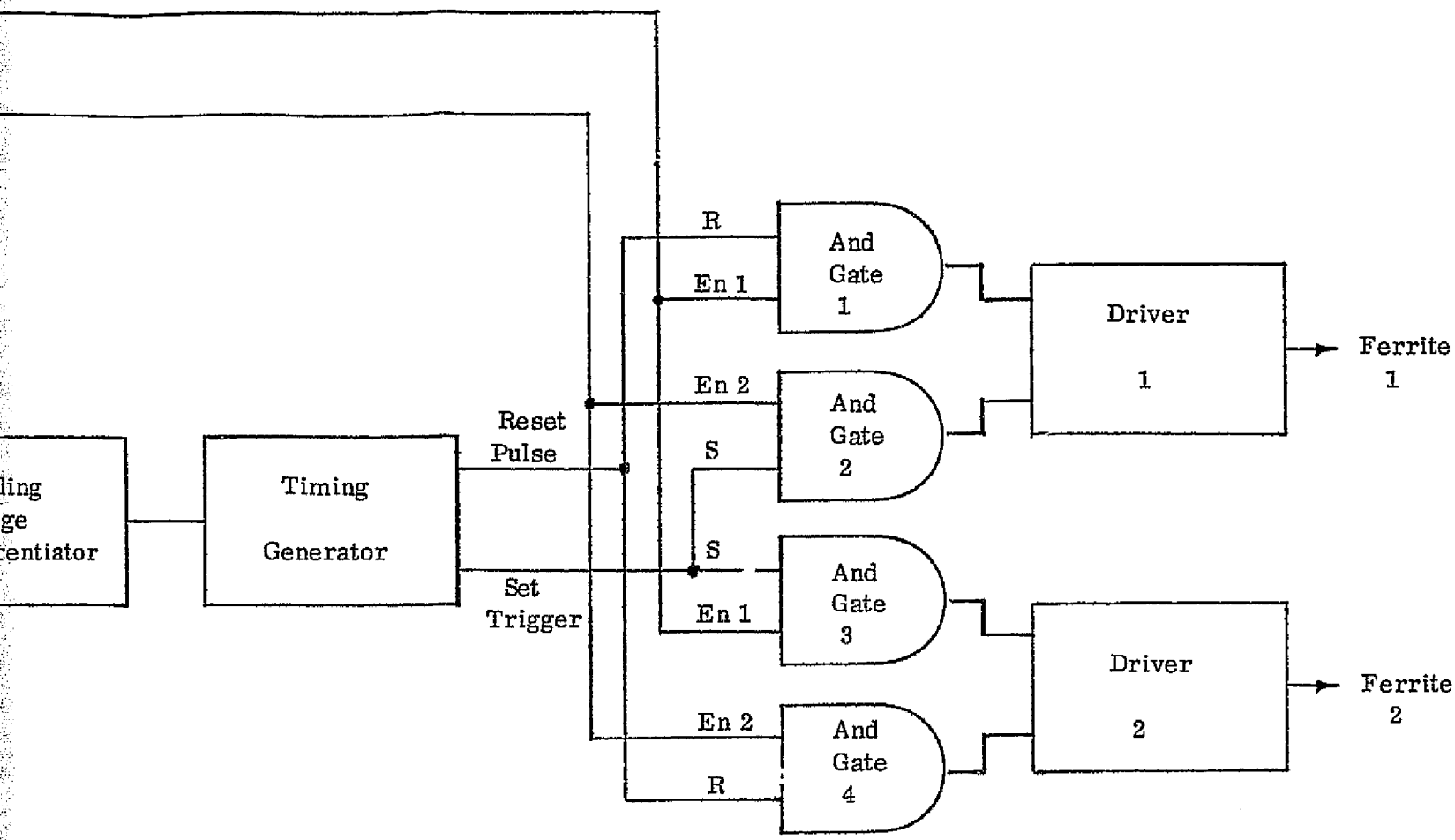

LECTRONIC DRIVER CIRCUIT FOR HIGH POWER MICROWAVE FERRITE SWITCH

Enable Steering Circuit as well as the generation of a pulse to the Leading Edge Differentiator. The Leading Edge Differentiator triggers the Timing Generator which puts out, in parallel, a reset pulse and set trigger pulse. The Enable Steering Circuit creates a 5-volt level on the Enable 1 Line and a 0-volt level on the Enable 2 Line. The 5-volt level from the Enable 1 Line enables AND Gates 1 and 3. Hence, the reset pulse output of the Timing Generator which is applied to AND Gate 1 is directed to Driver 1 and the set trigger pulse output of the Timing Generator which is applied to AND Gate 3 is directed to Driver 2. As a result, the ferrite in Phase Shifter 1 is put into a reset 0° differential phase state while the ferrite in Phase Shifter 2 is set to a 90° differential phase state. The set pulsewidth is determined by a manually adjusted control within Driver Circuit 2 and is adjusted to generate exactly 90° of differential phase shift in Phase Shifter 2.

To set the High Power Microwave Ferrite Switch to Position 2, a 5-volt level signal is applied to the Position 2 Input. This causes all of the subsequent circuitry to create the same signals as before, except that the Enable Steering Circuit creates a 5-volt level on the Enable 2 Line whereas the Enable 1 Line is at the 0-volt level. Since the Enable 2 Line is connected to AND Gates 2 and 4, a set trigger pulse is now directed to Driver 1 while a reset pulse is directed to Driver 2. Hence, Phase Shifter 1 is set to a 90° while Phase Shifter 2 is reset to 0°.

If a 5-volt command signal is applied to either the Position 1 or the Position 2 Inputs of the Position Memory Flip-Flop when the circuit is in the state commensurate with that input, no circuit activity occurs since the High Power Microwave Ferrite Switch would already be in the position that is being called for. Therefore, only a change in position state activates the electronic circuitry. A schematic diagram of the Electronic Driver Circuit is given in Figure 16.

The Update Generator is used to cycle the High Power Microwave Ferrite Switch in the event that position commands do not occur at regular intervals. The purpose of the update cycle is to overcome any switch drift caused by long term thermal or magnetic interference. Two update rates have been provided; one is at one update every five seconds while the other is a rapid update of approximately 1,000 updates per second. This latter update rate is really provided so that the device may be observed in a free run oscillating switching mode independent of the inputs to the Position Memory Flip-Flop. The Activate input is provided so that the update cycle may be manually initiated at any arbitrary rate dictated by an operator or even an external activating circuit. The Update Generator performs a function similar to the Position Memory Flip-Flop except that it generates a pair of triggers which causes the Enable Steering Circuit and the Timing Generator to create two rapid switch position changes. In other words, it causes both phase shifters to cycle through a "set" and "reset" state back

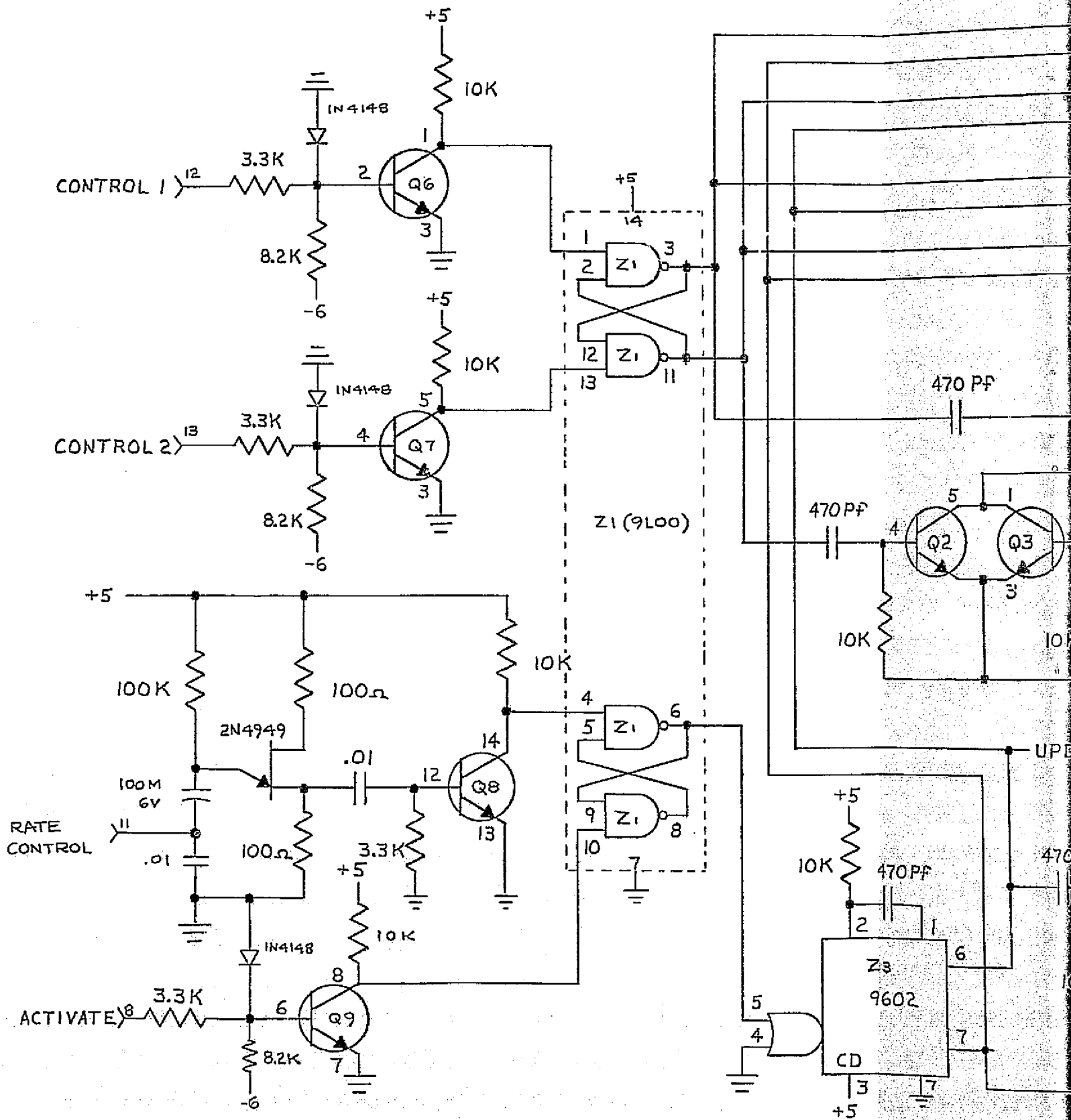

FIGURE 16 - SCHEMATIC DIAGRAM OF ELECTRONIC DRIVER CIRCUIT

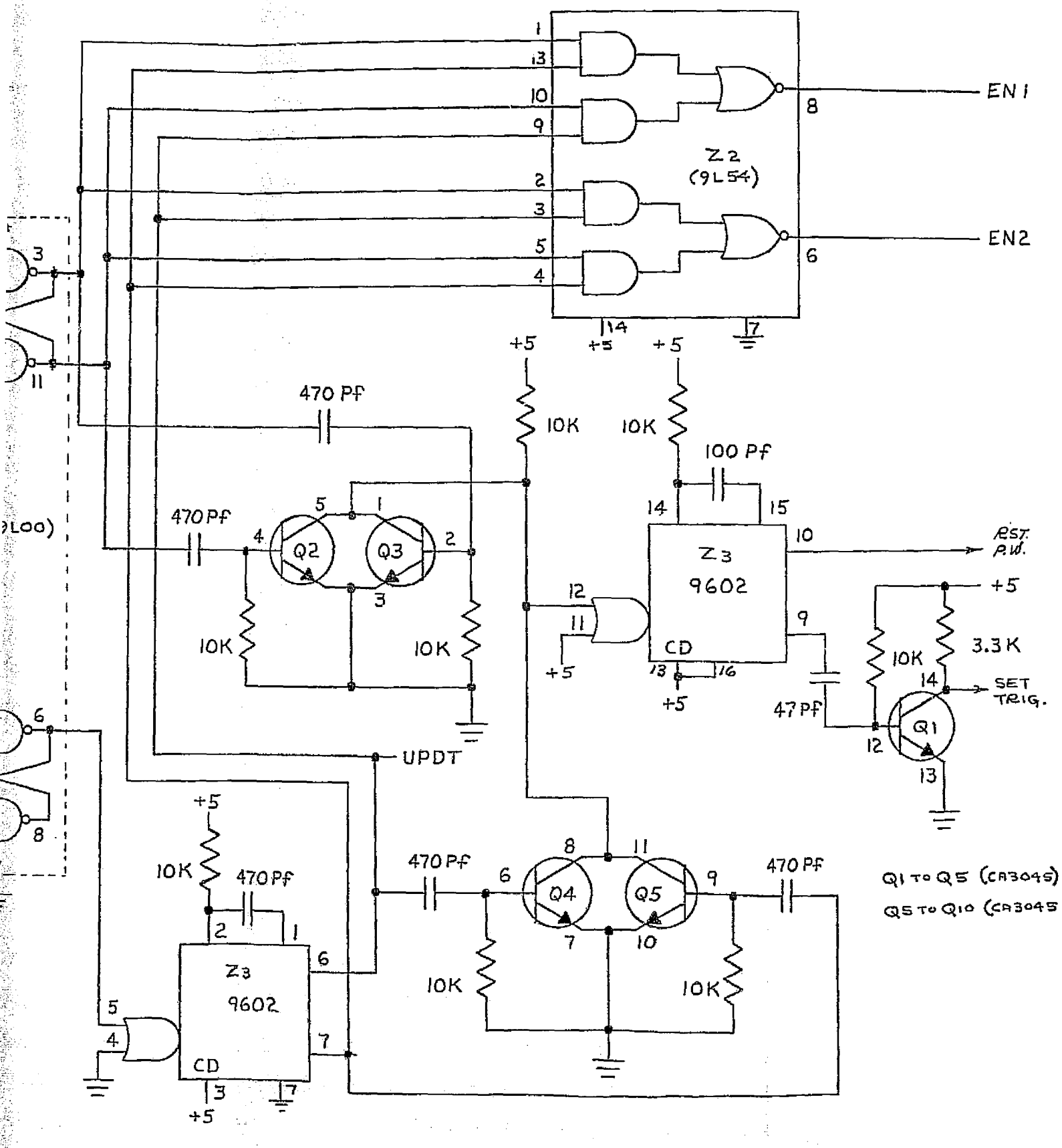
EN1
EN2
Z2
(9L54)
+5
10K
470 PF
100 PF
Z3
9602
CD
Q1
Q2
Q3
Q4
Q5
UPDT
47 PF
3.3 K
SET
TRIG.
RST.
P.W.
Q1 TO Q5 (CA3045)
Q5 TO Q10 (CA3045

to the original switch position before the initiation of the update pulse command. Hence, if the switch were in Position 1 and the Update Generator is triggered, the High Power Microwave Ferrite Switch will go to Position 2 and back to Position 1 in a matter of several microseconds. As stated earlier, the purpose of the update function is to overcome any long term drifts due to changes in either temperature or magnetic environment in the absence of position input control signals for long periods of time.

A Control Electronics Test Box was provided with the High Power Microwave Ferrite Switches. A photograph of this test box and a switch is shown in Figure 17. Figure 18 is a sketch and schematic diagram of the Control Electronics Test Box. The position inputs are generated by SPDT Switch No. 1. This switch applies a 5-volt level to Position 1 Input or Position 2 Input. The free run or manual update control is provided by SPDT Switch No. 2. A trigger switch is provided in series with SPDT Switch No. 2 to allow for manual trigger operation when SPDT Switch No. 2 is in the manual mode position. SPDT Switch No. 3 is used to control the update rate and provides either the high or low rate control discussed earlier. The Control Electronics Test Box also provides the required d. c. voltage levels for operation of the driver circuits of the High Power Microwave Ferrite Switch.

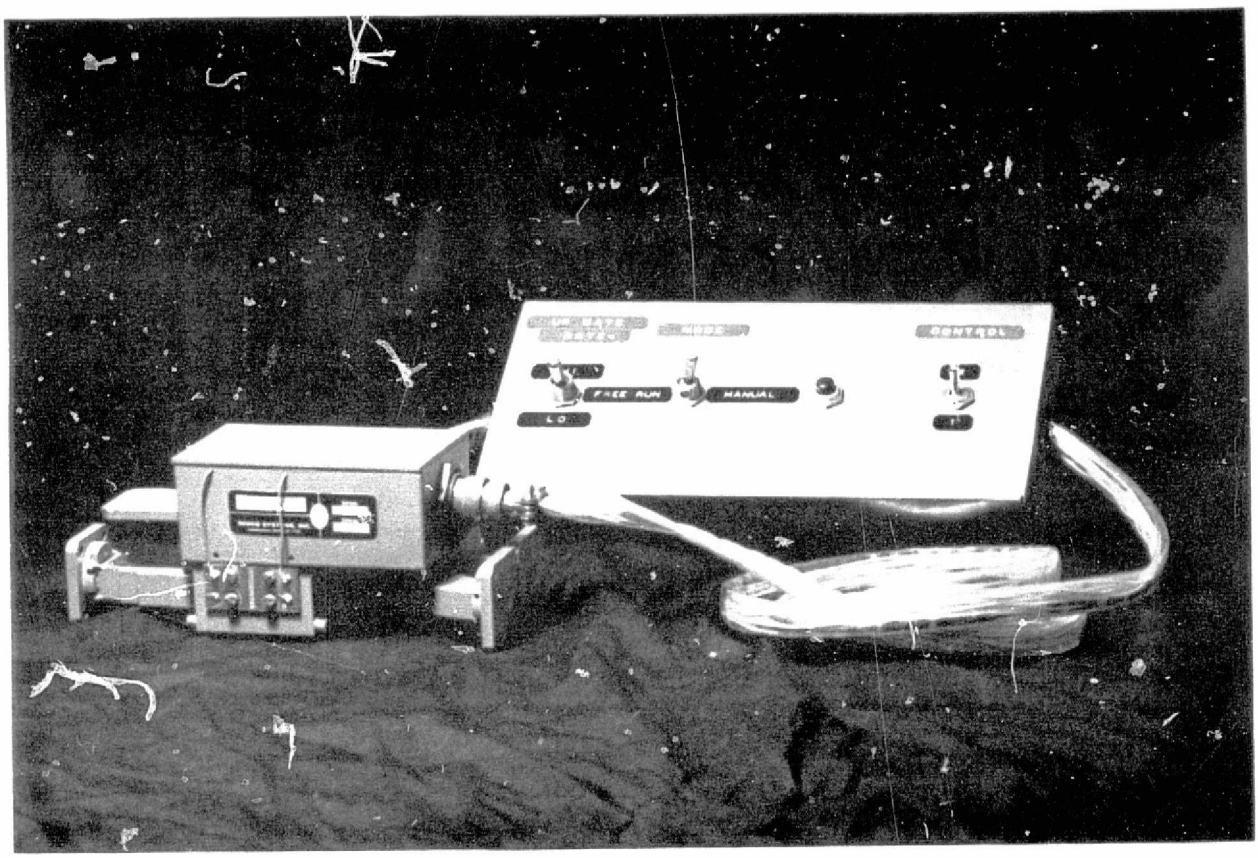

Figure 17 - Photograph of Control Electronics Test Box and High Power Ferrite Microwave Switch

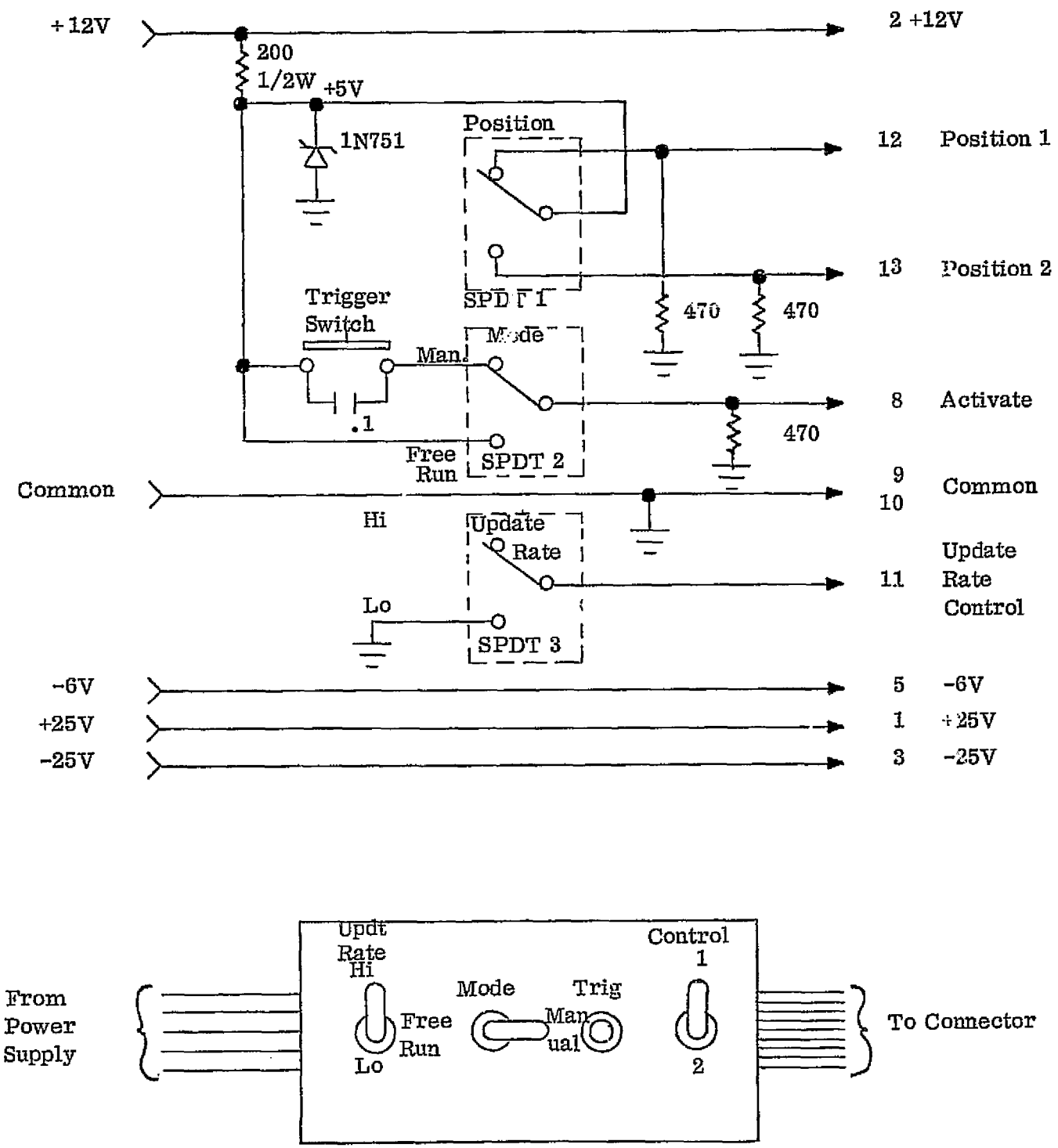

Figure 18 - Sketch and Schematic Diagram of the Control Electronics Test Box

C. High Power Ferrite Microwave Switch

A prototype High Power Ferrite Microwave Switch was constructed using two ferrite phase shifters, a folded magic tee, and a short-slot hybrid. Appropriate flanges were brazed into the hybrid and magic tee so that measurements from a WR75 waveguide setup could be made. A complete set of measurements were taken to determine the insertion loss, VSWR and isolation characteristics of this device.

Figure 19 illustrates two curves of insertion loss vs frequency of the High Power Ferrite Microwave Switch with the switch connected to output port 1 or output port 2. In general, the insertion loss appears to be about 0.3 db. In the frequency range close to 11.7 GHz the insertion loss gets as low as 0.2 db. Above 12 GHz the insertion loss appears to increase and has several slight resonances. This is caused by the fact that the phase shifter devices were optimally matched toward the low end of the band rather than the high end of the band. This was adjusted for the final devices so that optimum performance was achieved around the 12.0 GHz frequency range. The insertion loss data shown in Figure 19 illustrates that the 0.3 db maximum can be achieved and it was concluded that the final devices would exhibit an insertion loss of between 0.2 and 0.3 db in the required frequency band.

Figure 20 is a plot of VSWR vs frequency as seen looking into the sum arm of the input magic tee. In the frequency range around 11.7 GHz the

Switch Connection: Input--Output Port 2

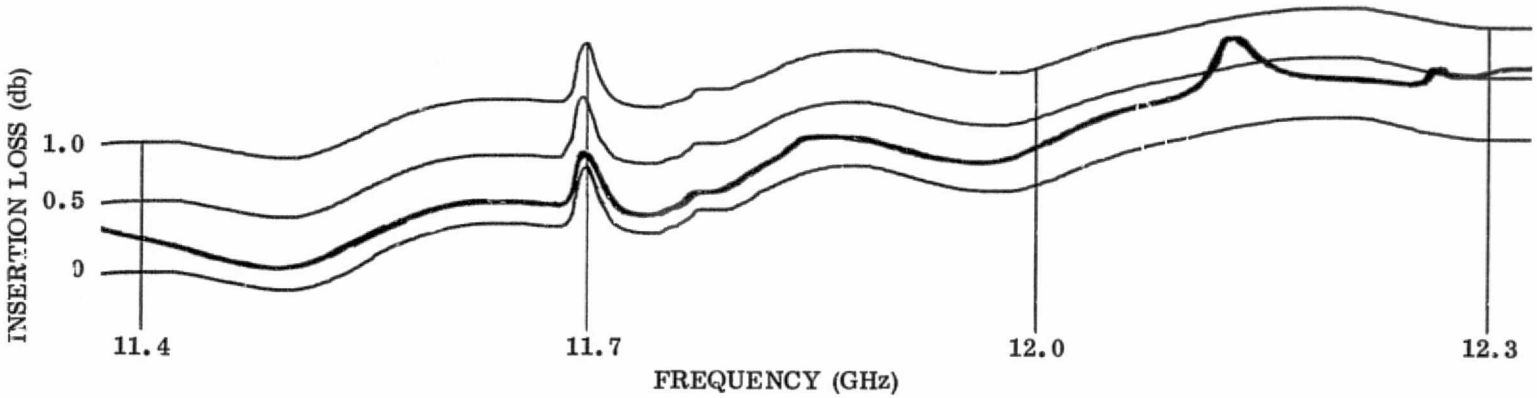

Switch Connection: Input--Output Port 1

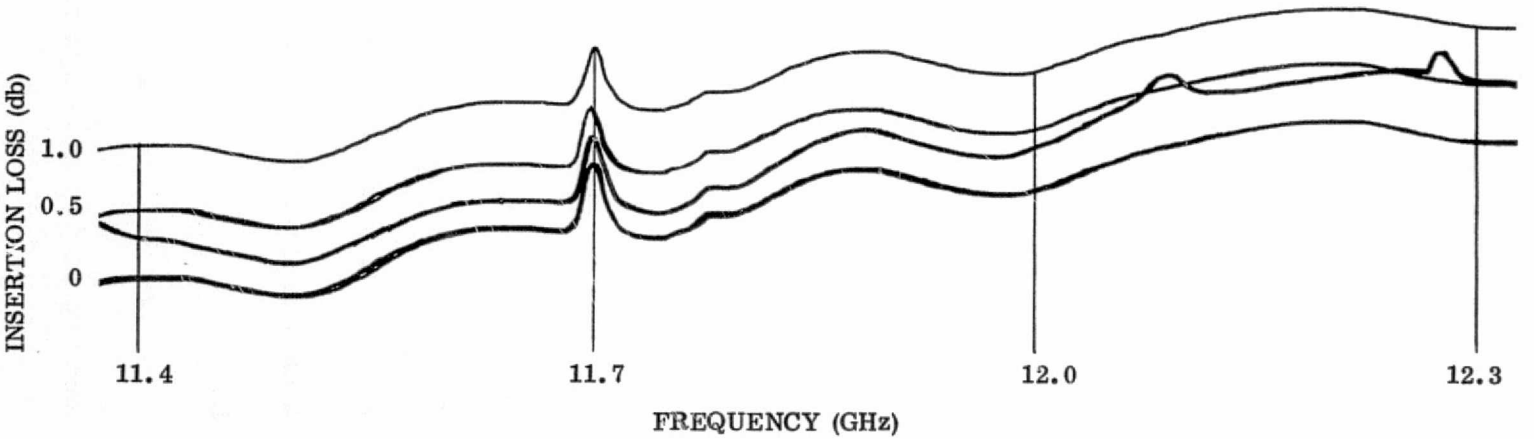

FIGURE 19 - INSERTION LOSS VS FREQUENCY OF HIGH POWER MICROWAVE SWITCH

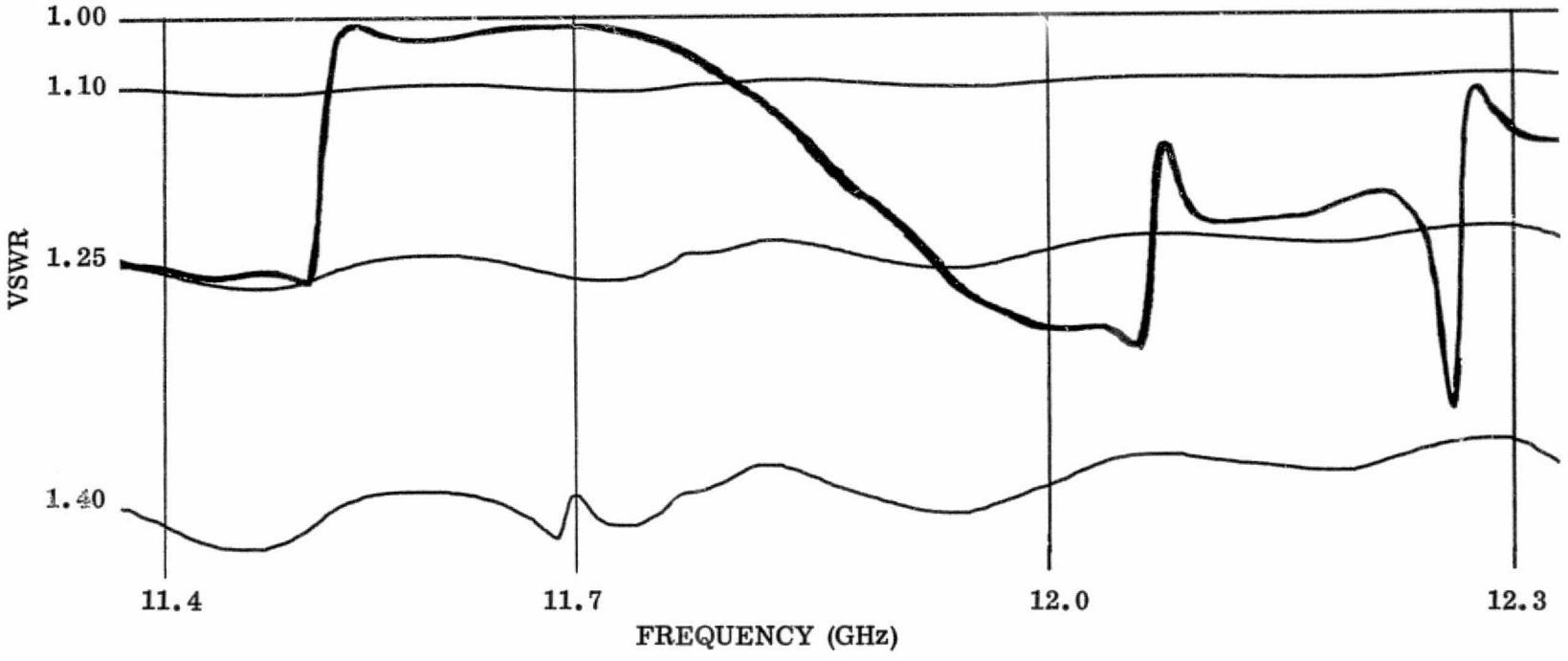

FIGURE 20 - INPUT VSWR VS FREQUENCY OF HIGH POWER FERRITE MICROWAVE SWITCH

VSWR was excellent and was under 1.10:1. At about 11.9 GHz the VSWR exceeded 1.25:1 and several slight resonances appeared about 12.0 GHz. At about 11.5 GHz the VSWR rose to approximately 1.25:1. This data indicates that a slight improvement in the VSWR performance was required and that the matched band had to be shifted up in frequency so that it would be centered on 12.0 GHz. Only one curve is illustrated in Figure 20 although the switch was programmed to propagate energy to both output ports. It was found that changing the switch state did not affect the VSWR characteristics of the device.

Figure 21 illustrates isolation vs frequency to the unswitched ports. When the device was switched to port 2, the isolation to port 1 exceeded 30 db from 11.4 GHz to 12.2 GHz. It appears that the isolation reached as high as 40 db for a good portion of this band. When the switch was positioned to output port 1, the isolation to port 2 was not quite as good as the previous curve. The upper portion of Figure 21 illustrates the isolation across the same band and it appears that the average isolation is somewhere around 27 db, and above 12 GHz reaches, at one point, as low as 20 db. The two curves shown are for two different phase settings of the phase shifters. When this data was taken it was not known why isolation greater than 30 db was not achieved. Changing phase settings varied the isolation characteristics slight, but greater than 30 db could not be achieved over the full band. Upon disassembling the switch it was found that the ferrite section used to

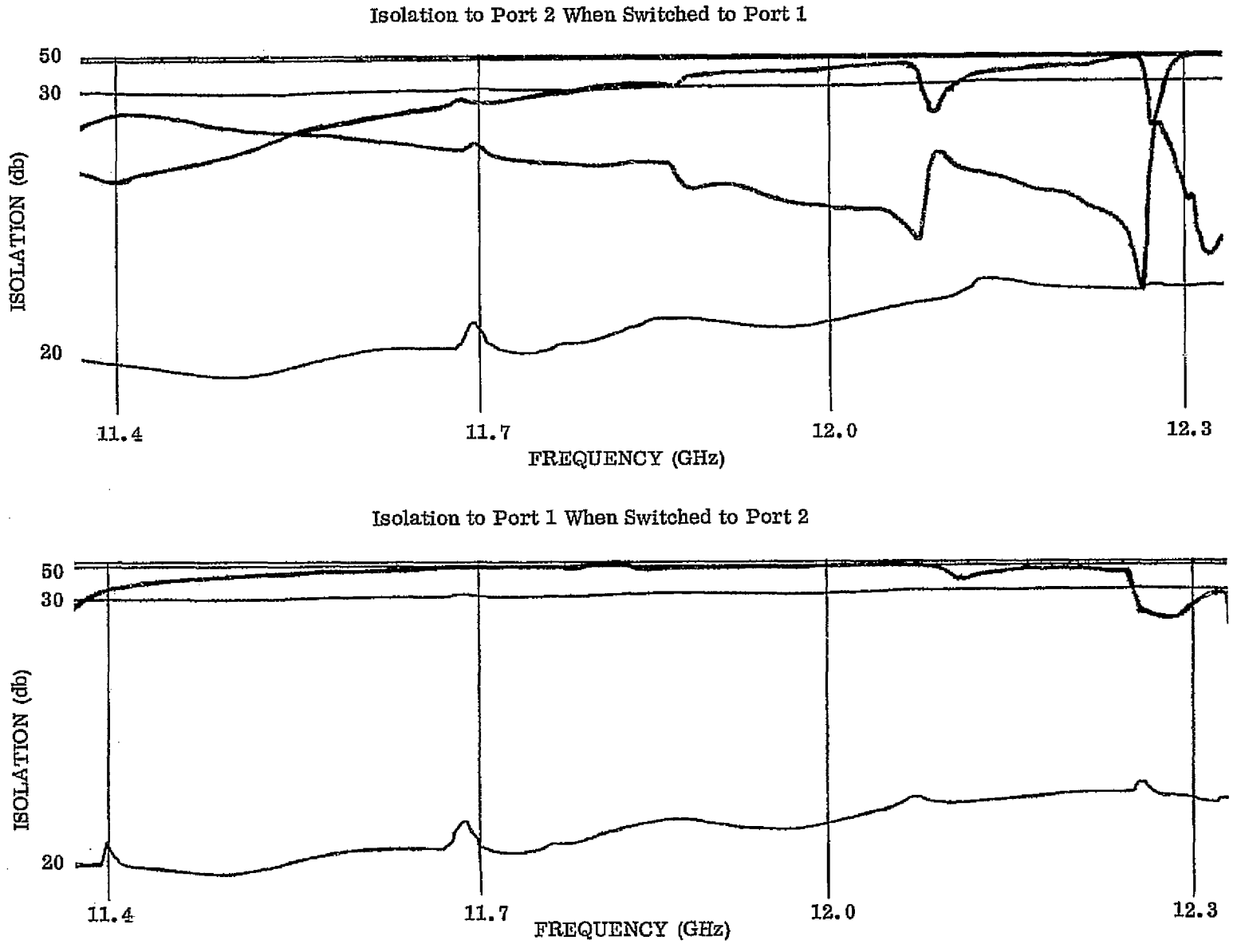

FIGURE 21 - ISOLATION VS FREQUENCY OF HIGH POWER FERRITE MICROWAVE SWITCH

"set" the required 90° of differential phase shift to produce isolation to port 2 was cracked. It therefore did not provide a frequency insensitive phase setting and in addition created VSWR and insertion loss spikes. This in turn caused the relatively poor isolation characteristics shown in the upper portion of Figure 21 as well as the VSWR and insertion loss resonances in the upper end of the frequency band as shown in Figures 19 and 20.

A complete set of high power measurements was made on the repaired prototype High Power Ferrite Microwave Switch. In addition a second thermal analysis was made to see if the measured data correlated with the theoretically predicted results.

Because of some difficulties with the high power test set, 500 watts of average power was used rather than the full 1,000 watts. When the switch was subjected to the 500 watt level a temperature rise of approximately 16°C was measured on the phase shift sections of the switch. This is well below maximum temperature rises that can be tolerated by this type of device. Since the thermal rise is directly related to the power dissipated, a maximum rise of 32°C (2 x 16°C) is anticipated under full power operation.

The insertion loss of the High Power Switch was measured to be between 0.2 and 0.3 db. Table 2 lists dissipated power for a 1,000 watt applied input to the switch for several levels of insertion loss.

Insertion Loss (db)	Dissipated Power for 1,000 Watt Input (watts)
0.1	23
0.2	45
0.3	67
0.4	88
0.5	109

Table 2 - Dissipated Power for 1,000 Watt Input for Several Insertion Loss Values

For a 0.2 db loss, a total dissipated power of 45 watts is expected upon applying 1,000 watts to the input of the switch. A dissipated energy of 45 watts would in turn produce a thermal rise of 29.9°C in the switch. This estimate is based on the thermal analysis that was described earlier. A thermal rise of 16°C was measured for 500 watts applied implying that a 32°C rise would occur upon the application of 1,000 watts of average power. This further implies that the insertion loss is slightly higher than 0.2 db. Measurements on the insertion loss of this device as shown in Figure 19 indicate that the loss is indeed slightly higher than 0.2 db. It is satisfying to see that the theoretically predicted temperature rises and the actual measured temperature rises are very close to one another.

The first of the three deliverable High Power Ferrite Microwave Switches was then built and tested. Tests included input VSWR, insertion loss to both output ports, and isolation to both output ports. In addition high power tests at atmospheric pressure was conducted. This first production unit had all of the modifications and changes required to center the frequency characteristics of the switch about 12.0 GHz.

Figure 22 is a plot of VSWR vs frequency covering the band from 11.6 through 12.4 GHz. In that band the VSWR was below 1.2:1. Over the required band of 11.75 to 12.25 GHz the VSWR appears to be below 1.12:1. This data was taken with r.f. terminations whose VSWR is greater than 1.1 and it is therefore felt that the overall switch VSWR falls below 1.1:1 in the required frequency band. Two traces are shown in Figure 22, one for each switch position. It can be seen from the data that the VSWR is virtually independent of switch position. This is highly desirable for proper performance in a high power system application.

Figures 23 and 24 are plots of Insertion Loss vs Frequency over the frequency band 11.6 to 12.4 GHz. (Figure 23 indicates insertion loss from the input port to output port 1, and Figure 24 indicates the insertion loss from the input port to output port 2). Note that in the design band of 11.75 to 12.25 GHz the switch insertion loss to either output port is about 0.2 db maximum. Above the design band there are indications of the present of higher order modes. These modes are characterized by slight resonances

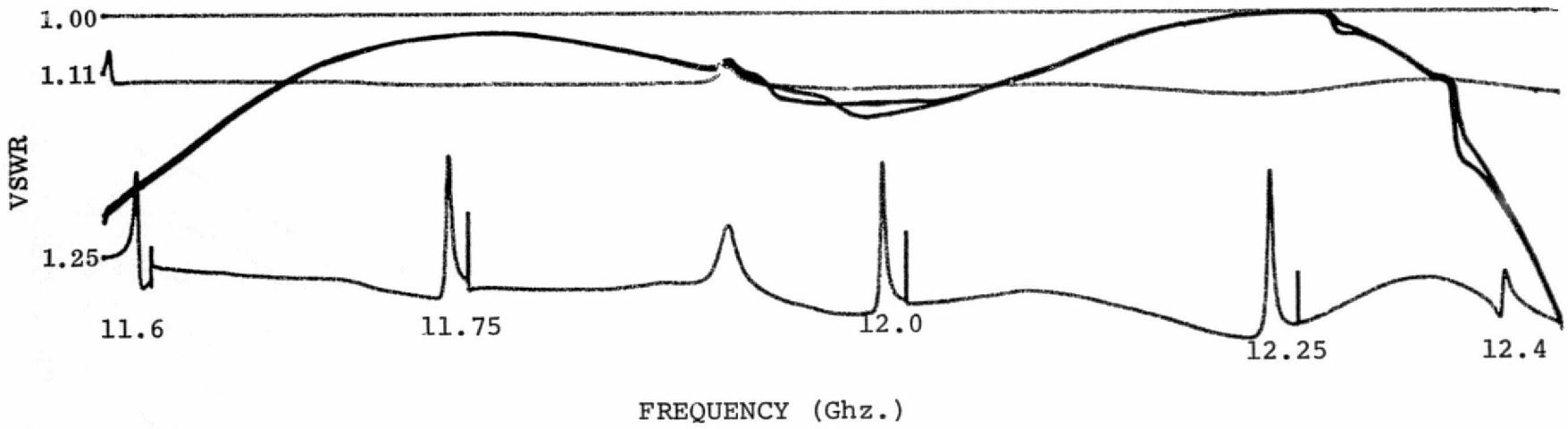

FIGURE 22 - INPUT VSWR VS. FREQUENCY OF HIGH POWER FERRITE MICROWAVE SWITCH

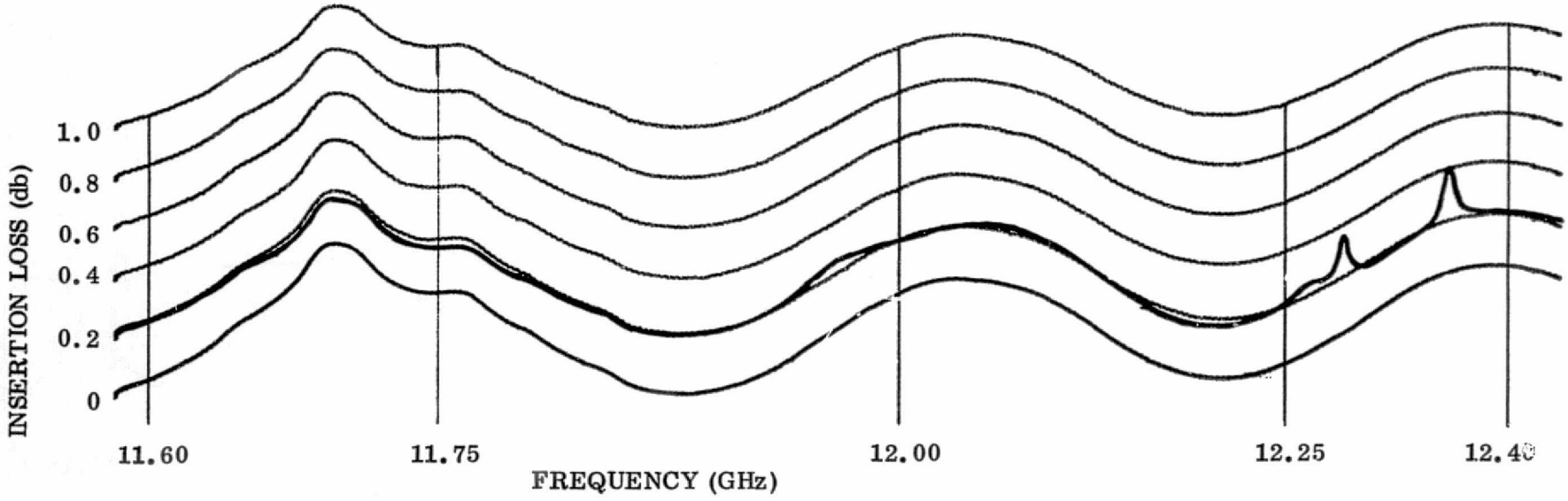

FIGURE 23 - INSERTION LOSS VS. FREQUENCY OF HIGH POWER FERRITE MICROWAVE SWITCH
(Connection - Input to Output Port 1)

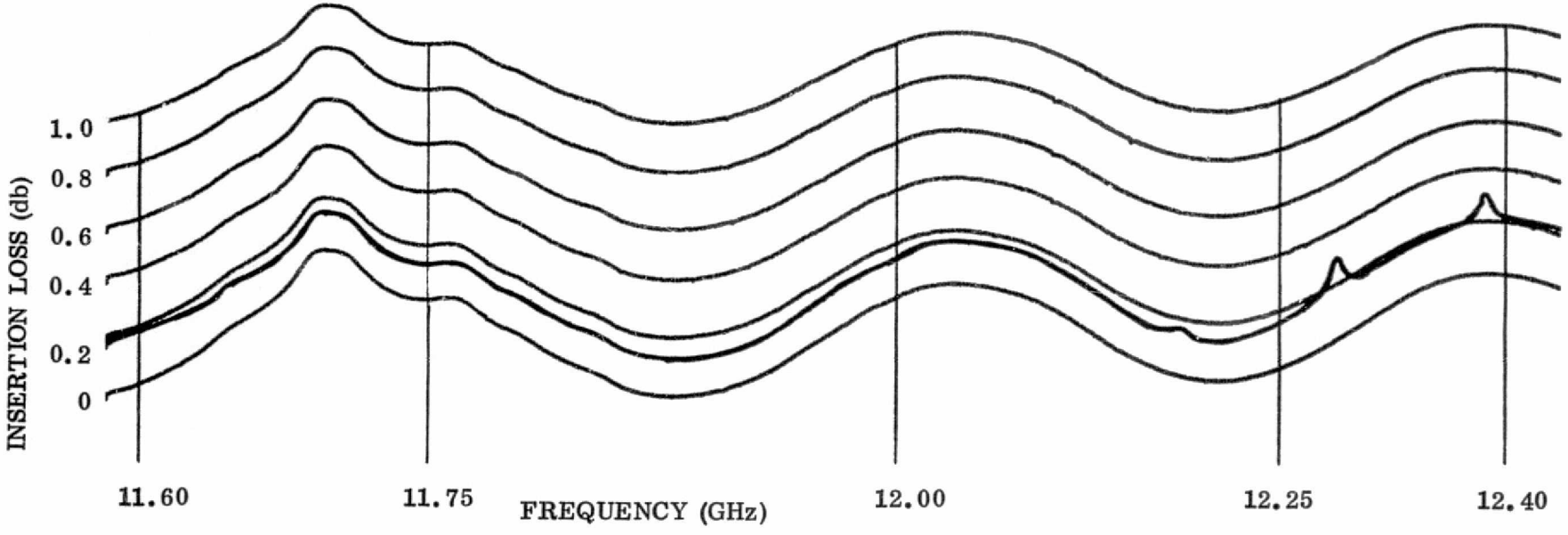

FIGURE 24 - INSERTION LOSS VS. FREQUENCY OF HIGH POWER FERRITE MICROWAVE SWITCH
(Connection - Input to Output Port 2)

that produce insertion loss peaks. The data indicates that these peaks may reach a level of 0.4 db maximum. The generation of these higher order modes was expected above the operating frequency band and was mentioned earlier. It was stated that higher order modes would probably propagate at around 12.4 GHz and that is indeed what was measured. However, since these resonances occur above the design band they do not influence required switch performance.

Figures 25 and 26 illustrate Isolation vs Frequency over the frequency range 11.6 to 12.4 GHz. (Figure 25 is the isolation to port 1 when the switch is in position 2, and Figure 26 is the isolation to port 2 when the switch is in position 1). It is difficult to measure the exact isolation, but over the design band the isolation to port 1 is never less than 35 db and in the center of the band is approximately 40 db. The isolation to port 2 appears to be never less than about 32 db and in the center of the band is approximately 38 db. These isolation measurements indicate that the required 30 db level across the entire band has been achieved. The main reason for this success is due to the optimization of the phase shifter matching sections across the required design band.

Initial power tests were made on the prototype switch at atmospheric pressure at power levels in excess of 1 Kw. A thermal rise of approximately 29°C was measured when the switch was exposed to this power level for more than a half hour. A steady state thermal condition was reached in about

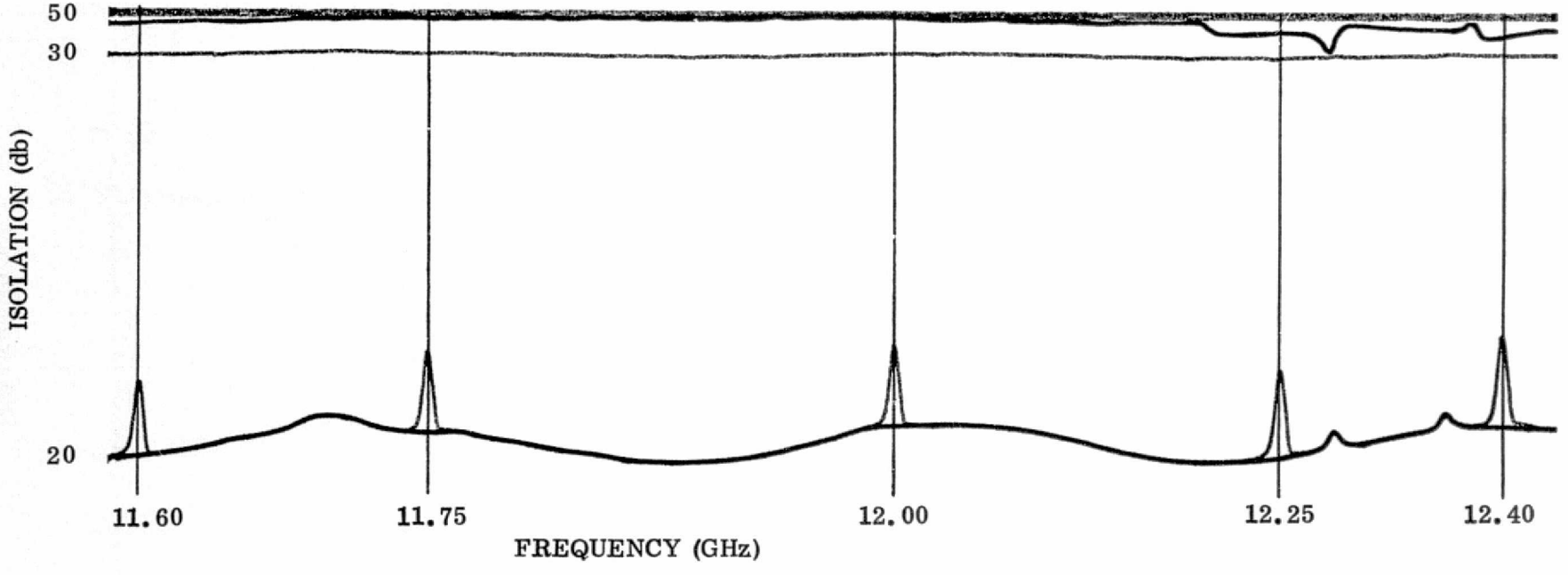

FIGURE 25 - ISOLATION VS. FREQUENCY OF HIGH POWER FERRITE MICROWAVE SWITCH
(Connection - Input to Output Port 1 with Switch in Position 2)

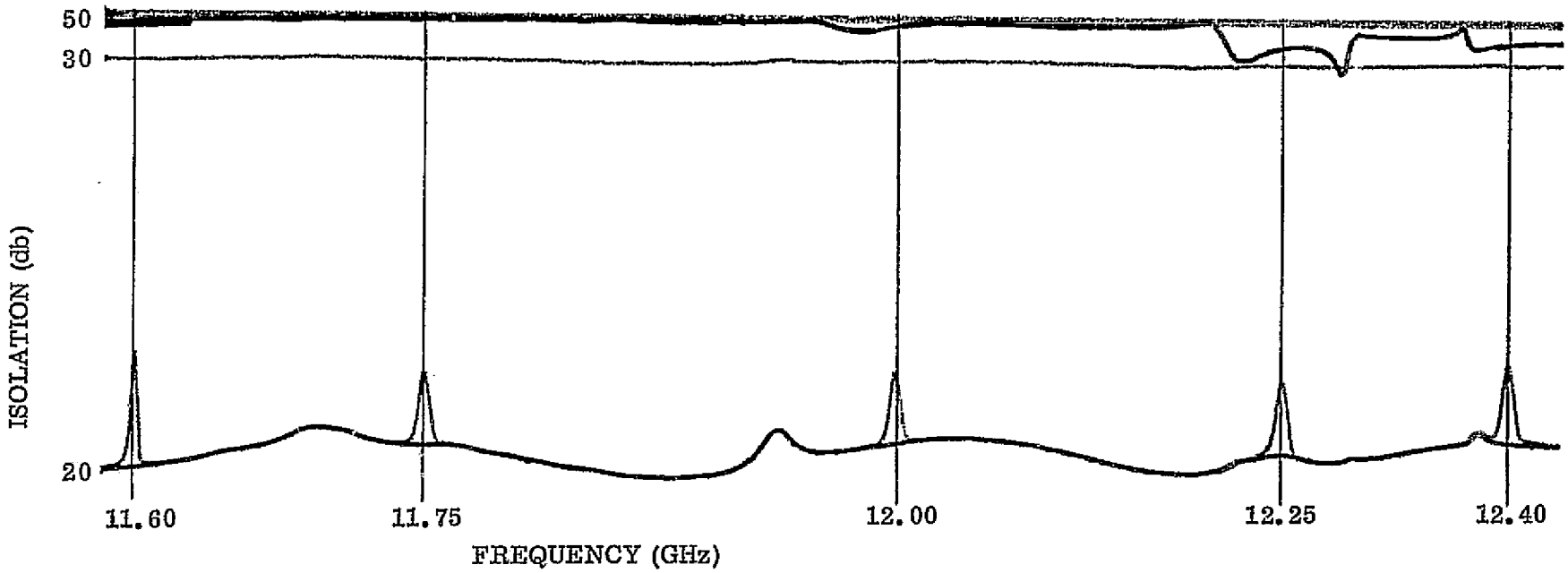

FIGURE 26 - ISOLATION VS. FREQUENCY OF HIGH POWER FERRITE MICROWAVE SWITCH
(Connection - Input to Output Port 2 with Switch in Position 1)

15 minutes. It was therefore felt that extending the test for more than a half hour would produce no additional changes and the test was stopped. High power tests were then conducted in a vacuum chamber. Some problems were encountered which were initially thought to be related to the instrumentation. It was later found that the VSWR of the pressure window in the test setup was excessive and was causing the power set to "turn off". This pressure window was changed as well as those on the output ports of the switch.

Additional difficulty was encountered with the high power test set. One of the diaphragms in the reentry cavities of the klystron ruptured and the tube was returned to the manufacturer for repairs. After a three month delay high power measurements were again conducted.

Serial No. 2 of the three High Power Ferrite Microwave Switches was subjected to rated high power. Under laboratory conditions and using the required 50°C cooling plate the unit functioned properly. Initial tests made in a vacuum appeared to indicate that the unit would satisfy the outer-space environment requirement. The following tests were made at a pressure of 10^{-6} torr. The unit was operated at 100 watts input for 3 hours; 200 watts input for 1 hour, 400 watts input for 1-1/2 hours, and 600 watts input for 2 hours at which time the switch failed. Upon opening the switch one ferrite-transformer interface was charred. It was believed that a slight misalignment of the fused silica dielectric transformer at this interface caused an arc to occur and resultant charring.

The unit was rebuilt and retested at low power to make sure that the required low loss and low VSWR operation existed. Upon satisfying these requirements the unit was again subjected to high power in a vacuum environment. The following tests were made at 10^{-6} torr. The unit was operated at 400 watts for 4 hours. The cool plate temperature was kept at 50°C and the switch top plate temperature was recorded at 60°C. The unit was then operated at 600 watts. After one half hour a rapid deterioration in isolation was noted. When the isolation dropped to 8 db the power was turned off. Two hours later the power was turned on again at 600 watts and the isolation was measured at 35 db. After one half hour, it decreased to 28 db and after an additional 45 minutes it dropped to 10 db. The switch was then cycled with the electronic driver circuit which increased the isolation to 20 db. However, after operation for another hour the switch failed. Examination of the insides of the switch showed that the same charring occurred at the same interface as was observed after the first failure.

It was concluded that the fused silica-ferrite interface was a high temperature zone and that long term exposure to high temperature caused the fused silica to outgas which then creates a runaway condition leading to eventual failure. It was decided to modify this interface by building a 0.020 inch gap between the fused silica-ferrite interface and to redesign the transformer dimension to achieve low VSWR performance. This was done and the low power swept measurements indicated that excellent

switch performance, as before, had been realized. A series of high power tests were then made. At the 600 watt level no problems were observed. The unit was then subjected to 800 watts. After one half hour the isolation level began to decrease. Power was turned off and the unit was taken apart. It was noted that the magnetizing wire in the ferrite toroid had melted at one spot and that in several other areas the tinned surface had bubbled slightly. A solid copper wire was then used in place of the tinned wire.

All subsequent tests made showed that at the 600 watt level the device functioned properly but at a level of 800 watts the unit would eventually breakdown and fail. A complete re-evaluation of all design procedures and materials characteristics was initiated which resulted in the achievement of a successful High Power Ferrite Microwave Switch. This redesign effort and resultant test results are presented in the next section.

IV REDESIGN AND FINAL TEST RESULTS

A. Phase Shifter

Due to repeated failure at high power it was concluded that a thorough evaluation of all the aggregate components of the latching ferrite phase shifters would have to be made. Several of the assumptions made during the early stages of the design effort were restudied. It was concluded that all of the epoxy adhesives used for securing the ferrite, beryllia heat sinks, and fused silica transformers would have to be eliminated. The epoxies used were specified by the manufacturer to be suitable for use in an outer space environment. However, it was concluded that slow outgassing from the epoxy caused localized breakdown at high power levels which eventually led to catastrophic failure. The outgassing procedure was a function of time and r.f. power level. Short term exposure to high power in a vacuum appeared to result in no apparent damage. However, with time, the epoxies degraded and caused eventual failure of the switch. This conclusion was based on the fact that all switches which failed showed that the epoxies used were slightly discolored. In fact, even in cases where the switch did not fail, slight discoloration of the epoxy adhesives was observed. The decision was therefore made to eliminate all epoxy.

In addition, the beryllia heat sinks were removed from the phase shift sections of the switch. It was believed that if the epoxy characteristic changed, the thermal path from the heat sinks to the sidewalls of the phase

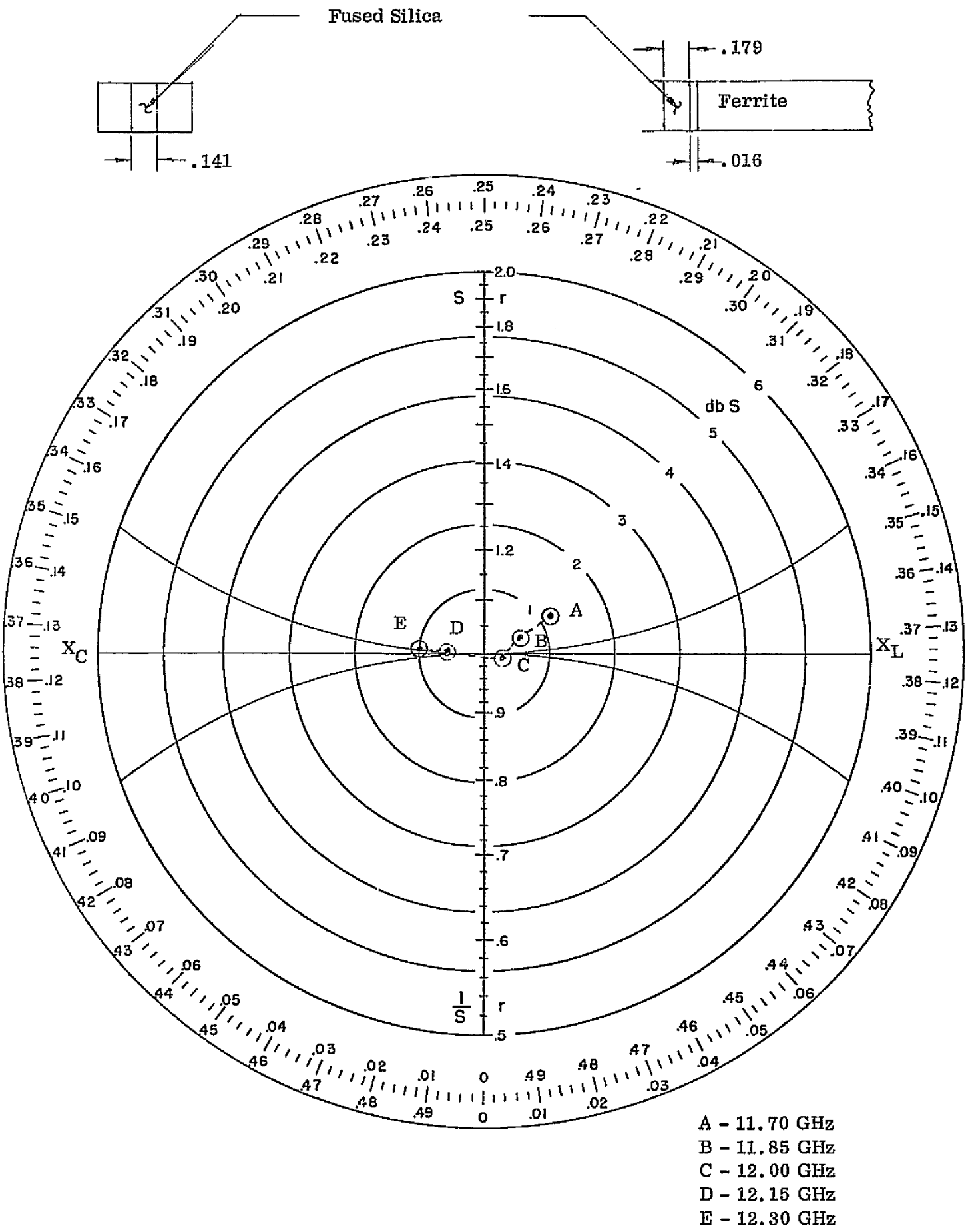

Figure 27 - Impedance of Phase Shifter at Waveguide/Phase Shifter Junction

shifter section would deteriorate thereby causing a rise in temperature in the ferrite toroid with time. It was expected that the ferrite portion of the phase shifter would experience a higher temperature without the beryllia heat sinks, but the resultant temperature would not cause the device to fail.

By eliminating the heat sinks from the phase shifter section the impedance of the phase shifter was changed and the waveguide/phase shifter interface was rematched. Figure 27 is an impedance plot of the waveguide/phase shifter interface referenced at the interface. The left half of the chart is capacitive while the right side is inductive. The numbers on the vertical line are the real part of the impedance ratio. Note that the VSWR of the matched phase shifter section falls between 1.15:1 and 1.13:1 across the frequency band 11.7 to 12.3 GHz. This impedance is more than sufficient to meet the VSWR specification for the High Power Ferrite Microwave Switch.

A phase shifter was built using two transformers with these characteristics. The measured VSWR and insertion loss was very similar to the results achieved earlier in the program. The major advantage of this new configuration is that it contained no materials other than the basic ferrite, ceramic, and fuse silica to achieve the required phase shift performance. The unit was subjected to 500 watts of power and exhibited no evidence of breakdown. It was therefore concluded that this newly designed phase shift section would satisfy the high power requirements for the complete switch.

B. High Power Ferrite Microwave Switch

A complete switch was fabricated and tested across the frequency band 11.7 to 12.3 GHz and it was found that the VSWR, insertion loss, and isolation satisfied all of the specified requirements. The unit was then subjected to high power at a level of 700 watts. No evidence of breakdown was observed when the measurements were made at atmospheric conditions nor when tested in a vacuum. The unit was then subjected to a power level of 750 watts for a continuous period of 30 hours. During that time no deterioration whatsoever in switch performance was observed. It was concluded that the redesigned High Power Ferrite Microwave Switch therefore satisfied all requirements of the program. The Test Data Sheets of all tests made on the final unit are given in Figures 28 through 44. The Acceptance Test Procedure taking this data may be found in Appendix A of this report.

FIGURE 28 - SEDCO SYSTEMS INC. TEST DATA SHEET 1

TEST: Input VSWR PRE POWER S/N 001

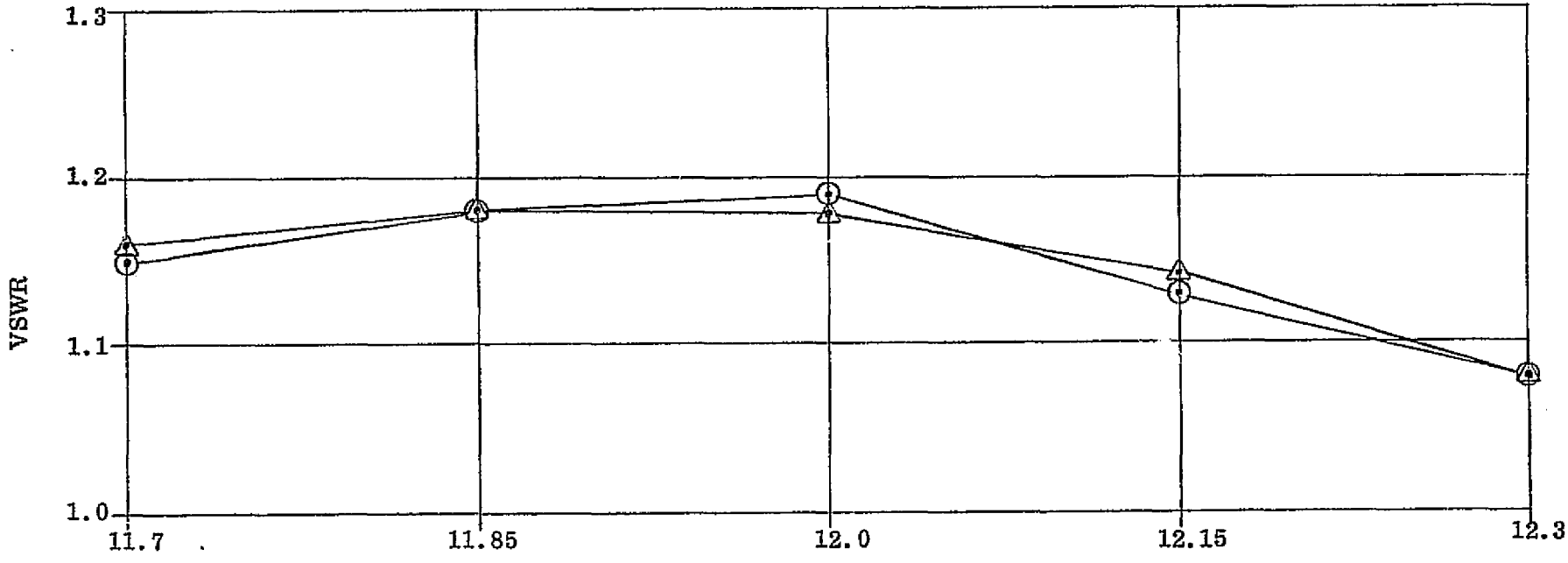

ATP. No. TPD-2011-001 DATE 1/24/75

PROCEDURE No. 3.2.1 INITIALS AED

⊙ SWITCHED TO 1
△ SWITCHED TO 2

FIGURE 29 - SEDCO SYSTEMS INC. TEST DATA SHEET 1

TEST: Input VSWR POST POWER

S/N 001

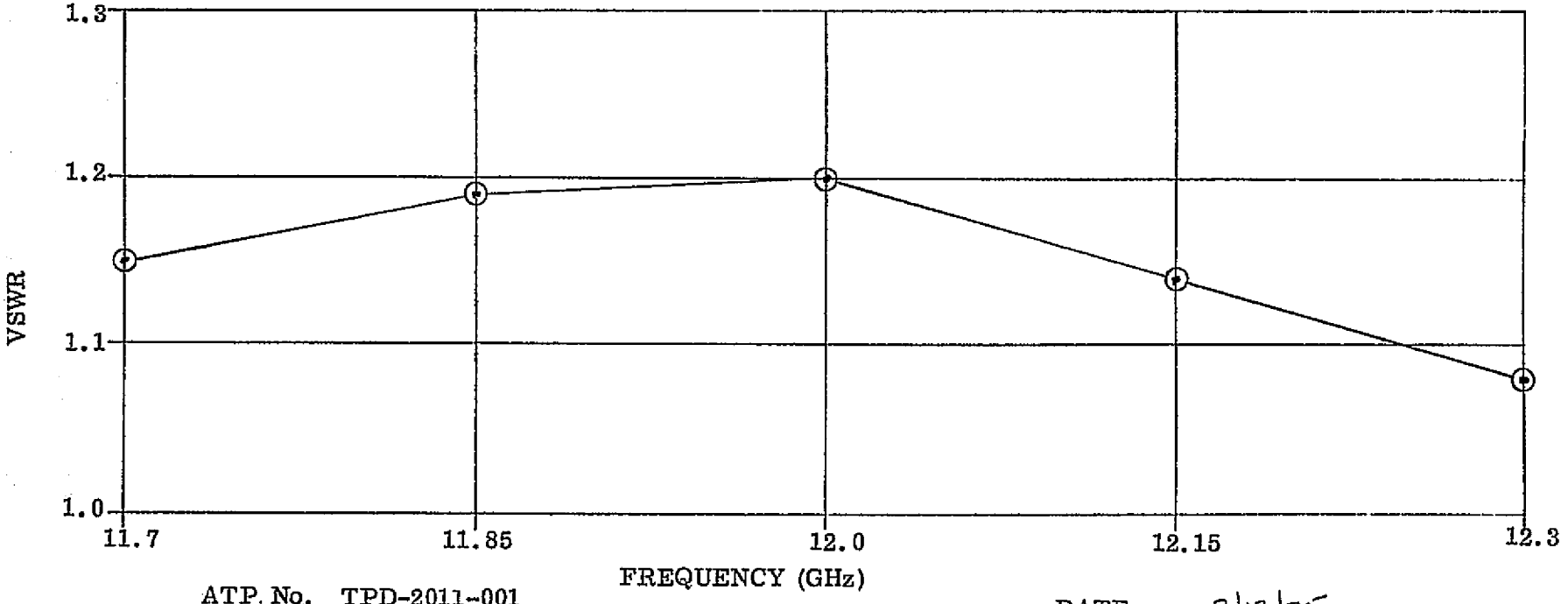

ATP. No. TPD-2011-001

DATE 2/13/75

PROCEDURE No. 3.2.1

INITIALS AED

⊙ SWITCHED TO 1
△ SWITCHED TO 2

FIGURE 30 - SEDCO SYSTEMS INC. TEST DATA SHEET 2

TEST: Insertion Loss (Input-Output) POST POWER S/N 001

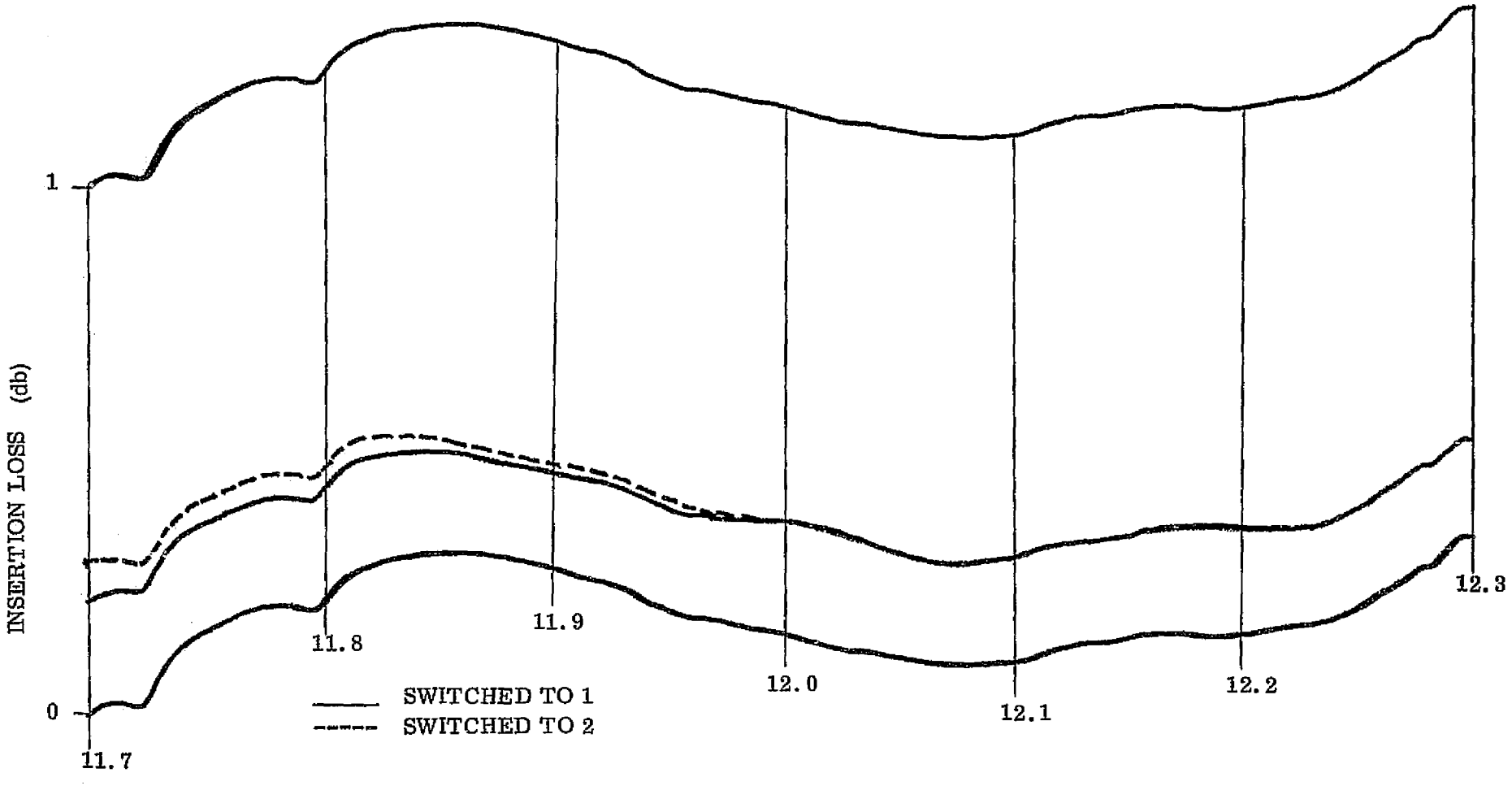

ATP No. TPD-2011-001 DATE 2/14/75

PROCEDURE No. 3.2.2 INITIALS AED

FIGURE 31 - SEDCO SYSTEMS INC. TEST DATA SHEET 3

TEST: Isolation (Input-Output) POST POWER S/N 001

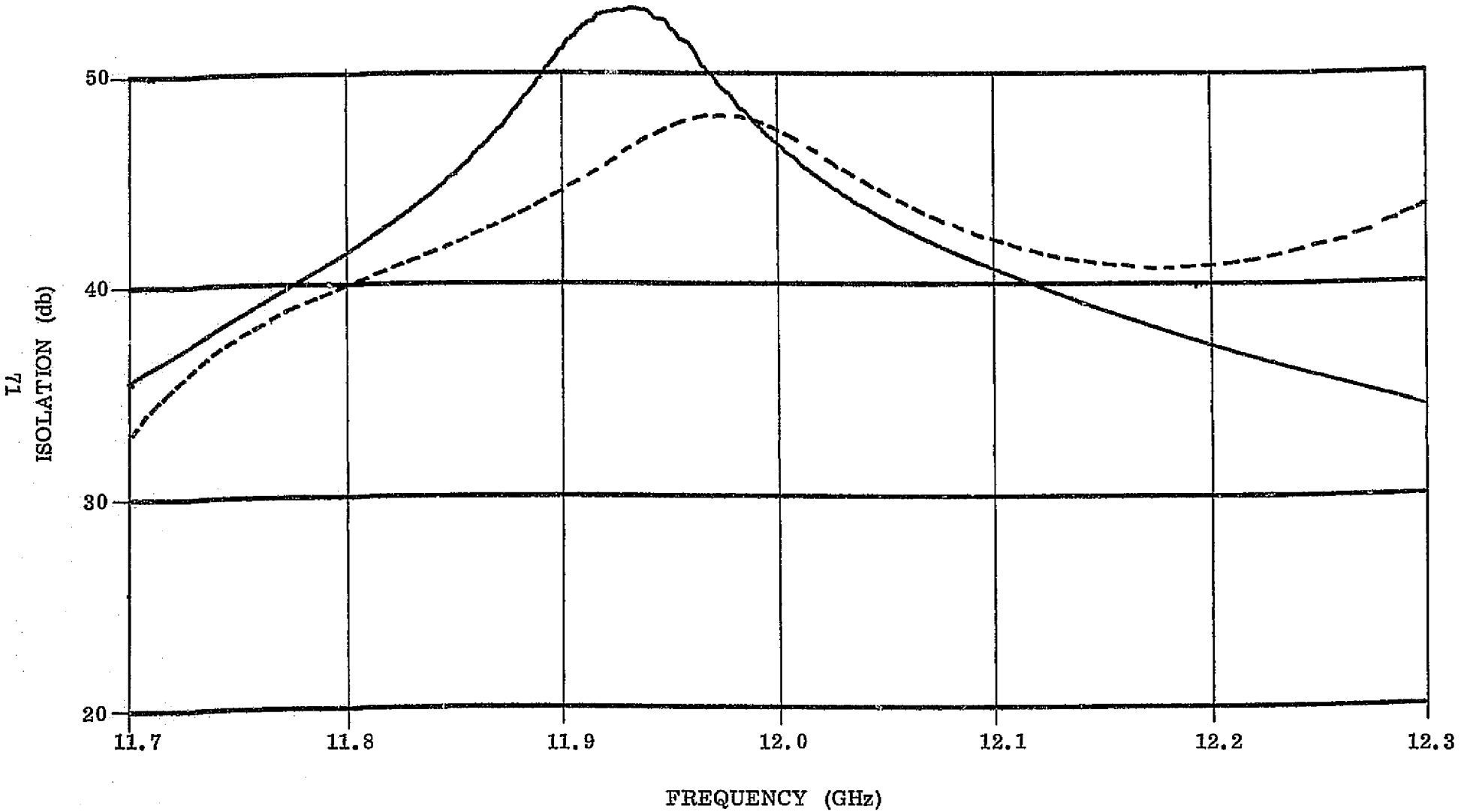

ATP No. TPD-2011-001 DATE 2/14/75

PROCEDURE No. 3.2.3

——— SWITCHED TO 1
- - - - - SWITCHED TO 2

INITIALS AED

FIGURE 32 - SEDCO SYSTEMS INC. TEST DATA SHEET 4

TEST: R. F. Power S/N 001

OBSERVATION: (Check appropriate box)

- [x] No evidence of breakdown was observed
- [ ] Breakdown was evidenced by change in loss
- [ ] Breakdown was evidenced by sound of arcing
- [ ] Other _____

POWER LEVEL CALCULATION

	INPUT	OUTPUT
Power Meter Rdg. (dbm)	+8.75	+8.42
Calibration Factor (db)	50	50
True Average Level (dbm)	+58.75	+58.42
Average Power (watts)	749.89	696.02

ATP No. TPD-2011-001

Procedure No. 3.2.4

DATE 11/27/75

INITIALS WKL

FIGURE 33 - SEDCO SYSTEMS INC. TEST DATA SHEET 5

TEST: Vacuum Environment S/N 001

OBSERVATION: (Check appropriate box)

- [x] No evidence of breakdown was observed
- [ ] Breakdown was evidenced by change in loss
- [ ] Breakdown was evidenced by sound of arcing
- [ ] Other _____

PRESSURE: 4.5×10^{-6} Torr

POWER LEVEL CALCULATION

	INPUT	OUTPUT
Power Meter Rdg. (dbm)	+8.75	+7.56
Calibration Factor (db)	50	50
True Average Level (dbm)	+58.75	+57.56
Average Power (watts)	749.89	570.16

RF THERMAL HEATING

	THERMAL COUPLES #1	#2
Temperature	45°C	45°C

Location #1 TERMINATION ON DIFF PORT OF HYBRID

Location #2 CASE PLATE

ATP No. TPD-2011-001

Procedure No. 3.2.5

DATE 1/29/75

INITIALS NVR

FIGURE 34 - SEDCO SYSTEMS INC. TEST DATA SHEET 6

TEST: Vacuum Environment - CONTINUOUS OPERATION S/N 001

OBSERVATION: (Check appropriate box)

- [x] No evidence of breakdown was observed
- [ ] Breakdown was evidenced by change in loss
- [ ] Breakdown was evidenced by sound of arcing
- [ ] Other _____

PRESSURE: 8×10^{-6} Torr

DATE & TIME-ON 2/3/75 0930

DATE & TIME-OFF 2/4/75 1530

ATP No. TPD-2011-001

Procedure No. 3.2.6

POWER LEVEL CALCULATION

	INPUT	OUTPUT
Power Meter Rdg. (dbm)	+8.75	+7.56
Calibration Factor (db)	50	50
True Average Level (dbm)	+58.75	+57.56
Average Power (watts)	749.89	570.16

RF THERMAL HEATING

	THERMAL COUPLES #1	#2
Temperature	45°C	16°C

Location #1 TERMINATION ON DIFF. PORT OF HYBRID

Location #2 CHILL PLATE

DATE 2/4/75

INITIALS ACD / NKE

FIGURE 35 - SEDCO SYSTEMS INC. TEST DATA SHEET 1

TEST: Input VSWR PRE POWER

S/N 002

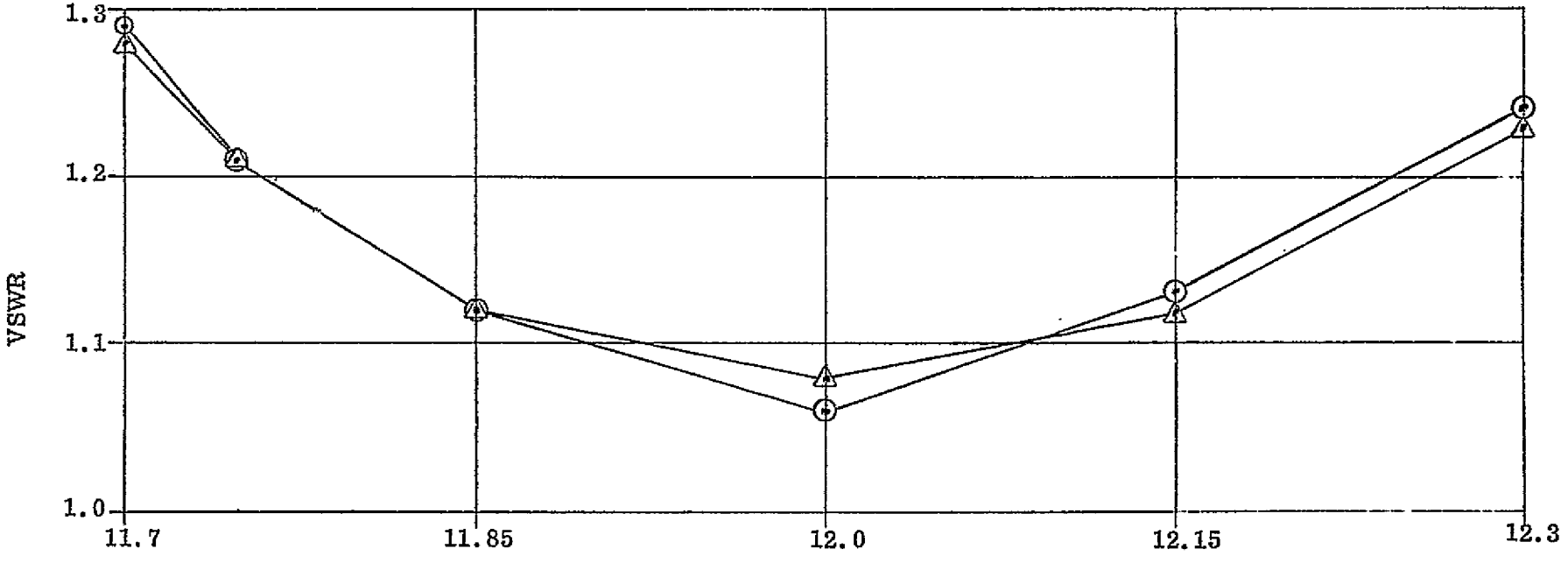

ATP No. TPD-2011-001

DATE 1/24/75

PROCEDURE No. 3.2.1

INITIALS AED

⊙ SWITCHED TO 1
△ SWITCHED TO 2

FIGURE 36 - SEDCO SYSTEMS INC. TEST DATA SHEET 1

TEST: Input VSWR POST POWER

S/N 002

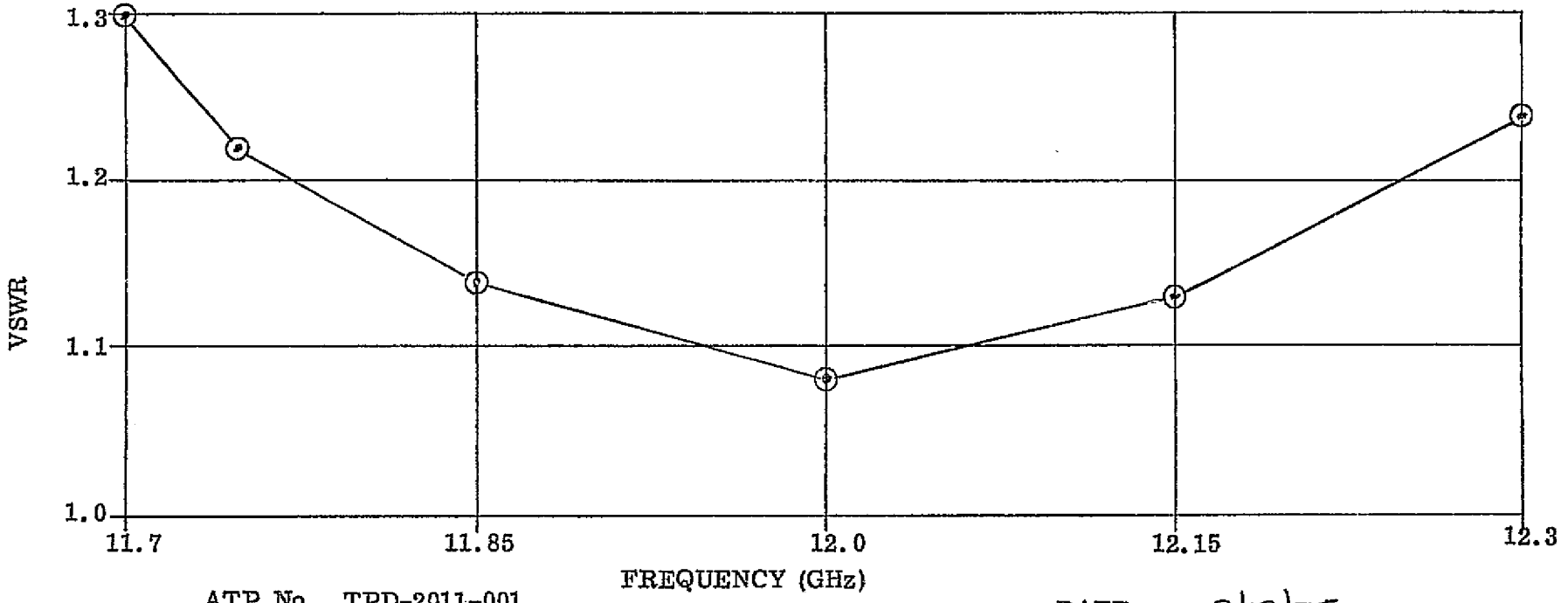

ATP No. TPD-2011-001

DATE 2/13/75

PROCEDURE No. 3.2.1

INITIALS AED

⊙ SWITCHED TO 1

△ SWITCHED TO 2

FIGURE 37 - SEDCO SYSTEMS INC. TEST DATA SHEET 2

TEST: Insertion Loss (Input-Output) POST POWER S/N 002

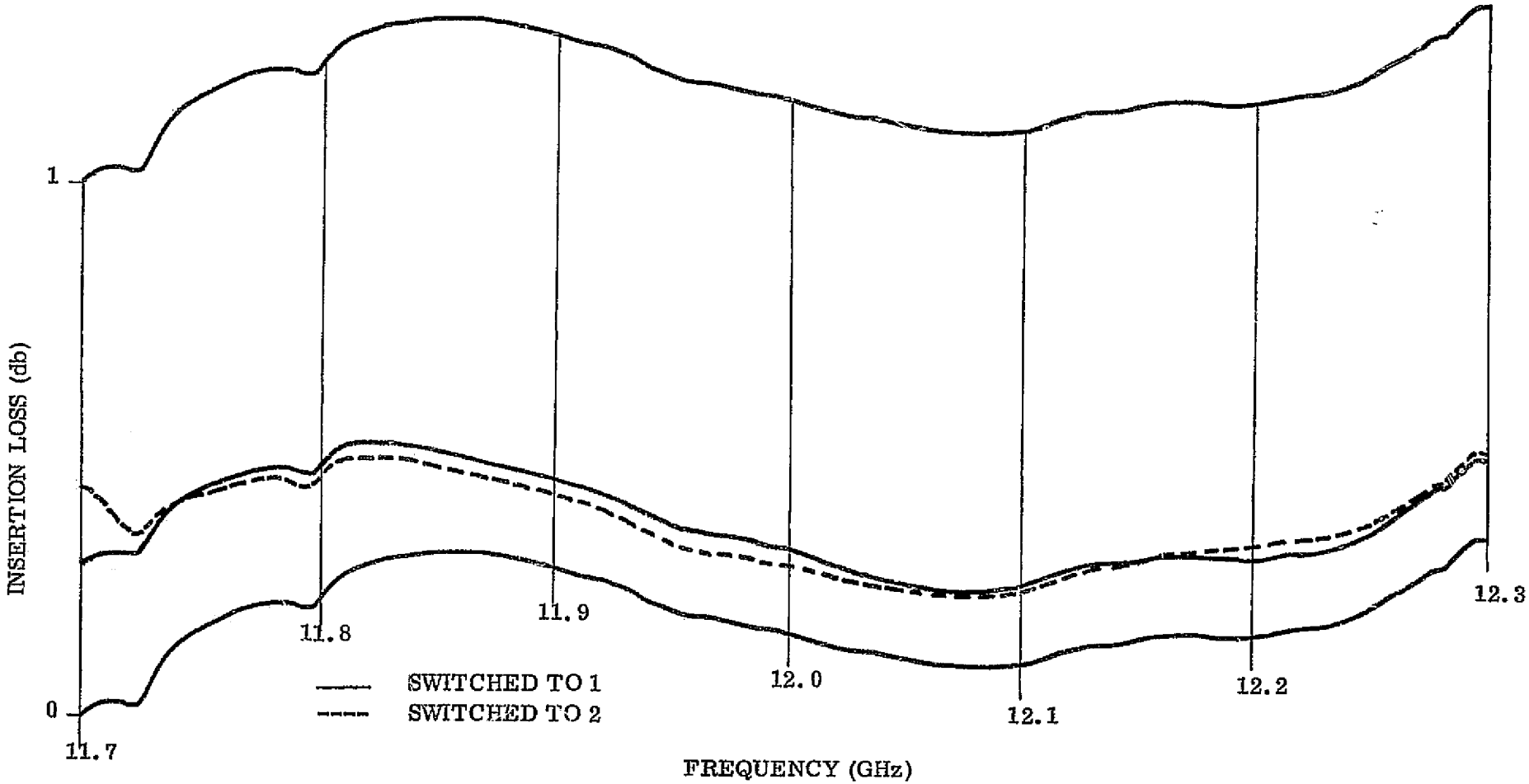

ATP No. TPD-2011-001

PROCEDURE No. 3.2.2

DATE 2/14/75

INITIALS AED

FIGURE 38 - SEDCO SYSTEMS INC. TEST DATA SHEET 3

TEST: Isolation (Input-Output) POST POWER S/N 002

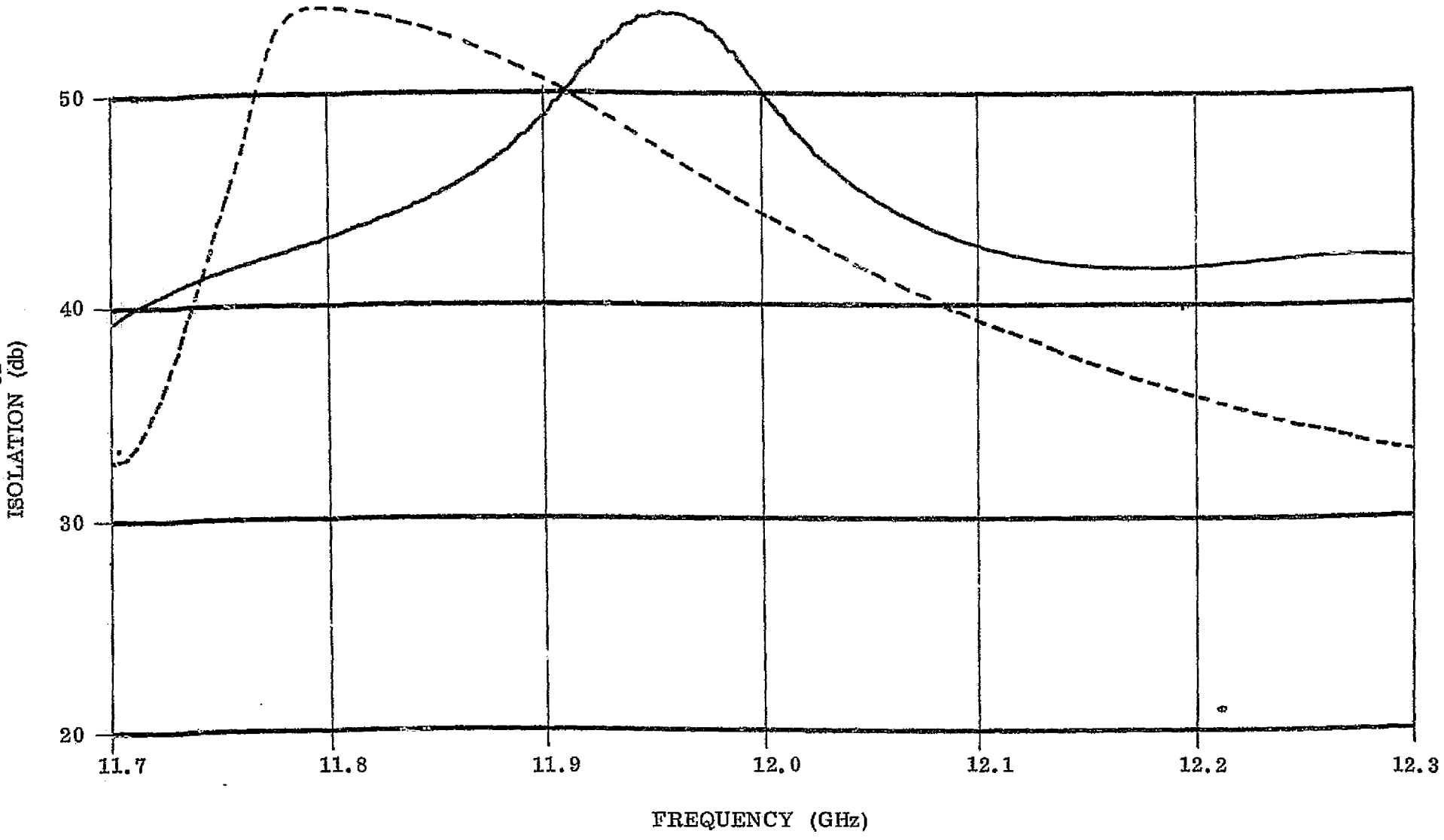

ATP No. TPD-2011-001

PROCEDURE No. 3.2.3

——— SWITCHED TO 1
----- SWITCHED TO 2

DATE 2/14/75

INITIALS AED

FIGURE 39 - SEDCO SYSTEMS INC. TEST DATA SHEET 6

TEST: Vacuum Environment - CONTINUOUS OPERATION S/N 002

OBSERVATION: (Check appropriate box)

- ☐ No evidence of breakdown was observed
- ☐ Breakdown was evidenced by change in loss
- ☐ Breakdown was evidenced by sound of arcing
- ☐ Other _____

POWER LEVEL CALCULATION

	INPUT	OUTPUT
Power Meter Rdg. (dbm)	+8.75	+8.06
Calibration Factor (db)	50	50
True Average Level (dbm)	+58.75	+58.06
Average Power (watts)	749.89	639.73

PRESSURE: 8.6×10^{-6} Torr

DATE & TIME-ON 2/4/75 1630

DATE & TIME-OFF 2/5/75 2230

RF THERMAL HEATING

	THERMAL COUPLES #1	#2
Temperature	45°C	46°C

Location #1 TERMINATION ON DIFF. PORT OF HYBRID

Location #2 CHILL PLATE

ATP No. TPD-2011-001

Procedure No. 3.2.6

DATE 2/5/75

INITIALS AGD/HKR

FIGURE 40 - SEDCO SYSTEMS INC. TEST DATA SHEET 1

TEST: Input VSWR PRE POWER S/N 003

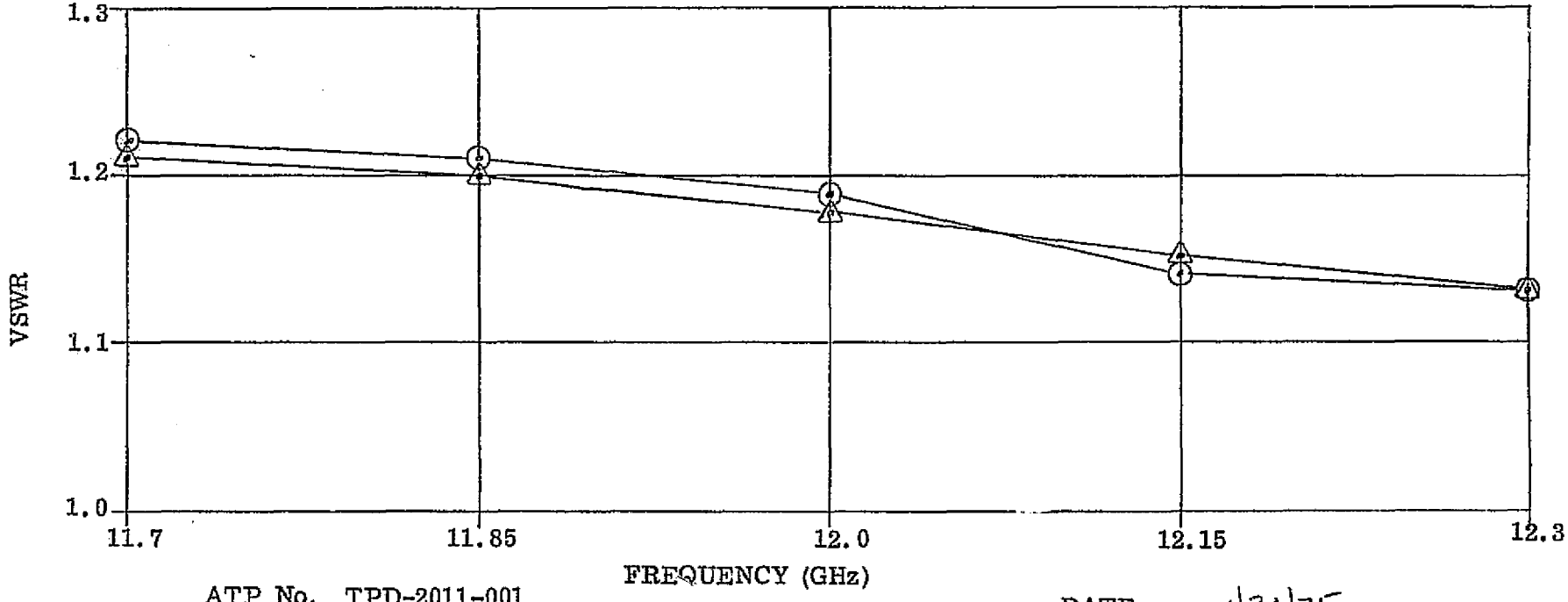

ATP No. TPD-2011-001

PROCEDURE No. 3.2.1

DATE 1/24/75

INITIALS AED

⊙ SWITCHED TO 1
△ SWITCHED TO 2

FIGURE 41 - SEDCO SYSTEMS INC. TEST DATA SHEET 1

TEST: Input VSWR POST POWER S/N 003

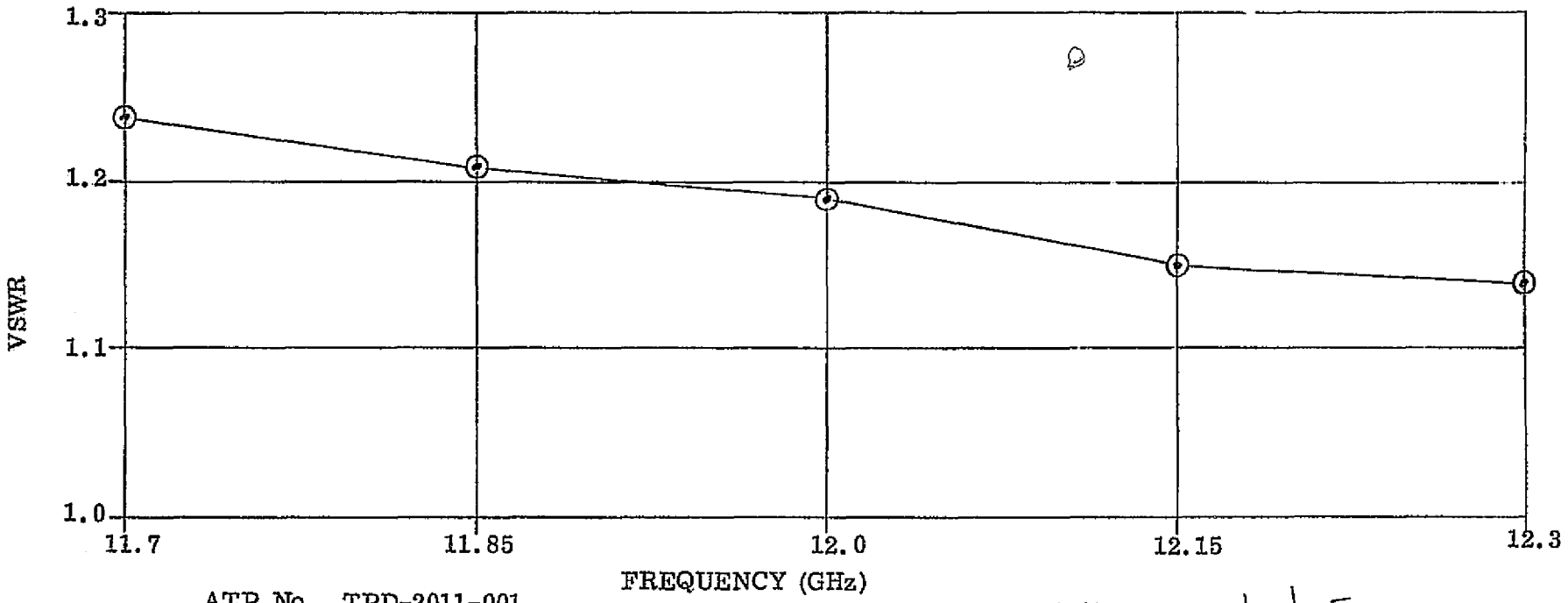

ATP No. TPD-2011-001 DATE 2/13/75

PROCEDURE No. 3.2.1 INITIALS AED

⊙ SWITCHED TO 1
△ SWITCHED TO 2

FIGURE 42 - SEDCO SYSTEMS INC. TEST DATA SHEET 2

TEST: Insertion Loss (Input-Output) POST POWER S/N 003

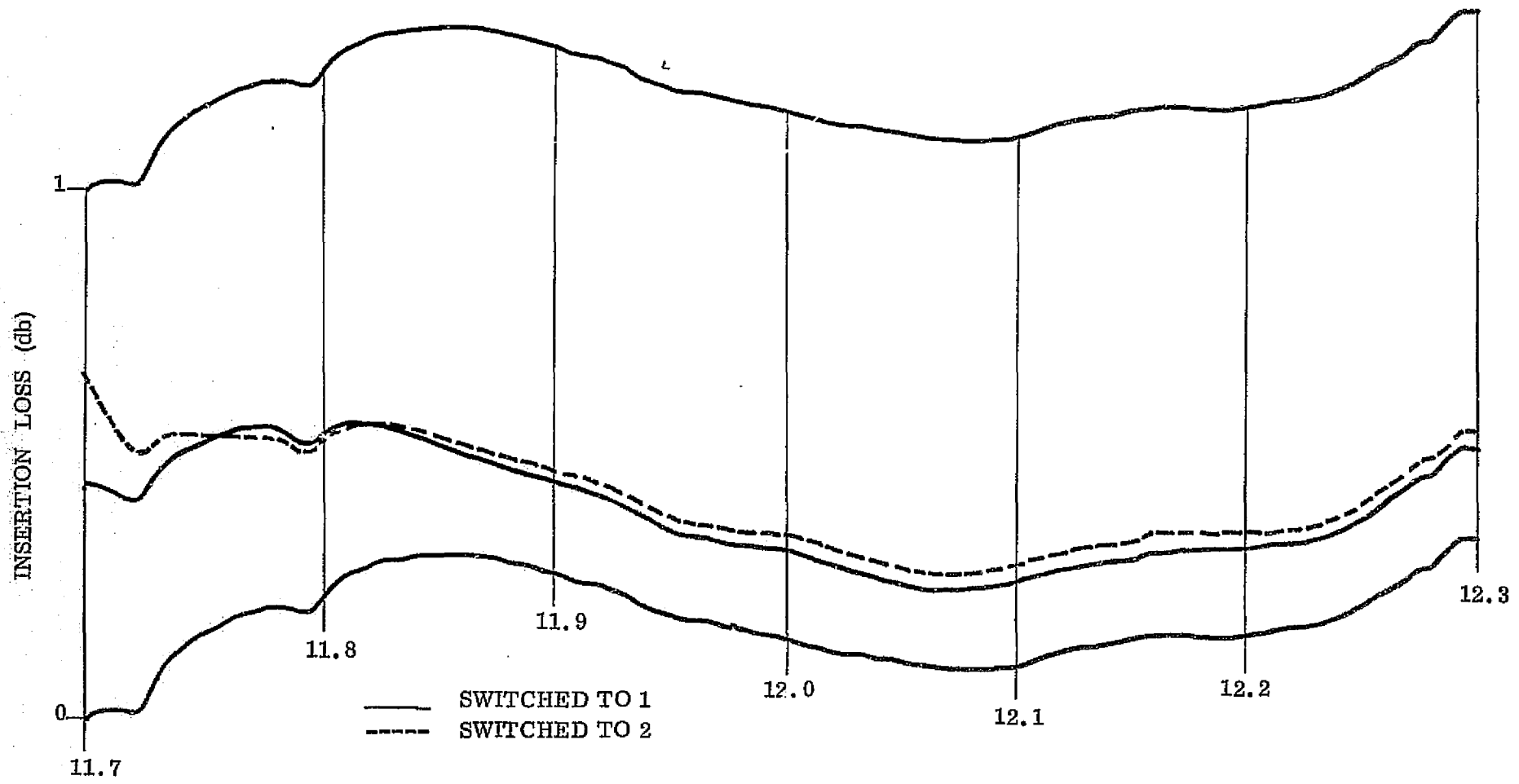

ATP No. TPD-2011-001 DATE 2/14/75

PROCEDURE No. 3.2.2 INITIALS AED

FIGURE 43 - SEDCO SYSTEMS INC. TEST DATA SHEET 3

TEST: Isolation (Input-Output) POST POWER S/N 003

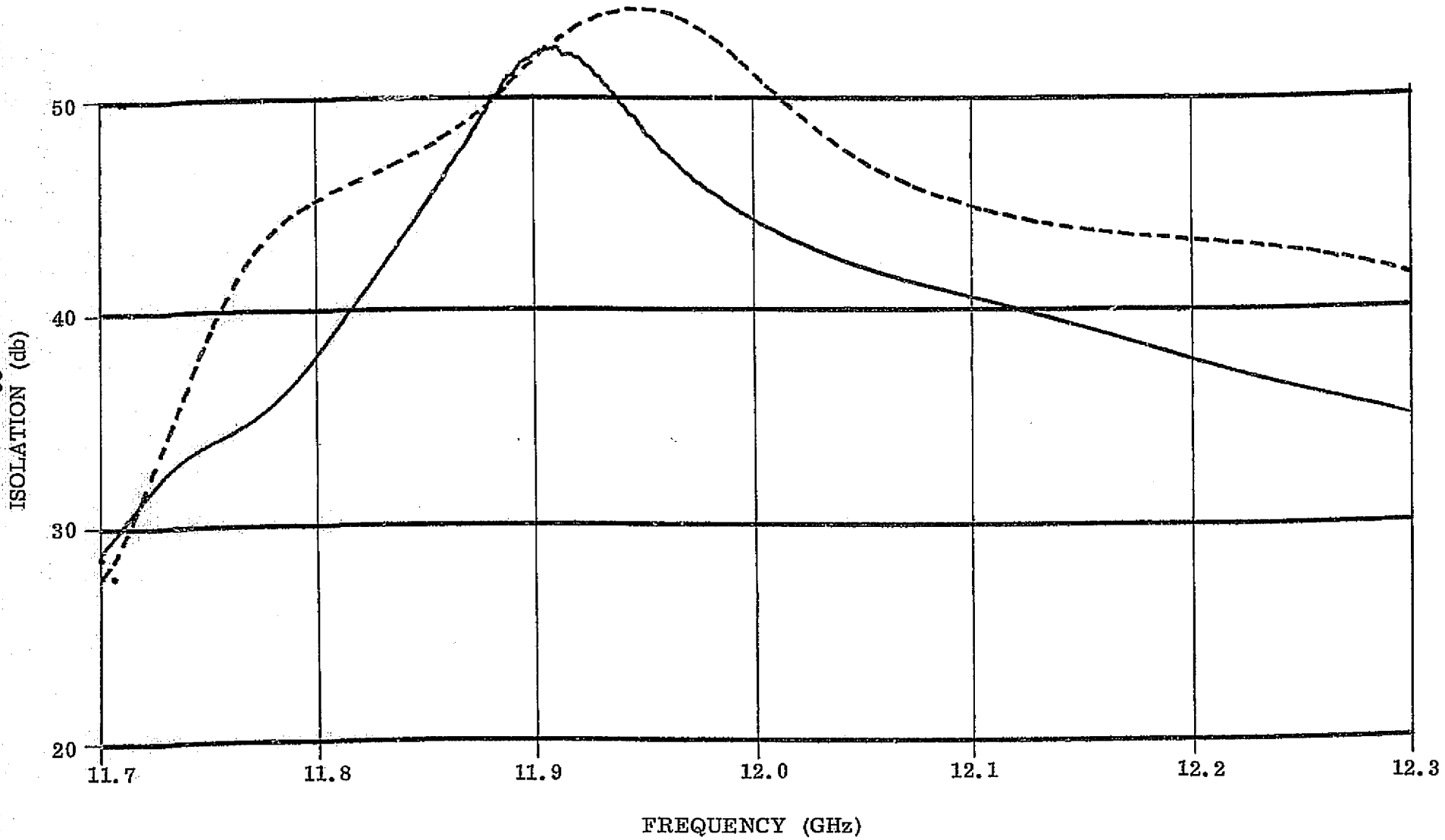

ATP No. TPD-2011-001

PROCEDURE No. 3.2.3

——— SWITCHED TO 1

----- SWITCHED TO 2

DATE 2/14/75

INITIALS AED

FIGURE 44 - SEDCO SYSTEMS INC. TEST DATA SHEET 6

TEST: Vacuum Environment - CONTINUOUS OPERATION S/N 003

OBSERVATION: (Check appropriate box)

- [X] No evidence of breakdown was observed
- [ ] Breakdown was evidenced by change in loss
- [ ] Breakdown was evidenced by sound of arcing
- [ ] Other _____

POWER LEVEL CALCULATION

	INPUT	OUTPUT
Power Meter Rdg. (dbm)	+6.99	+6.02
Calibration Factor (db)	50	50
True Average Level (dbm)	+56.99	+56.02
Average Power (watts)	500	399.9

PRESSURE: 9.0×10^{-6}

DATE & TIME-ON 2/6/75 1000

DATE & TIME-OFF 2/7/75 0900

RF THERMAL HEATING

	THERMAL COUPLES #1	#2
Temperature	45°C	46°C

Location #1 TERMINATION ON DIFF PORT OF HYBRID

Location #2 CHILL PLATE

ATP No. TPD-2011-001

Procedure No. 3.2.6

DATE 2/7/75

INITIALS ACD/NKC

V CONCLUSIONS AND RECOMMENDATIONS

Test results presented in the previous section indicate that a High Power Ferrite Microwave Switch capable of handling 750 watts in a space environment can be built, and that such a device will exhibit very low insertion loss (less than 0.3 db), very high isolation (greater than 30 db), and very low VSWR (less than 1.25:1).

Difficulty in achieving acceptable high power performance was traced to the use of supposedly space-qualified epoxy adhesive. It was concluded that epoxy adhesives are not appropriate for use in high power, r.f. equipment which must operate in a space environment. The failure mode was not immediately apparent since deterioration of the originally used epoxy adhesives occurred only after relatively long periods of time. It is therefore recommended that no epoxy be used for fabricating this type of hardware.

With the exception of the problem related to the epoxy adhesive, all other aspects of the program were relatively straightforward. The developed High Power Ferrite Microwave Switches should find successful application in spaceborne high power microwave transmitters in geostationary orbit.

APPENDIX A

ACCEPTANCE TEST PROCEDURE

FOR

HIGH POWER

FERRITE MICROWAVE SWITCH

Prepared for:

NASA-Lewis Research Center
Cleveland, Ohio

NASA Contract NAS3 - 16752

Prepared by:

Sedco Systems Inc.
Farmingdale, New York

Procedure Prepared by: L Bankard

Procedure Approved by: M. Hauser
Q.A. Mgr., Sedco Systems

Approved by NASA: _____

TABLE 1

ORDER AND TABLE OF TEST

Page	Test	Procedure	Specification*
3	VSWR	3.2.1	4.2.11
4	Insertion Loss	3.2.2	4.2.9
4	Isolation	3.2.3	4.2.10
5	R.F. Power	3.2.4	5.2
6	Vacuum Environment	3.2.5	5.4.2
6	Vacuum Environment Continuous Operation	3.2.6	3.4.j

*Paragraphs in NASA Specification NAS3-16752 Exhibit A

1.0 SCOPE

This document summarizes the test procedures applicable to electrical testing of a High Power Ferrite Microwave Switch to determine conformance with NASA Specification NAS3-16752 Exhibit A.

2.0 APPLICABLE DOCUMENTS

NASA Specification NAS3-16752 Exhibit A Sedco Test Data Sheets 1 through 18 for ATP-2011-001.

3.0 TEST REQUIREMENTS

3.1 Test Conditions

3.1.1 Environmental Conditions

All tests will be conducted at ambient laboratory conditions except those tests specifically related to temperature, power, and high vacuum performance.

3.1.2 Frequency Increments

All VSWR, Insertion Loss and Isolation tests will be conducted on a swept basis over the entire frequency band of 11.7 to 12.3 GHz. R.F. power tests will be made at 12.0 GHz.

3.2 Detailed Test Procedure

3.2.1 Input VSWR (Record results on TEST DATA SHEET 1)

Step 1 Connect test equipment as shown in Figure 1. Set sweeper markers for required band edges.

Step 2 Connect shorting plate to the output port of the directional-coupler.

Step 3 Using variable attenuators, calibrate paper in X-Y recorder in accordance with the following table:

Attenuation Setting (db)	dB R	VSWR
		1.00
37.3	32.3	1.05
28.1	23.1	1.15
24.1	19.1	1.25
21.5	16.5	1.35
19.7	14.7	1.45

Step 4 Set variable attenuator to 5.0 db and replace short with terminated High Power Ferrite Microwave Switch. (Switch is to be terminated with loads whose VSWR is not to exceed 1.15.)

Step 5 Set High Power Ferrite Microwave Switch to position 1 by applying trigger pulse to Input Terminal 1 of Switch Driver Circuit.

Step 6 Using manual-trigger capability of sweeper, record VSWR trace on TEST DATA SHEET 1.

Step 7 Repeat Step 6 after applying trigger pulse to Input Terminal 2 of Switch Driver Circuit.

3.2.1.1 Specification Limits: VSWR (Min.) -1.0:1 VSWR (Max.) -1.25:1

3.2.2 Insertion Loss (Input to Output) - (Record results on TEST DATA SHEET 2)

Step 1 Connect test equipment as shown in Figure 2 with input and output waveguide pads connected directly to each other (High Power Ferrite Microwave Switch removed from set-up). Set sweeper markers for required band edges.

Step 2 Using variable attenuator, calibrate TEST DATA SHEET 2 in X-Y Recorder for settings of 0.0, 0.2, 0.4, and 0.6 db.

Step 3 Set variable attenuator to 0 db and insert High Power Ferrite Microwave Switch into set-up with output waveguide pad connected to Output 1 of Switch.

Step 4 Set High Power Ferrite Microwave Switch to position 1 by applying trigger pulse to Input Terminal 1 of Switch Driver Circuit.

Step 5 Using manual-trigger capability of sweeper, record Insertion Loss trace on TEST DATA SHEET 2.

Step 6 Repeat Steps 1 and 2.

Step 7 Set variable attenuator to 0 db and insert High Power Ferrite Microwave Switch into set-up with output waveguide pad connected to Output 2 of Switch.

Step 8 Repeat Step 4 but apply trigger pulse to Input Terminal 2 of Switch Driver Circuit.

Step 9 Repeat Step 5.

3.2.2.1 Specification Limits

Insertion Loss (Min.) -0.1 db Insertion Loss (Max.) -0.3 db

3.2.3 Isolation (Input to Output)-(Record results on TEST DATA SHEET 3)

Step 1 Connect test equipment as shown in Figure 3 with input and output waveguide pads connected directly to each other (High Power Ferrite Microwave Switch removed from set-up). Set sweeper markers for required band edges.

Step 2 Using variable attenuator, calibrate TEST DATA SHEET 3 in X-Y Recorder for settings of 20, 25, 30, 40 and 50 db.

Step 3 Set variable attenuator to 0 db and insert High Power Ferrite Microwave Switch into set-up with output waveguide pad connected to Output 1 of Switch.

Step 4 Set High Power Ferrite Microwave Switch to position 2 by applying trigger pulse to Input Terminal 2 of Switch Driver Circuit.

Step 5 Using manual-trigger capability of sweeper, record Isolation trace on TEST DATA SHEET 3.

Step 6 Repeat Steps 1 and 2.

Step 7 Set variable attenuator to 0 db and insert High Power Ferrite Microwave Switch into set-up with output waveguide pad connected to Output 2 of Switch.

Step 8 Repeat Step 4 but apply trigger pulse to Input Termianl 1 of Switch Driver Circuit.

Step 9 Repeat Step 5.

3.2.3.1 Specification Limits - Isolation (Min.) -25 db

3.2.4 R.F. Power - (Record results on TEST DATA SHEET 4)

Step 1 Connect test equipment as shown in Figure 4 (R.F. input to input port, R.F. output at Output Port 1, Output Port 2 terminated).

Step 2 Apply rated power (800 watts C.W. minimum) to input port as monitored by Input Power Meter.

Step 3 Measure and record output power level at Output Port 1 as monitored by Output Power Meter.

Step 4 Observe if breakdown occurs by monitoring reflected energy, drop in output power, or audible evidence of arcing.

Step 5 Record observation on TEST DATA SHEET 4.

Step 6 Connect test equipment as shown in Figure 4 but with R.F. output at Output Port 2 and Output Port 1 terminated.

Step 7 Repeat Steps 2, 3, 4 and 5.

3.2.4.1 Specification Limits

Insertion Loss - Same as 3.2.2
Breakdown - Go/No Go test

C-2

3.2.5 Vacuum Environment - (Record results on TEST DATA SHEET 5)

Step 1 Connect test equipment as shown in Figure 4 except that High Power Ferrite Microwave Switch is to be placed in a vacuum chamber, with thermocouples attached to the switch to check R.F. Heating.

Step 2 Set pressure in vacuum chamber to equivalent of theoretical multipactor breakdown region (10-6 Torr). Maintain pressure for ½ hour.

Step 3 Repeat Procedure 3.2.4.

Step 4 Record observations on TEST DATA SHEET 5.

3.2.5.1 Specification Limits

No evidence of breakdown shall be observed.

3.2.6 Vacuum Environment - Continuous operation - (Record results Test Data Sheet 6)

Step 1 Repeat Procedure 3.2.5 Step 1

Step 2 Repeat Procedure 3.2.5 Step 2

Step 3 Repeat 3.2.4 Steps 1,2,3,--Operate for 60 continuous hours at a R.F. power level of 800 watts minimum --activating the switch every 8 hours.

Step 4 Observe if breakdown occurs by monitoring reflected energy, drop in output power, or audible evidence of arcing.

Step 5 Record observations on TEST DATA SHEET 6.

3.2.6.1 Specification Limits

No evidence of breakdown shall be observed.

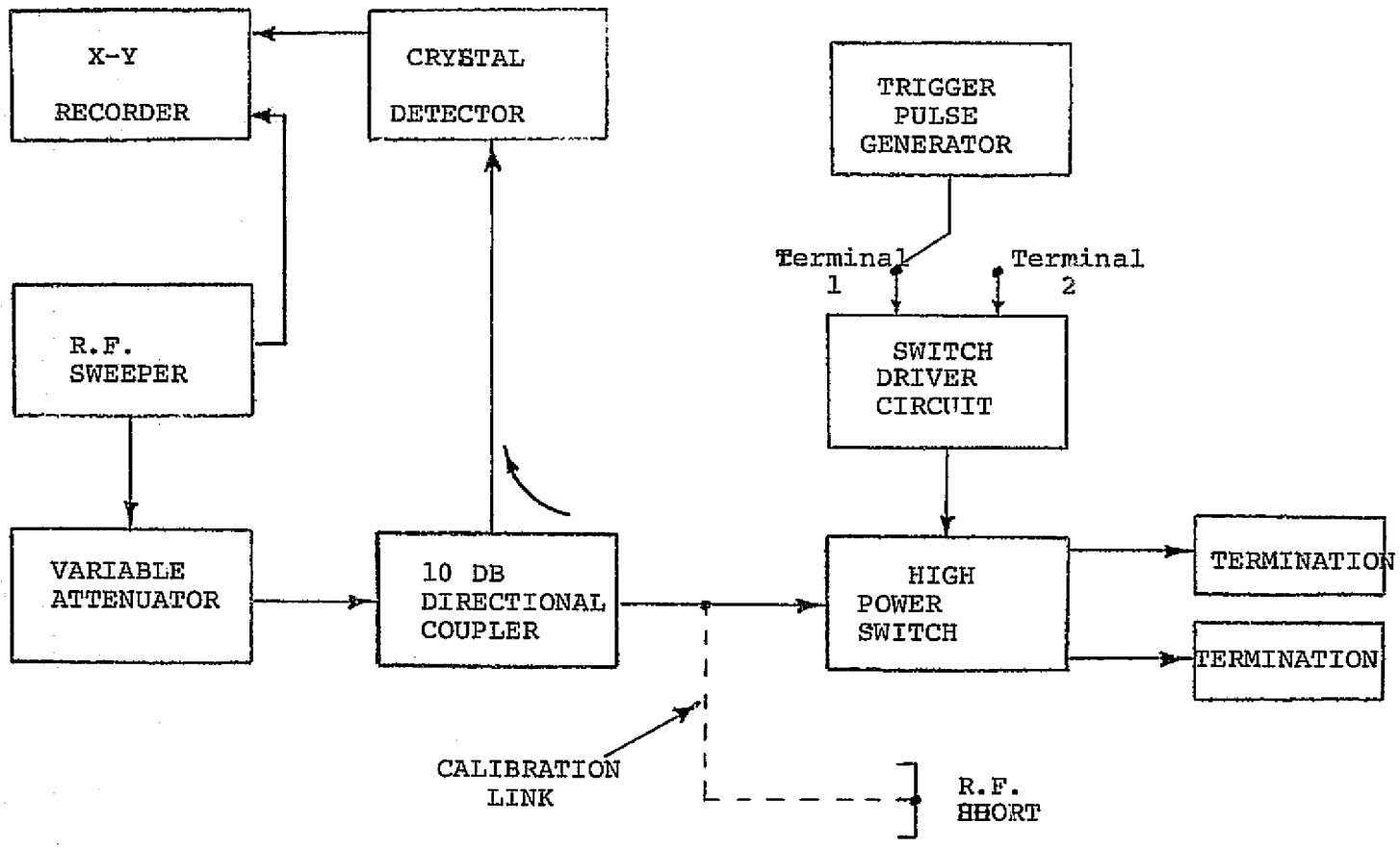

FIGURE 1 - BLOCK DIAGRAM FOR INPUT VSWR TESTS

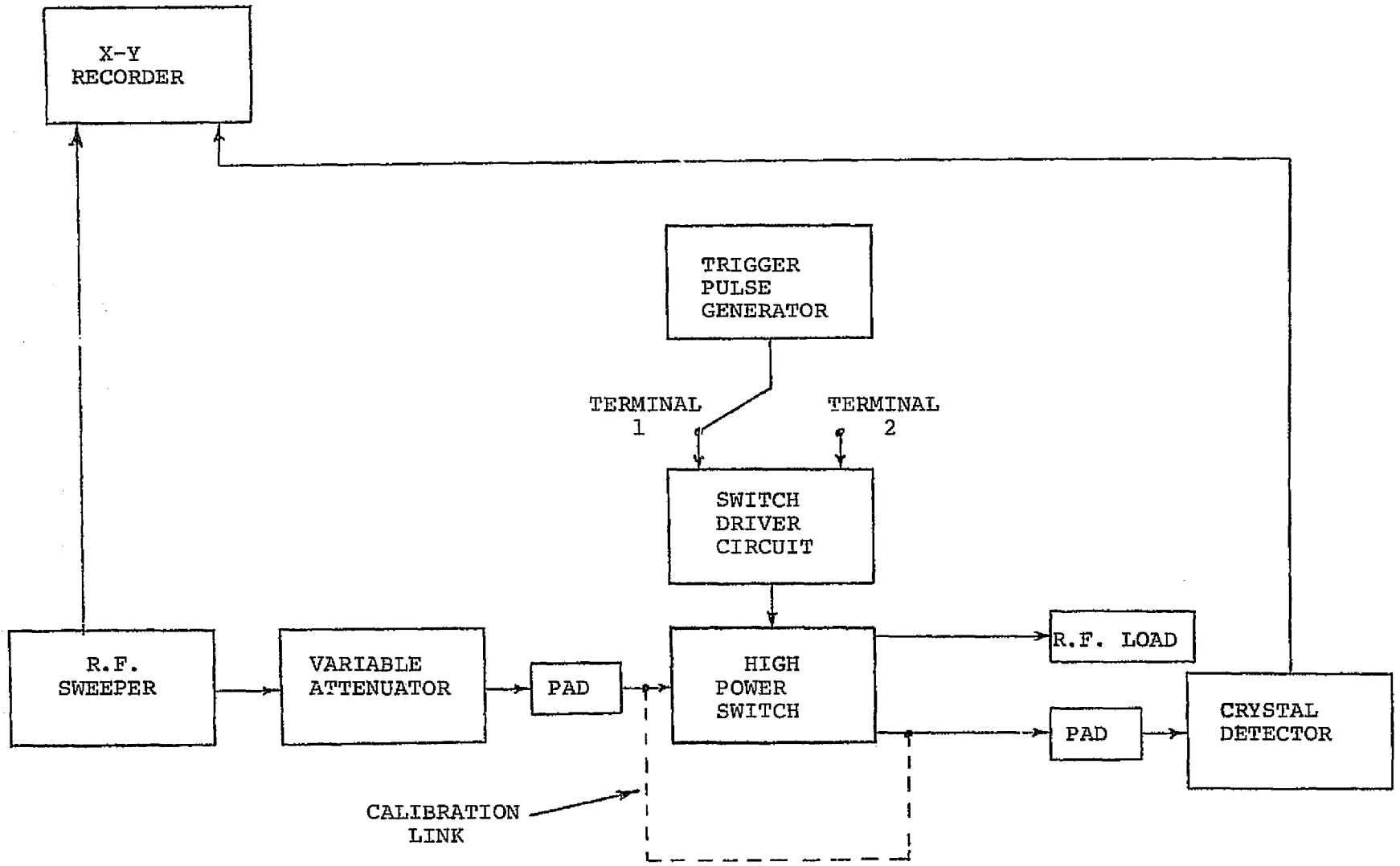

FIGURE 2 - BLOCK DIAGRAM FOR INSERTION LOSS TESTS (INPUT TO OUTPUT)

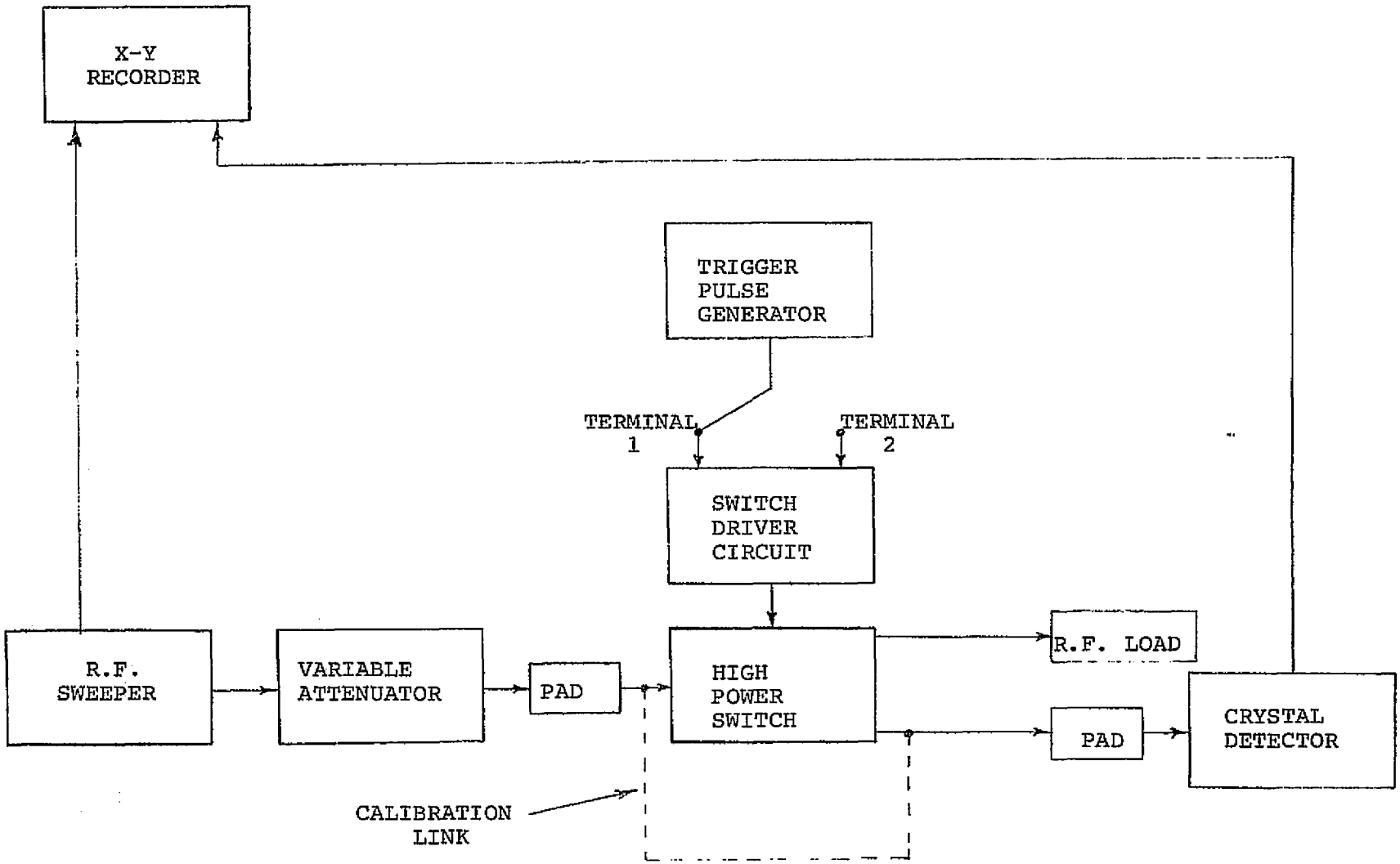

FIGURE 3 - BLOCK DIAGRAM FOR ISOLATION (INPUT TO OUTPUT)

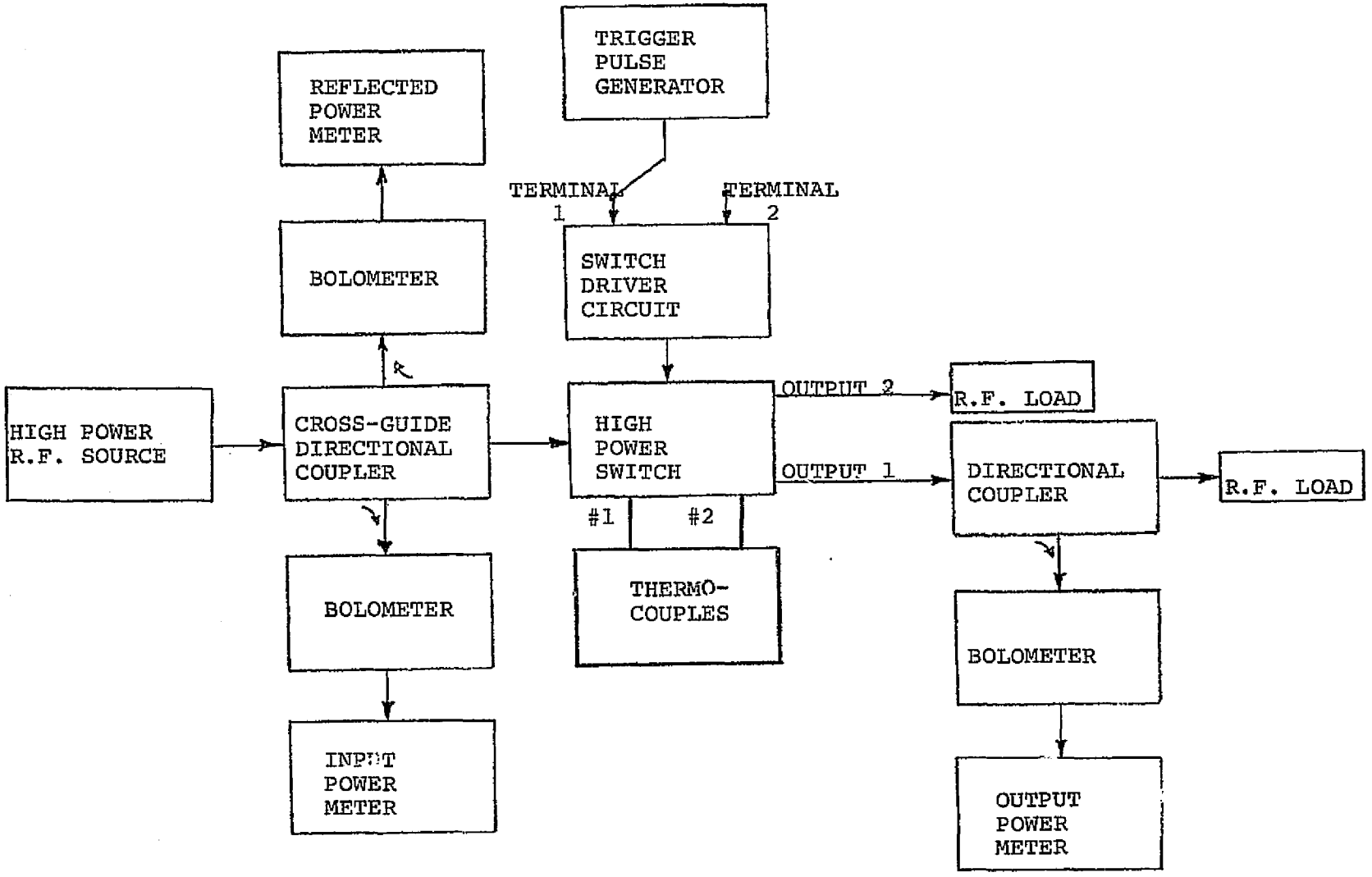

FIGURE 4 - BLOCK DIAGRAM FOR R.F. POWER TESTS